Application of Plasma Phenomena

Po-Yu Chang

Institute of Space and Plasma Sciences, National Cheng Kung University

Lecture 8

2024 spring semester

Tuesday 9:10-12:00

Materials:

https://capst.ncku.edu.tw/PGS/index.php/teaching/

Online courses:
https://nckucc.webex.com/nckucc/j.php?MTID=m4082f23c59af0571015416f6e58dd803

Electromagnetic wave can be used to measure the density or the magnetic field in the plasma

- **Nonmagnetized isotropic plasma (interferometer needed):**

$$n^2 = 1 - \frac{X(1-X)}{1 - X - \frac{1}{2}Y^2\sin^2\theta \pm \left[\left(\frac{1}{2}Y^2\sin^2\theta\right)^2 + (1-X)^2 Y^2\cos^2\theta\right]^{1/2}}$$

$$= 1 - X = 1 - \frac{\omega_p^2}{\omega^2} = 1 - \frac{n_e}{n_{cr}} \qquad \left(Y \equiv \frac{\Omega}{\omega} \equiv 0\right)$$

Note: $\qquad \omega_p^2 = \dfrac{n_e e^2}{\epsilon_0 m_e} \qquad n_{cr} = \dfrac{\epsilon_0 m_e \omega^2}{e^2}$

- **Magnetized isotropic plasma (Polarization detected needed):**

Parallel to B$_0$

$$n^2 = 1 - \frac{\omega_p^2}{\omega(\omega \pm \Omega)} \qquad\qquad \frac{E_x}{E_y} = \pm i \qquad \Omega \equiv \frac{eB_0}{m_e}$$
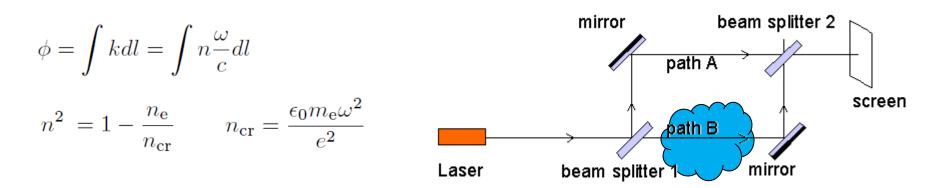
Faraday rotation: linear polarization rotation caused by the difference between the speed of LHC and RHC polarized wave.

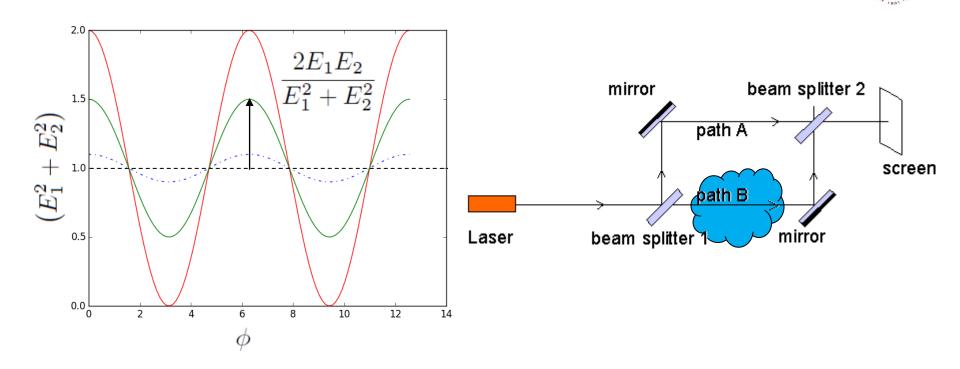# The phase different depends on the line integral of the electron density along the path

$$\phi = \int k\,dl = \int n\frac{\omega}{c}\,dl$$

$$n^2 = 1 - \frac{n_e}{n_{cr}} \qquad n_{cr} = \frac{\epsilon_0 m_e \omega^2}{e^2}$$

$$
\begin{aligned}
\Delta\phi &= \int (k_{\text{plasma}} - k_0)\,dl = \frac{\omega}{c}\int (n-1)\,dl \\
&= \frac{\omega}{c}\int\left(\sqrt{1 - \frac{n_e}{n_c}} - 1\right)dl \approx \frac{\omega}{c}\int\left(1 - \frac{1}{2}\frac{n_e}{n_c} - 1\right)dl \\
&= -\frac{\omega}{2cn_c}\int n_e\,dl
\end{aligned}
$$

Note that $n_e \ll n_{cr}$ **is assumed,** $\qquad \sqrt{1 - \frac{n_e}{n_{cr}}} \approx 1 - \frac{1}{2}\frac{n_e}{n_{cr}}$

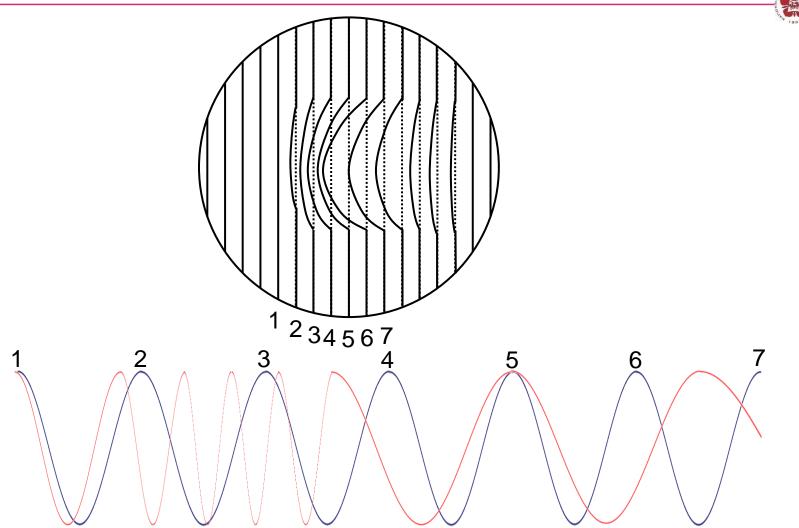# The intensity on screen depends on the phase different between two paths

$$I = (E_1^2 + E_2^2)\left(1 + \frac{2E_1 E_2}{E_1^2 + E_2^2}\cos\phi\right)$$

The phase is determined by comparing to the pattern without the phase shift

Fourier transform can be used to retrieve the data from the interferometer image

$$I(x, y) = I_0(x, y) + m(x, y)\cos[2\pi\nu_0 x + \phi(x, y)] \qquad \cos(x) = \frac{e^{ix} + e^{-ix}}{2}$$

$$= I_0(x, y) + \frac{1}{2}m(x, y)\left(e^{i[2\pi\nu_0 x + \phi(x,y)]} + e^{-i[2\pi\nu_0 x + \phi(x,y)]}\right)$$

$$= I_0(x, y) + \frac{1}{2}m(x, y)e^{i\phi(x,y)}e^{i2\pi\nu_0 x} + \frac{1}{2}m(x, y)e^{-i\phi(x,y)}e^{-i2\pi\nu_0 x}$$
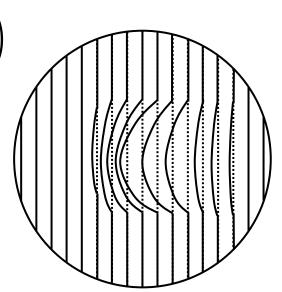
$$= I_0(x, y) + c(x, y)e^{i2\pi\nu_0 x} + c^*(x, y)e^{-i2\pi\nu_0 x}$$

$$c(x, y) \equiv \frac{1}{2}m(x, y)e^{i\phi(x,y)} \qquad \phi(x, y) = \tan^{-1}\left(\frac{\text{Im}[c(x, y)]}{\text{Re}[c(x, y)]}\right)$$

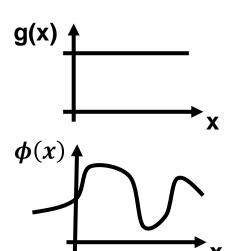$$\hat{g}(f_x, y) \equiv \text{FT}[g(x, y)]$$

$$\hat{g}(f_x - \nu_0, y) = \text{FT}\left[g(x, y)e^{i2\pi\nu_0 x}\right]$$

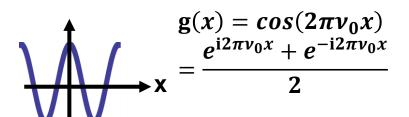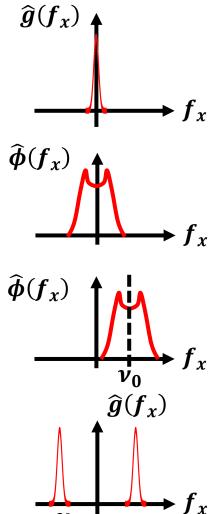$$\hat{I}(f_x, y) = \hat{I}_0(f_x, y) + \hat{c}(f_x - \nu_0, y) + \hat{c}^*(f_x + \nu_0, y)$$

Basic knowledge of Fourier transform

g(x)

$\widehat{g}(f_x)$

$\phi(x)$

$\widehat{\phi}(f_x)$

$$\mathbf{h}(x) = \boldsymbol{\phi}(x) \times e^{-i2\pi v_0 x}$$

$\widehat{\phi}(f_x)$

v_0

$$g(x) = cos(2\pi v_0 x)$$
$$= \frac{e^{i2\pi v_0 x} + e^{-i2\pi v_0 x}}{2}$$

$\widehat{g}(f_x)$

$-v_0$ v_0
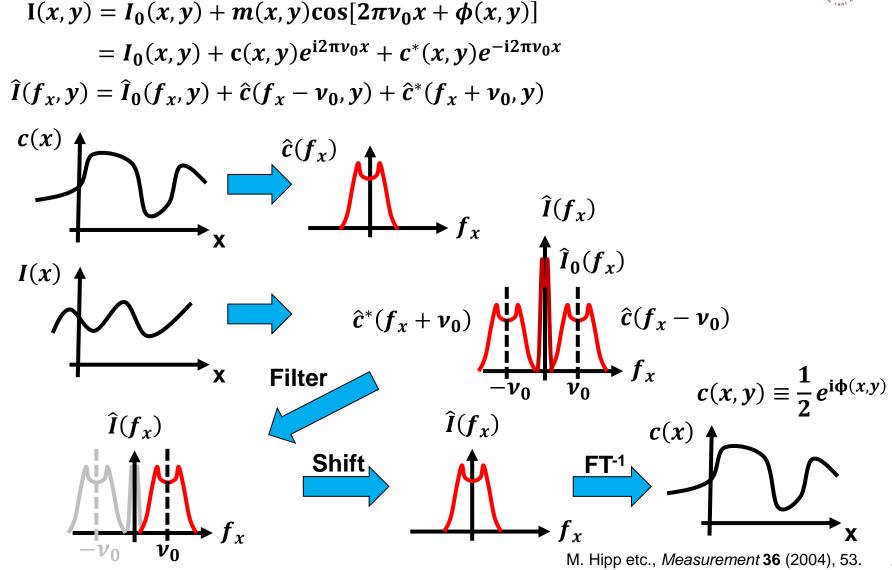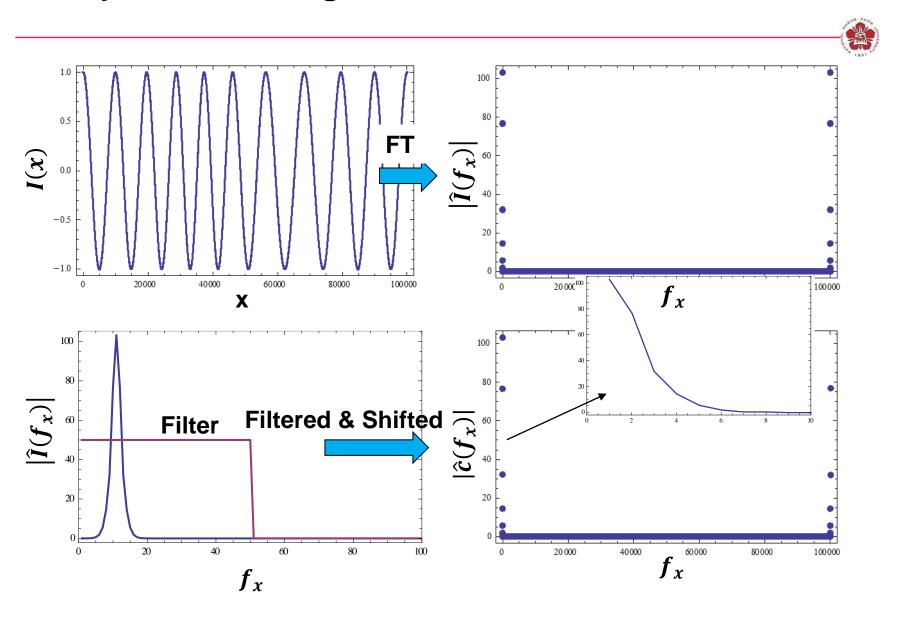
$$I(x) = I_0(x) + m(x)\cos[2\pi\nu_0 x + \phi(x)]$$

Procedure of retrieving data

$$I(x, y) = I_0(x, y) + m(x, y)\cos[2\pi\nu_0 x + \phi(x, y)]$$
$$= I_0(x, y) + c(x, y)e^{i2\pi\nu_0 x} + c^*(x, y)e^{-i2\pi\nu_0 x}$$
$$\hat{I}(f_x, y) = \hat{I}_0(f_x, y) + \hat{c}(f_x - \nu_0, y) + \hat{c}^*(f_x + \nu_0, y)$$

$$c(x, y) \equiv \frac{1}{2}e^{i\phi(x,y)}$$
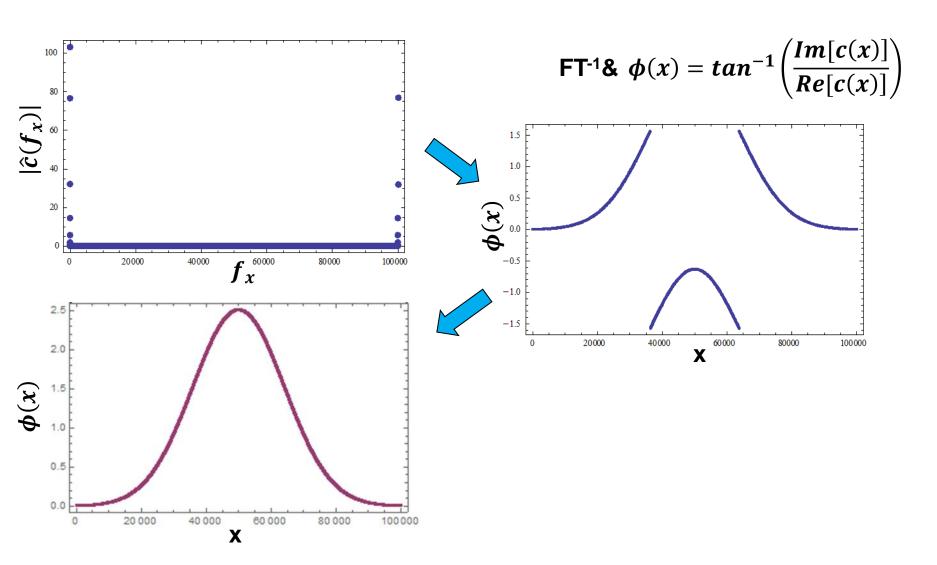
M. Hipp etc., *Measurement* **36** (2004), 53.

Example of retrieving data from 1D interferometer
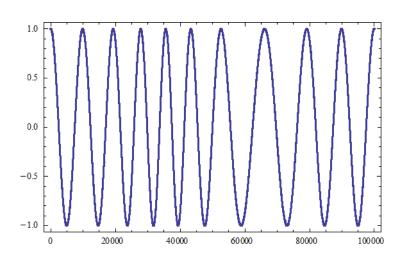
The retrieved data need to be modified if the phase change is too much

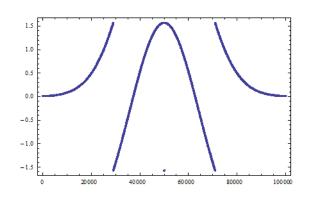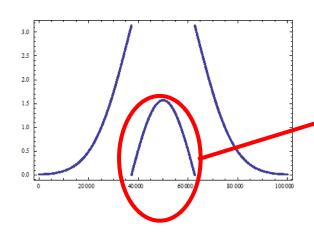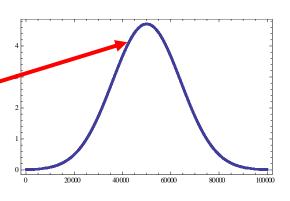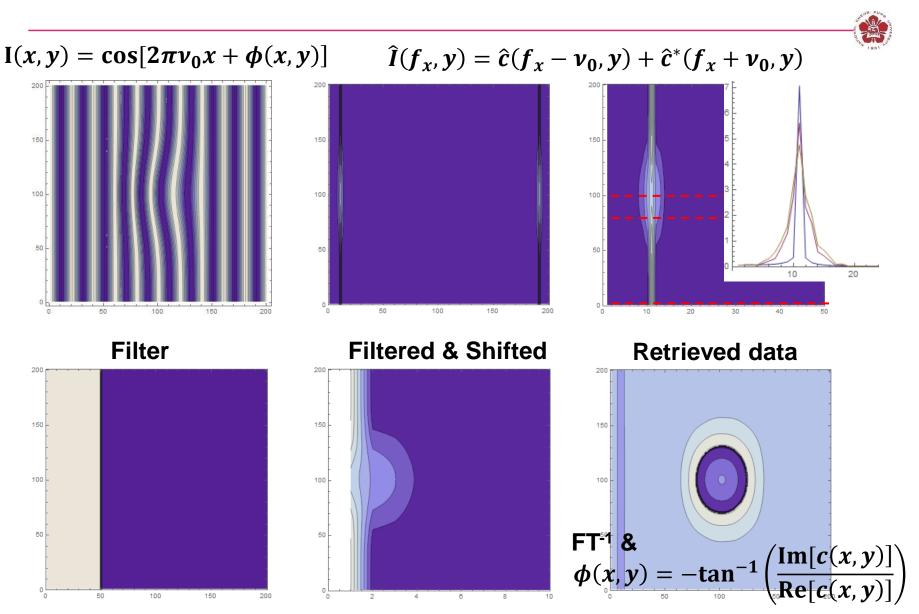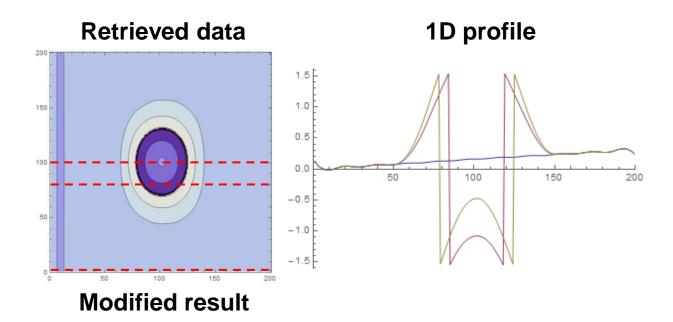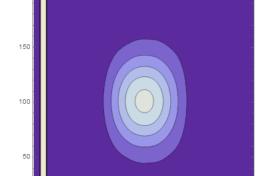$$FT^{-1} \& \; \phi(x) = tan^{-1}\left(\frac{Im[c(x)]}{Re[c(x)]}\right)$$

The final phase difference needs to be determined manually since it may exceeds 2π

Example of retrieving data from 2D interferometer

$$\mathbf{I}(x,y) = \cos[2\pi\nu_0 x + \phi(x,y)]$$

$$\hat{\mathbf{I}}(f_x, y) = \hat{c}(f_x - \nu_0, y) + \hat{c}^*(f_x + \nu_0, y)$$

Filter   **Filtered & Shifted**   **Retrieved data**

$\mathbf{FT^{-1}}$ &

$$\phi(x,y) = -\tan^{-1}\left(\frac{\mathbf{Im}[c(x,y)]}{\mathbf{Re}[c(x,y)]}\right)$$

The retrieved data may need to be modified if the phase change is too large

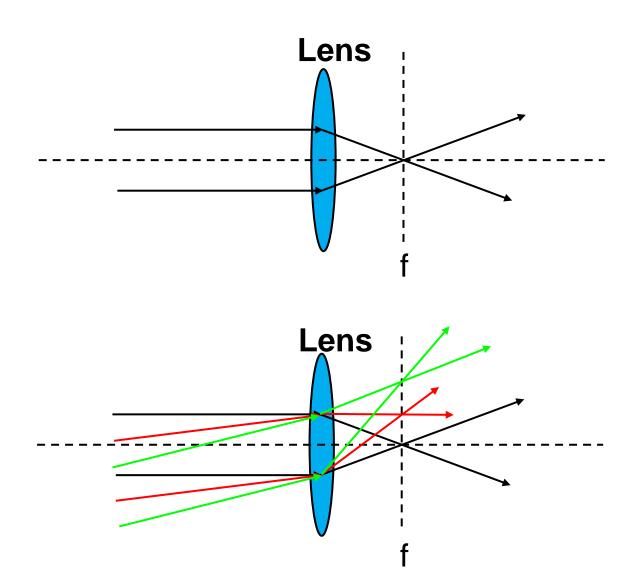**Retrieved data**

1D profile

Modified result

- Slope came from the non-integer spatial frequency of the fringes.
- Noise came from rectangular function as the filter.

13

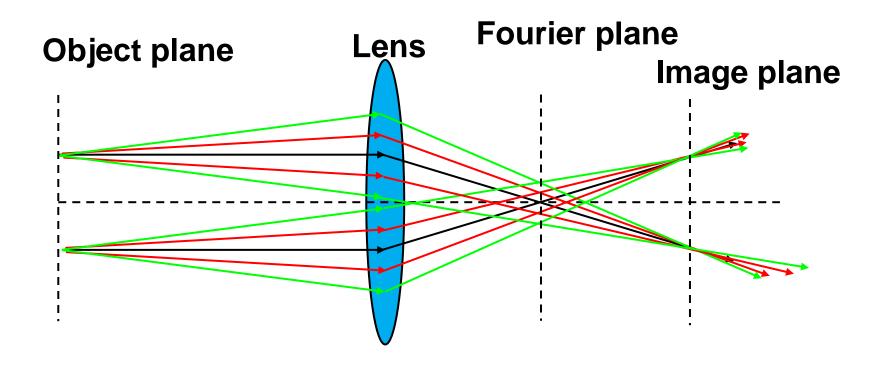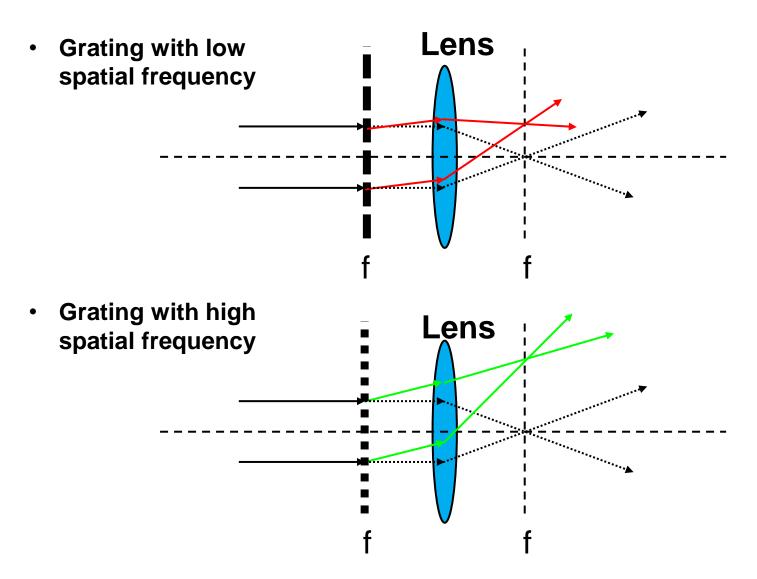# Angular spectrum of plane waves can be used for diagnostic

Lens

f

Lens

f

Rays with different angles go through different focal points on the focal points

Object plane   **Lens**   **Fourier plane**

Image plane
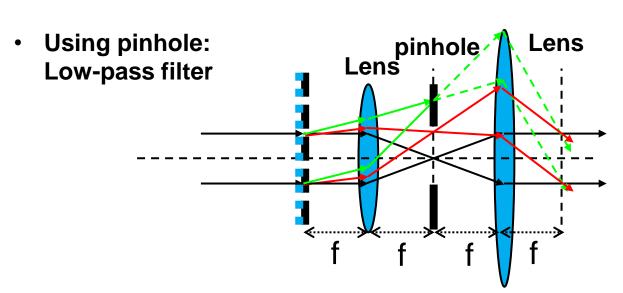
Parallel beams are deflected to different angles with grating with different spatial frequencies

- **Grating with low spatial frequency**

Lens

f   f

- **Grating with high spatial frequency**

Lens

f   f
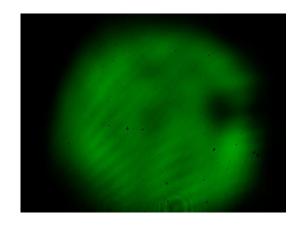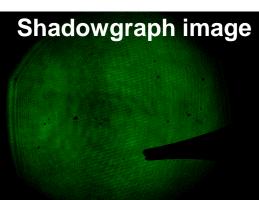
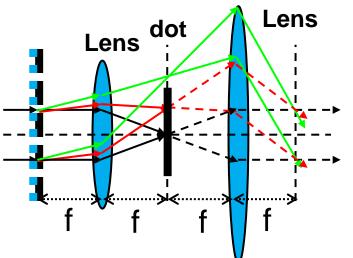# A pinhole or a dot acts like a low-pass / high-pass filter

- **Using pinhole: Low-pass filter**
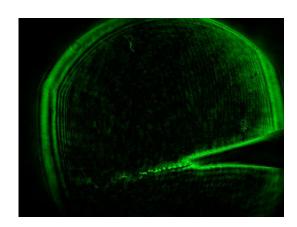
- **Using dot: High-pass filter**
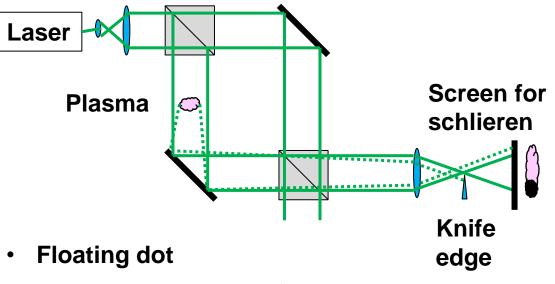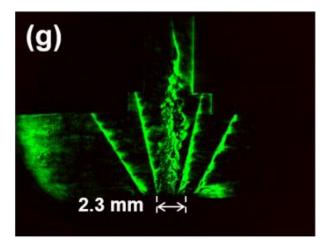

Shadowgraph image

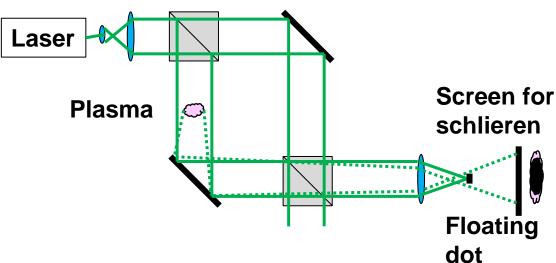# A symmetric Schlieren image can be obtained if the knife edge is replaced by a "floating dot"

- **Knife edge**

Laser

Plasma

Screen for schlieren

Knife edge

- **Floating dot**

Laser

Plasma

Screen for schlieren

Floating dot

(g)

2.3 mm
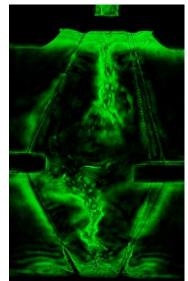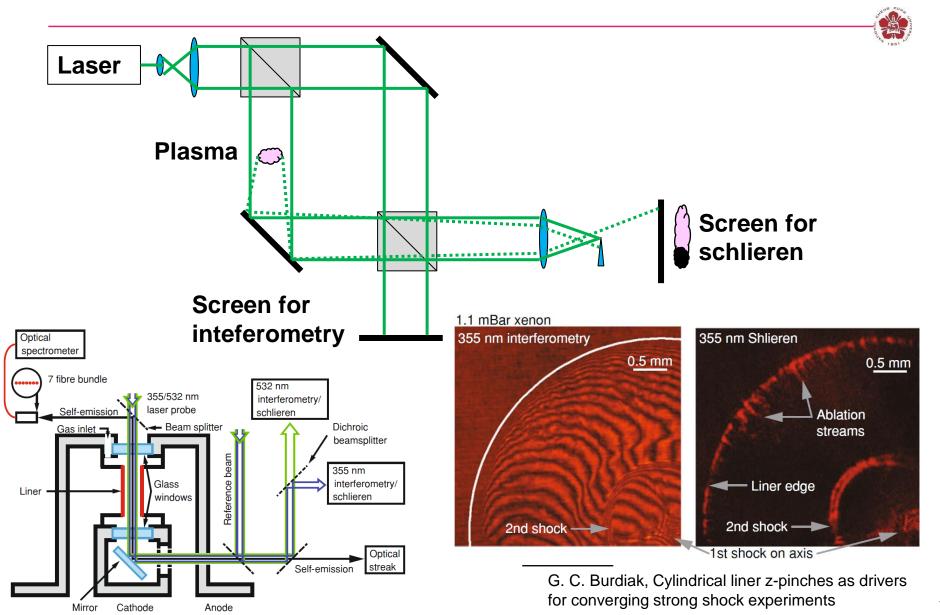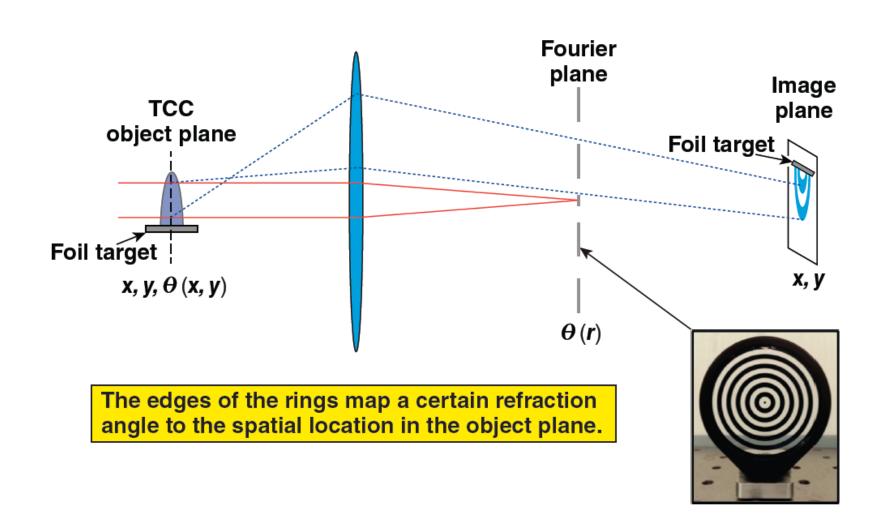
Schlieren imaging system can detect density gradient

Laser

Plasma

Screen for schlieren

Screen for inteferometry

Optical spectrometer

7 fibre bundle

Self-emission

Gas inlet

Liner

Glass windows

355/532 nm laser probe

Beam splitter

Reference beam

532 nm interferometry/ schlieren

Dichroic beamsplitter

355 nm interferometry/ schlieren

Optical streak

Self-emission

Mirror   Cathode   Anode

1.1 mBar xenon
355 nm interferometry
0.5 mm
2nd shock

355 nm Shlieren
0.5 mm
Ablation streams
Liner edge
2nd shock
1st shock on axis

G. C. Burdiak, Cylindrical liner z-pinches as drivers for converging strong shock experiments

19

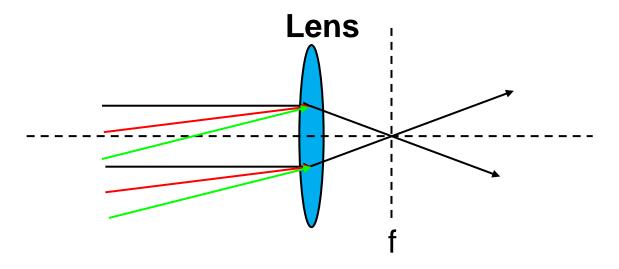# Angular filter refractometry (AFR) maps the refraction of the probe beam at TCC to contours in the image plane

The edges of the rings map a certain refraction angle to the spatial location in the object plane.

Angular spectrum of plane waves can be used for diagnostic

Lens

f

Angular spectrum of plane waves can be used for diagnostic

Lens

f

Lens

f

Rays with different angles go through different focal points on the focal points

Object plane   Lens   Fourier plane   Image plane

Rays with different angles can be selected by blocking different focal points
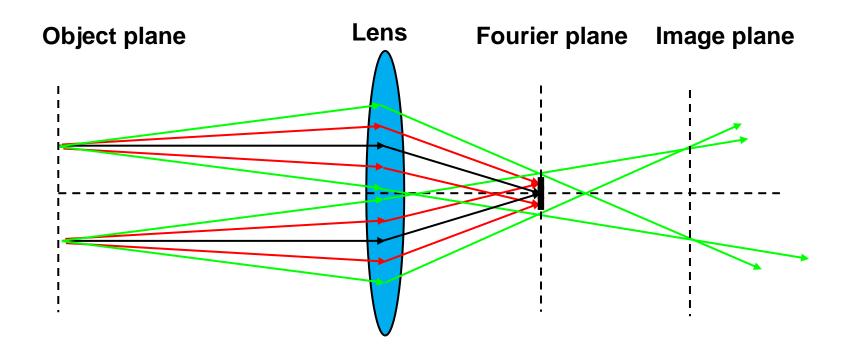
Object plane

Lens

Fourier plane

Image plane

Rays with different angles go through different focal points on the focal points

Object plane

Lens

Fourier plane

Image plane

Rays with different angles go through different focal points on the focal points

Object plane   **Lens**   **Fourier plane**   **Image plane**

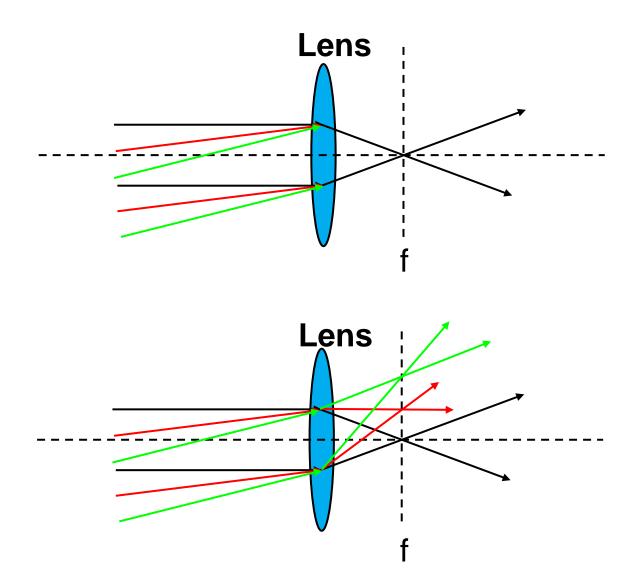# Angular filter refractometry (AFR) maps the refraction of the probe beam at TCC to contours in the image plane
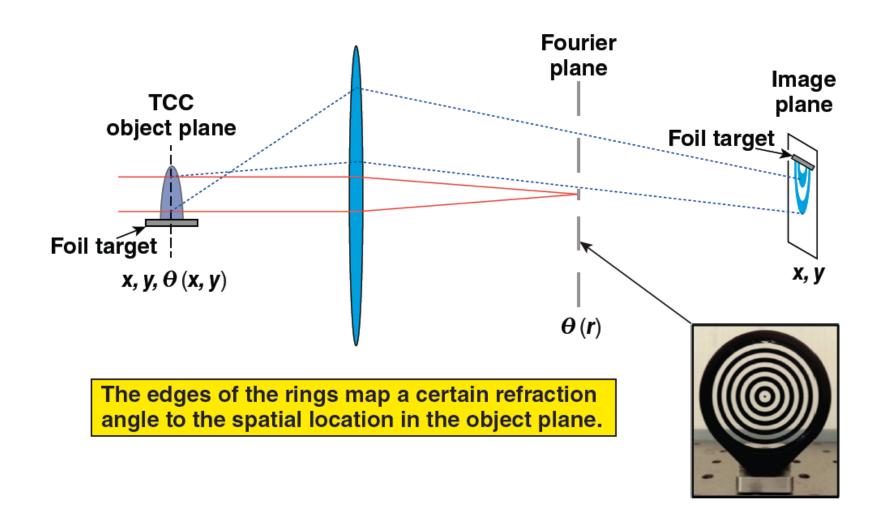
The edges of the rings map a certain refraction angle to the spatial location in the object plane.

Channeling of multi-kilojoule high-intensity laser beams in an inhomogeneous plasma was observed using AFR

S. Ivancic *et al.*, Phys. Rev. E 91 , 051101 (2015)

Electromagnetic wave can be used to measure the density or the magnetic field in the plasma

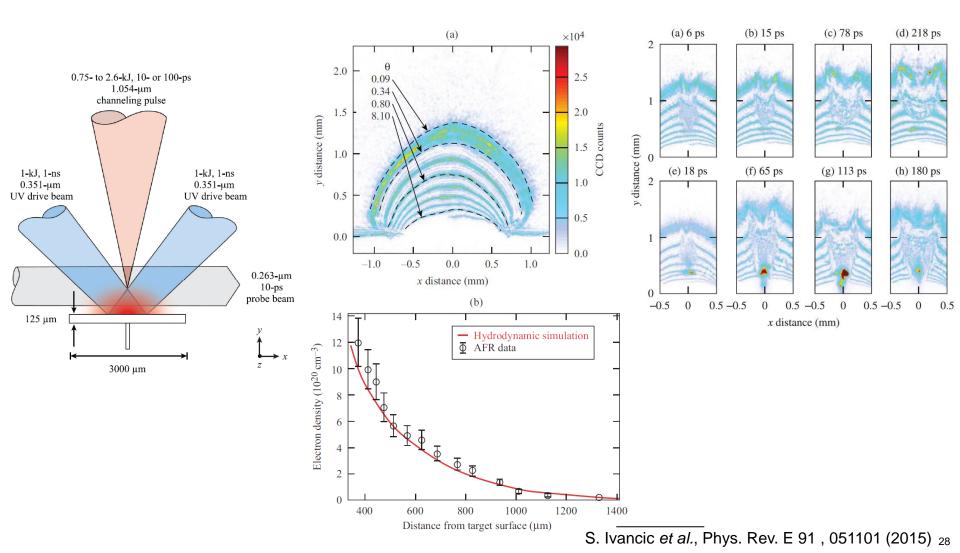- **Nonmagnetized isotropic plasma (interferometer needed):**

$$n^2 = 1 - \frac{X(1-X)}{1 - X - \frac{1}{2}Y^2\sin^2\theta \pm \left[\left(\frac{1}{2}Y^2\sin^2\theta\right)^2 + (1-X)^2 Y^2\cos^2\theta\right]^{1/2}}$$

$$= 1 - X = 1 - \frac{\omega_p^2}{\omega^2} = 1 - \frac{n_e}{n_{cr}} \qquad \left(Y \equiv \frac{\Omega}{\omega} \equiv 0\right)$$

Note: $\qquad \omega_p^2 = \dfrac{n_e e^2}{\epsilon_0 m_e} \qquad n_{cr} = \dfrac{\epsilon_0 m_e \omega^2}{e^2}$

- **Magnetized isotropic plasma (Polarization detected needed):**

Parallel to B$_0$

$$n^2 = 1 - \frac{\omega_p^2}{\omega(\omega \pm \Omega)} \qquad\qquad \frac{E_x}{E_y} = \pm i \qquad \Omega \equiv \frac{eB_0}{m_e}$$

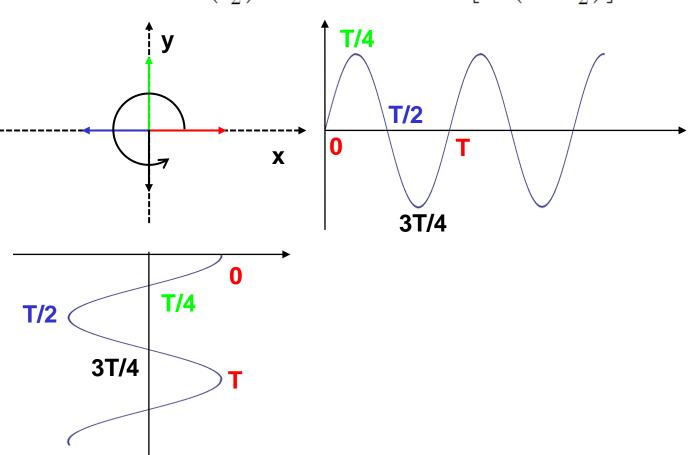**Faraday rotation: linear polarization rotation caused by the difference between the speed of LHC and RHC polarized wave.**

Circular polarization

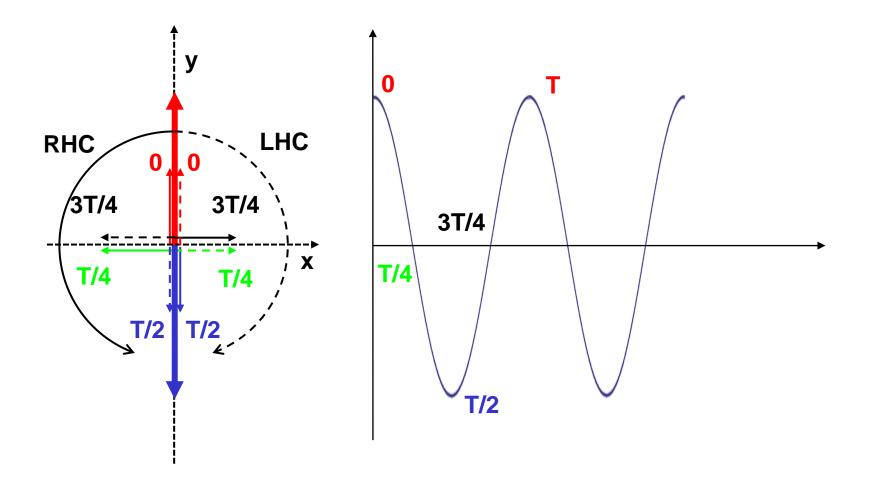$$E_{\mathrm{x}} = E_0 \exp\left(-i\omega t\right)$$

$$E_{\mathrm{y}} = iE_{\mathrm{x}} = iE_0 \exp\left(-i\omega t\right) = E_0 \exp\left(i\frac{\pi}{2}\right)\exp\left(-i\omega t\right) = E_0 \exp\left[-i\left(\omega t - \frac{\pi}{2}\right)\right]$$

Linear polarization rotates as the wave propagates with different speed in LHC and RHC polarization

$$\vec{E} = E_0 \hat{x} = \frac{E_0}{2}[(\hat{x} + i\hat{y}) + (\hat{x} - i\hat{y})] \qquad \vec{E}(z) = \vec{E}\exp(i\phi) \qquad \phi_R \neq \phi_L$$

$$\vec{E}(z) = \frac{E_0}{2}[(\hat{x} + i\hat{y})e^{i\phi_R} + (\hat{x} - i\hat{y})e^{i\phi_L}] \qquad \bar{\phi} \equiv \frac{\phi_R + \phi_L}{2} \qquad \Delta\phi \equiv \frac{\phi_R - \phi_L}{2}$$

$$= \frac{E_0}{2}[\hat{x}(e^{i\phi_R} + e^{i\phi_L}) + \hat{y}i(e^{i\phi_R} - e^{i\phi_L})]$$

$$= \frac{E_0}{2}\left[\hat{x}\left(e^{i\left(\bar{\phi}+\frac{\Delta\phi}{2}\right)} + e^{i\left(\bar{\phi}-\frac{\Delta\phi}{2}\right)}\right) + \hat{y}i\left(e^{i\left(\bar{\phi}+\frac{\Delta\phi}{2}\right)} - e^{i\left(\bar{\phi}-\frac{\Delta\phi}{2}\right)}\right)\right]$$

$$= E_0 e^{i\bar{\phi}}\left[\hat{x}\left(\frac{e^{i\frac{\Delta\phi}{2}} + e^{-i\frac{\Delta\phi}{2}}}{2}\right) + \hat{y}i\left(\frac{e^{i\frac{\Delta\phi}{2}} - e^{-i\frac{\Delta\phi}{2}}}{2}\right)\right]$$

$$= E_0 e^{i\bar{\phi}}\left[\hat{x}\cos\left(\frac{\Delta\phi}{2}\right) + \hat{y}\sin\left(\frac{\Delta\phi}{2}\right)\right]$$

A linear polarized wave can be decomposed into one left-handed circular polarized wave and a righ-handed circular polarized wave

The rotation angle of the polarization depends on the linear integral of magnetic field and electron density

$$\phi = \int k\,dl = \int n\frac{\omega}{c}\,dl \qquad\qquad \alpha = \frac{\Delta\phi}{2} = \frac{\omega}{2c}\int (n_R - n_L)\,dl$$
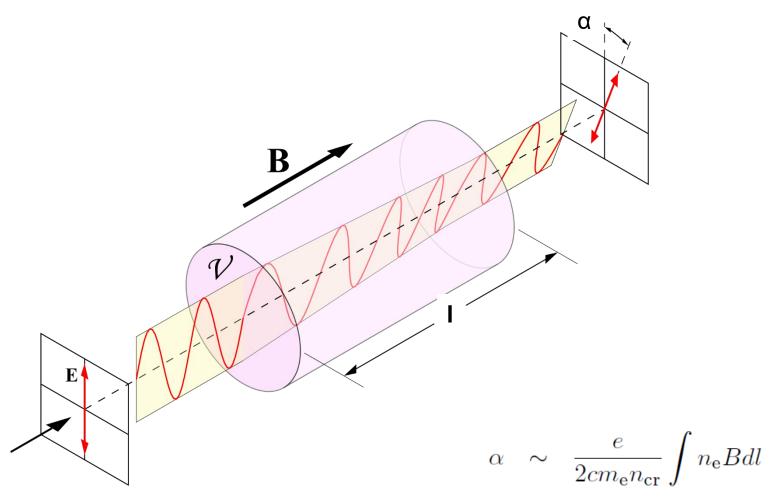
$$n_R = \sqrt{1 - \frac{X}{1+Y}} \sim 1 - \frac{1}{2}\frac{X}{1+Y} \qquad\qquad X, Y \ll 1$$

$$n_L \sim 1 - \frac{1}{2}\frac{X}{1-Y} \qquad\qquad\qquad \frac{X}{1\pm Y} \ll 1$$

$$n_R - n_L \sim \frac{X}{2}\left(\frac{1}{1-Y} - \frac{1}{1+Y}\right) = \frac{XY}{1-Y^2} \sim XY$$

$$\alpha \sim \frac{\omega}{2c}\int XY\,dl = \frac{\omega}{2c}\int \frac{\omega_p^2}{\omega^2}\frac{\Omega}{\omega}\,dl = \frac{1}{2c}\int \frac{n_e}{n_{cr}}\frac{eB}{m_e}\,dl$$

$$= \frac{e}{2cm_e n_{cr}}\int n_e B\,dl$$

The rotation angle of the polarization depends on the linear integral of magnetic field and electron density

$$\alpha \sim \frac{e}{2cm_{e}n_{cr}} \int n_{e}Bdl$$
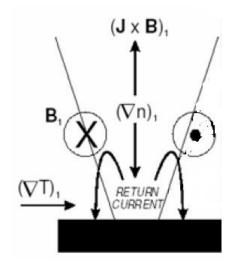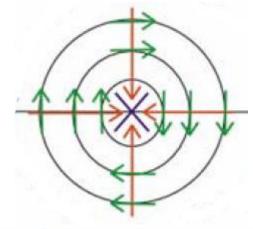
Magnetic field can be generated when the temperature and density gradients are not parallel to each other

$$\frac{\partial \vec{B}}{\partial t} = \nabla \times \left[\underbrace{\vec{u} \times \vec{B}}_{\text{Convection term}} + \underbrace{\frac{1}{\sigma \mu_0} \nabla \times \vec{B}}_{\text{Diffusion term}} + \underbrace{\frac{\nabla p_e}{n_e e}}_{\text{self generated field}} - \underbrace{\frac{1}{\mu_0} \left(\frac{\nabla \times \vec{B}}{n_e e} \times \vec{B} \right)}_{\text{Hall term}} \right]$$

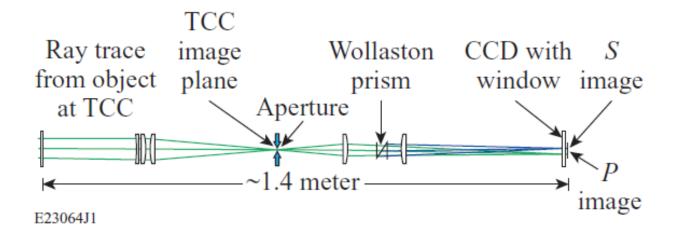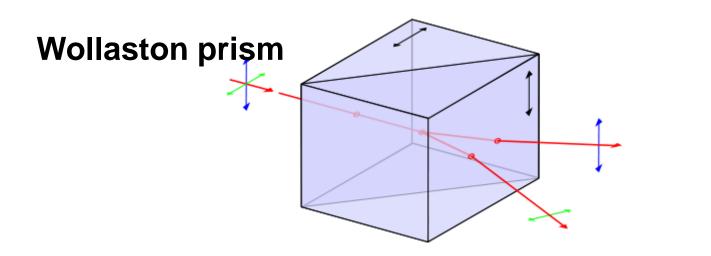$$\nabla \times \frac{\nabla p_e}{n_e e} = -\frac{k_B}{e} \frac{\nabla n_e \times \nabla T_e}{n_e}$$

$(J \times B)_1$

B_1 $(\nabla n)_1$

$(\nabla T)_1$ RETURN CURRENT

(grad n_e) $\times$ (grad T_e) $\longrightarrow$ B field $\longrightarrow$

P M Nilson *et al.*, Central Laser Facility Annual Report 2004/2005

Polarimetry diagnostic can be used to measure the magnetic field

TCC
Ray trace image Wollaston CCD with S
from object plane prism window image
at TCC Aperture

~1.4 meter

P image

E23064J1

Wollaston prism

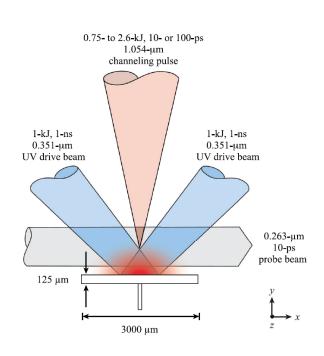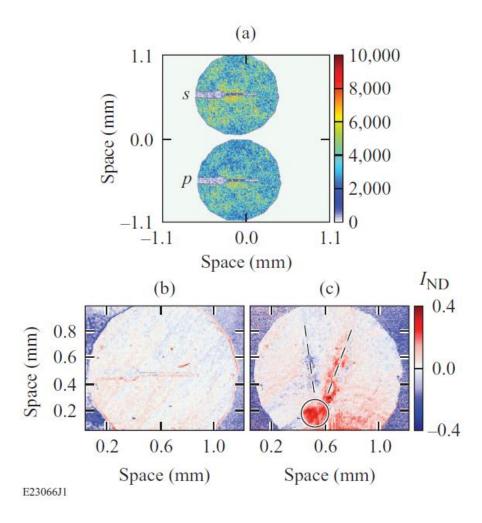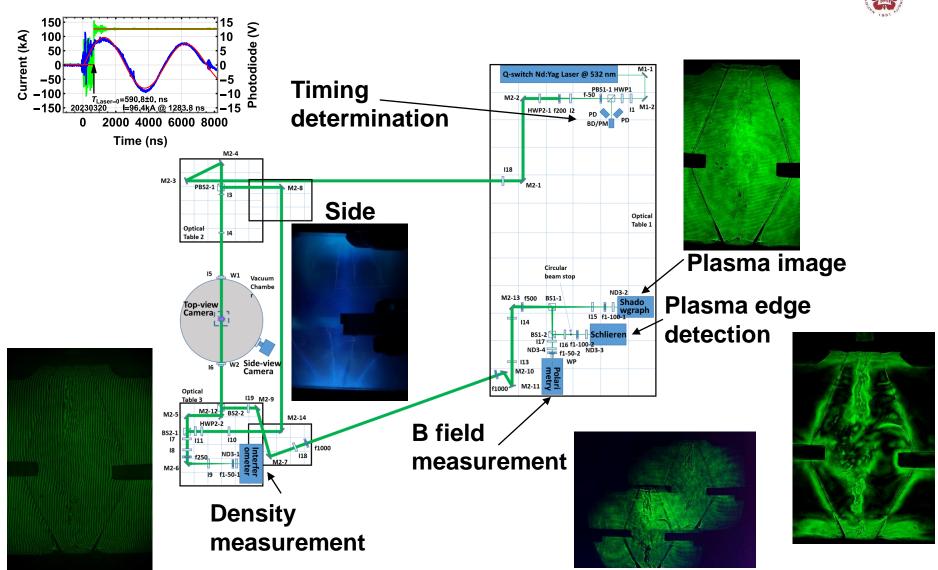A. Davies *et al.*, Rev. Sci. Instrum. **85**, 11E611 (2014)

Self-generated field was suggested when multi-kilojoule high-intensity laser beams illuminated on an inhomogeneous plasma
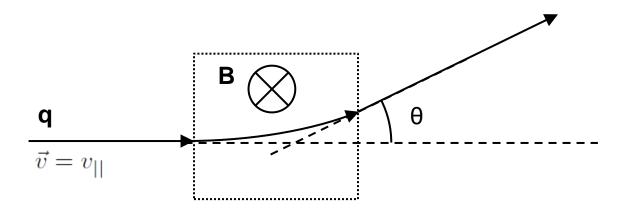

E23066J1

Time-resolved imaging system with temporal resolution in the order of nanoseconds was implemented

Timing determination

Side

Plasma image

Plasma edge detection

B field measurement

Density measurement

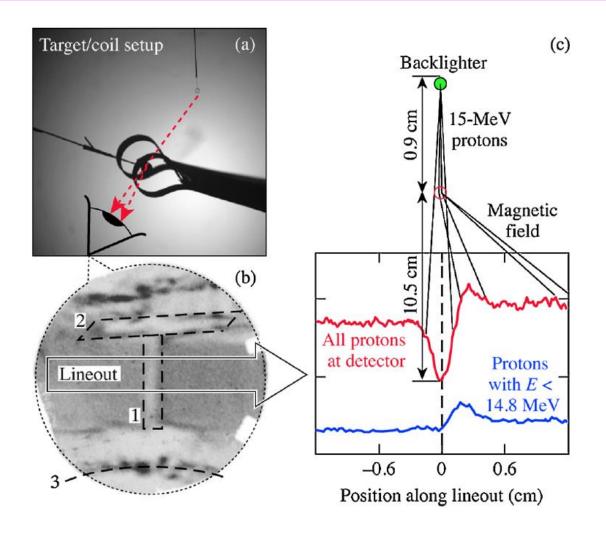# The magnetic field can be measured by measuring the deflected angle of charged particles

$$F_\perp = q\vec{v} \times \vec{B} = qv_{||}B = m\frac{dv_\perp}{dt}$$

$$v_\perp = \int \frac{qv_{||}B}{m}dt = \frac{qv_{||}}{m}\int Bdt\frac{dx}{dx} = \frac{qv_{||}}{m}\int \frac{B}{v_{||}}dx = \frac{q}{m}\int Bdx$$

$$\tan\theta = \frac{v_\perp}{v_{||}} = \frac{q}{mv_{||}}\int Bdx = \frac{q}{\sqrt{2mE}}\int Bdx \qquad \int Bdx = \frac{\sqrt{2mE}}{q}\tan\theta$$

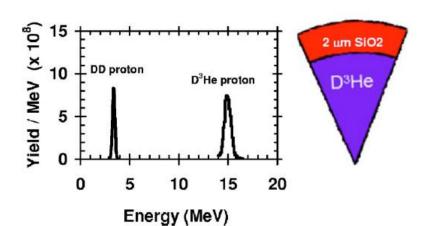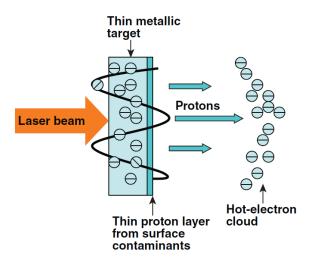# Magnetic field was measured using protons

O. V. Gotchev *et al.*, Phys. Rev. Lett. **103**, 215004 (2009)

Protons can be generated from fusion product or copper foil illuminated by short pulse laser
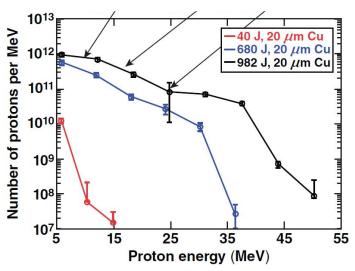
$$D + D \quad \rightarrow \quad T(1.01\text{MeV}) \quad + \quad p(3.02\text{MeV})$$

$$D + \text{He}^3 \quad \rightarrow \quad \text{He}^4(3.6\text{MeV}) \quad + \quad p(14.7\text{MeV})$$
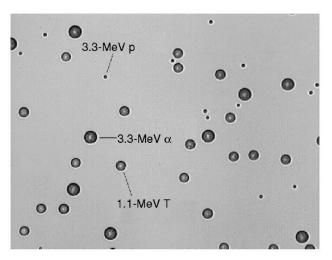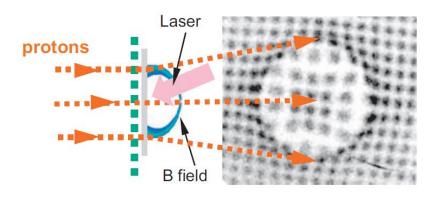

Target normal sheath acceleration (TNSA)

C. K. Li *et al.*, Rev. Sci. Instrum. **77**, 10E725 (2006)
L. Gao, PhD Thesis
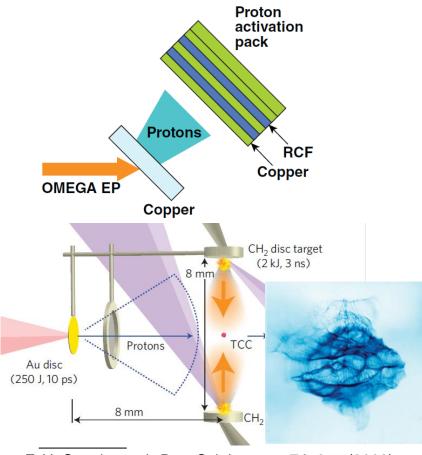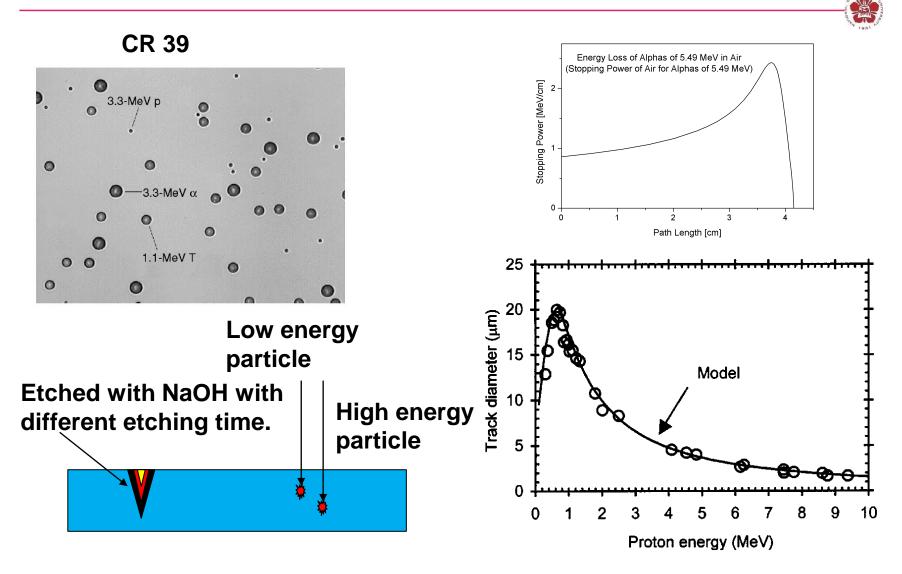
Protons can leave tracks on CR39 or film

CR 39

3.3-MeV p

3.3-MeV α

1.1-MeV T

protons

Laser

B field

Radiochromic film pack

Proton activation pack

Protons

RCF
Copper

OMEGA EP

Copper

CH$_2$ disc target
(2 kJ, 3 ns)

8 mm

Protons

TCC
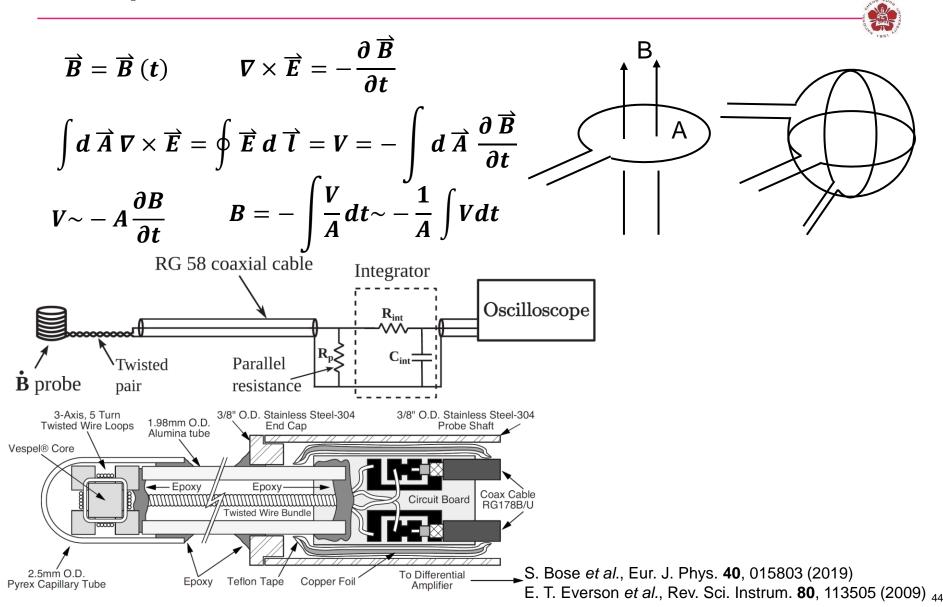
Au disc
(250 J, 10 ps)

8 mm

CH$_2$

F. H. Seguin *et al.*, Rev. Sci. Instrum. **74**, 975 (2003)
C. K. Li *et al.*, Phys. Plasmas **16**,056304 (2009)
L. Gao, PhD Thesis
N. L. Kugland et al., Nature Phys. B, 809 (2012)

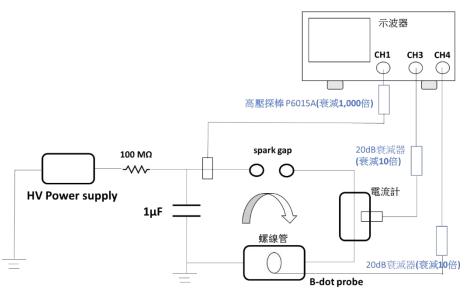# Track diameter on the CR39 is depended on the particle energy that incidents

CR 39

3.3-MeV p

3.3-MeV α

1.1-MeV T

Low energy particle

Etched with NaOH with different etching time.

High energy particle

Energy Loss of Alphas of 5.49 MeV in Air
(Stopping Power of Air for Alphas of 5.49 MeV)

Stopping Power [MeV/cm]

Path Length [cm]

Model

Track diameter (μm)

Proton energy (MeV)

F. H. Seguin *et al.*, Rev. Sci. Instrum. **74**, 975 (2003)

Time dependent magnetic field can be measured using B-dot probe

$$\vec{B} = \vec{B}(t) \qquad \nabla \times \vec{E} = -\frac{\partial \vec{B}}{\partial t}$$

$$\int d\vec{A}\, \nabla \times \vec{E} = \oint \vec{E}\, d\vec{l} = V = -\int d\vec{A}\, \frac{\partial \vec{B}}{\partial t}$$

$$V \sim -A\frac{\partial B}{\partial t} \qquad B = -\int \frac{V}{A} dt \sim -\frac{1}{A}\int V dt$$

S. Bose *et al.*, Eur. J. Phys. **40**, 015803 (2019)

E. T. Everson *et al.*, Rev. Sci. Instrum. **80**, 113505 (2009)
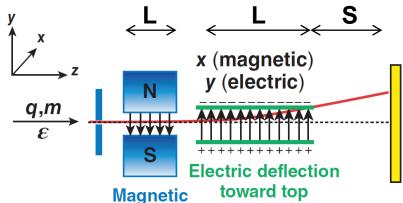
B-dot probe experiments
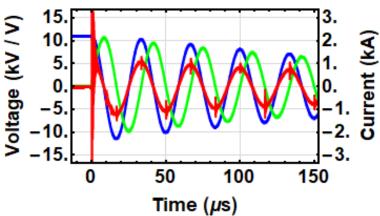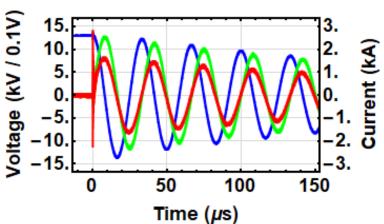
- **Without integrator**

- **With integrator**

A Thomson parabola uses parallel electric and magnetic fields to deflect particles onto parabolic curves that resolve q/m

y
x
z

L   L   S

x (magnetic)
y (electric)

N
S

q,m
ε

Magnetic deflection into page (x direction)

Electric deflection toward top of page (y direction)

- Deflection caused by magnetic field ~q/p
- Deflection caused by electric field ~q/KE
- Ion traces form parabolic curves on detector plane

$$y = \frac{m}{q}\frac{E}{B^2SL}x^2$$

$$F_x = qv_{||}B = m\frac{dv_x}{dt}$$

$$v_x = \frac{q}{m}v_{||}B\Delta t = \frac{q}{m}v_{||}B\frac{L}{v_{||}} = \frac{qBL}{m}$$

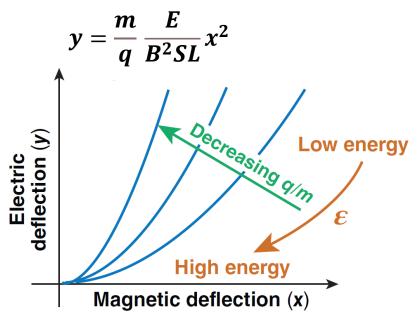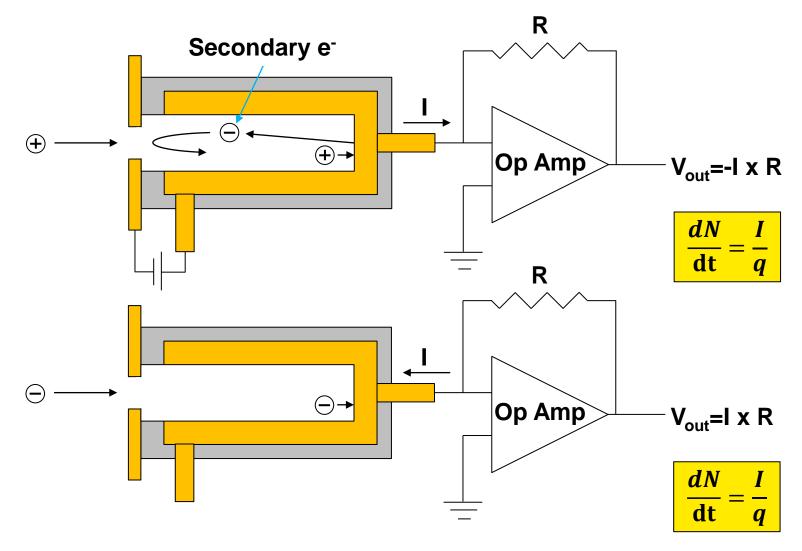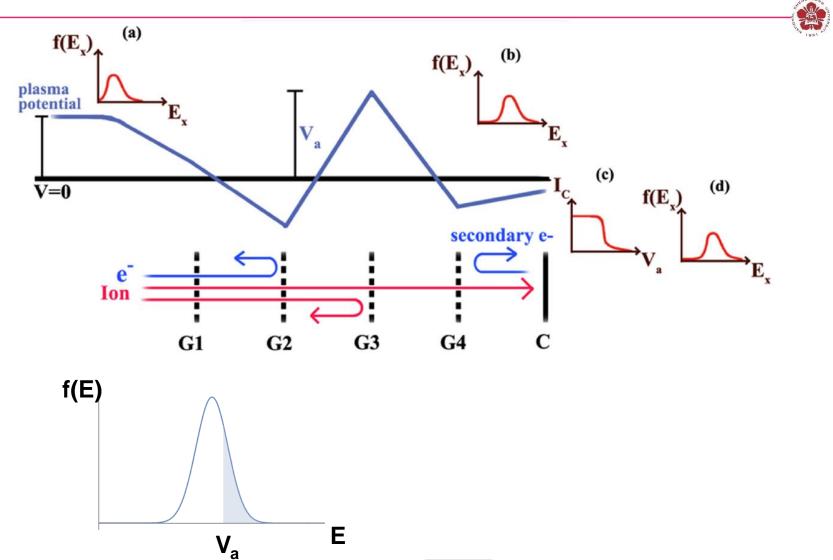$$\tan\theta_x = \frac{v_x}{v_{||}} = \frac{qBL}{mv_{||}} = \frac{qBL}{\sqrt{2m\epsilon}}$$

$$F_y = qE = m\frac{dv_y}{dt}$$

$$v_y = \frac{q}{m}E\Delta t = \frac{q}{m}E\frac{L}{v_{||}} = \frac{qEL}{mv_{||}}$$

$$\tan\theta_y = \frac{v_y}{v_{||}} = \frac{qEL}{mv_{||}^2} = \frac{qEL}{2\epsilon}$$

Electric deflection (y)

Magnetic deflection (x)

Decreasing q/m

Low energy

ε

High energy

E16717b

46

A faraday cup measures the flux of charge particles

Secondary e⁻

Op Amp

$V_{out} = -I \times R$

$$\frac{dN}{dt} = \frac{I}{q}$$

Op Amp

$V_{out} = I \times R$

$$\frac{dN}{dt} = \frac{I}{q}$$

R

R

I

I

Retarding potential analyzer measures the energy / velocity distribution function

48

The photon energy spectrum provides valuable information
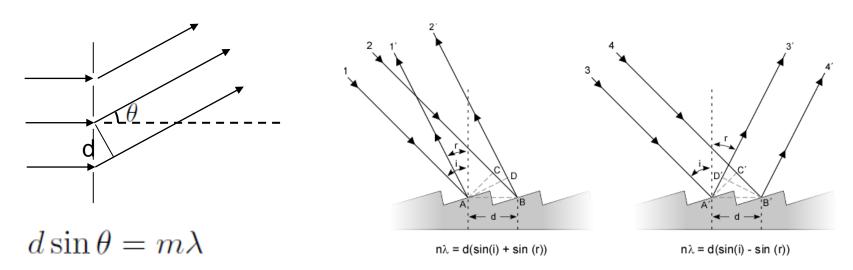
- **Plasma conditions can be determined from the photon spectrum**

  - **visible light: absorption and laser-plasma interactions**

  - **x rays: electron temperature, density, plasma flow, material mixing**

- **There are three basic tools for determining the spectrum detected**
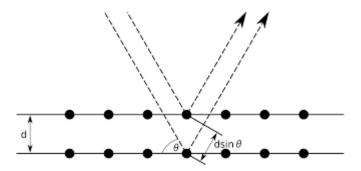
  - **filtering**

  - **grating spectrometer**

  - **Bragg spectrometer**

Spectrum can be obtained using grating

- **Grating is used to disperse the light**

$$d \sin \theta = m\lambda$$

$n\lambda = d(\sin(i) + \sin(r))$

$n\lambda = d(\sin(i) - \sin(r))$

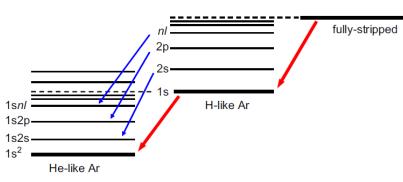- **Bragg condition in the crystal is used for X-ray.**
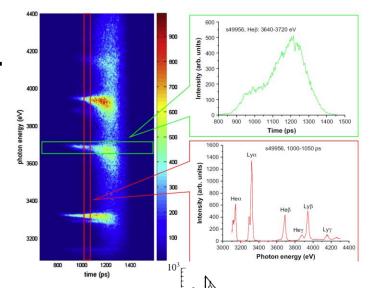

$$2d \sin \theta = m\lambda$$

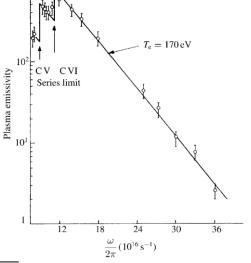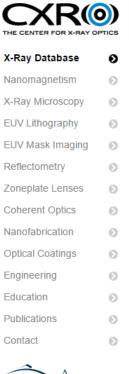# Temperature and density can be obtained from the emission

Line emission

Bremsstrahlung emission

$$\eta_\nu = \frac{16\pi}{3\sqrt{6\pi}} \frac{e^6}{m_e^2 c^3} \frac{Z_i^2 n_e}{\sqrt{k_B T_e/m_e}\, A m_p} \exp\left(-\frac{h\nu}{k_B T_e}\right)$$

R. Florido *et al.*, High Energy Dens. Phys. **6**, 70 (2010)

Information of x-ray transmission or reflectivity over a surface can be obtained from the Center for X-Ray Optics

- **http://henke.lbl.gov/optical_constants/**

CXRO
THE CENTER FOR X-RAY OPTICS

X-Ray Database
Nanomagnetism
X-Ray Microscopy
EUV Lithography
EUV Mask Imaging
Reflectometry
Zoneplate Lenses
Coherent Optics
Nanofabrication
Optical Coatings
Engineering
Education
Publications
Contact

BERKELEY LAB

The Center for X-Ray Optics is a multi-disciplined research group within Lawrence Berkeley National Laboratory's (LBNL)

X-Ray Interactions With Matter

Introduction

Access the atomic scattering factor files.
Look up x-ray properties of the elements.
The index of refraction for a compound material.
The x-ray attenuation length of a solid.
X-ray transmission
- Of a solid.
- Of a gas.
X-ray reflectivity
- Of a thick mirror.
- Of a single layer.
- Of a bilayer.
- Of a multilayer.
The diffraction efficiency of a transmission grating.
Related calculations:
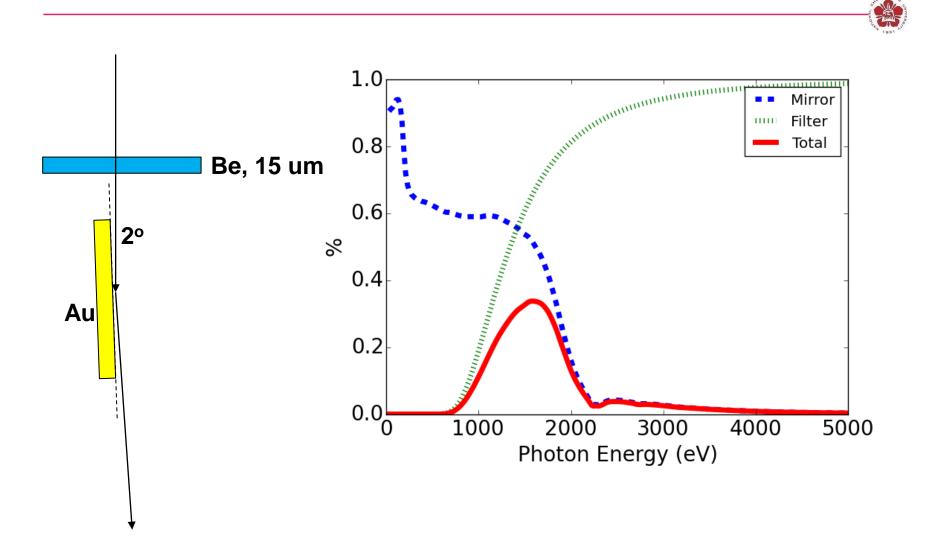- Synchrotron bend magnet radiation.

Other x-ray web resources.
X-ray Data Booklet

Reference

B.L. Henke, E.M. Gullikson, and J.C. Davis. *X-ray interactions: photoabsorption, scattering, transmission, and reflection at E=50-30000 eV, Z=1-92*, Atomic Data and Nuclear Data Tables Vol. **54** (no.2), 181-342 (July 1993).
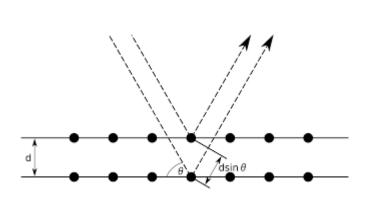
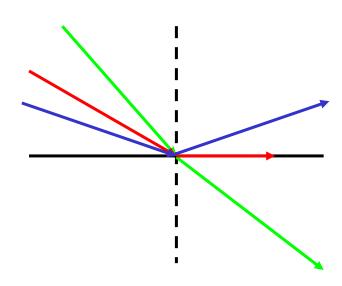# A band pass filter is obtained by combing a filter and a mirror

Be, 15 um

2°

Au

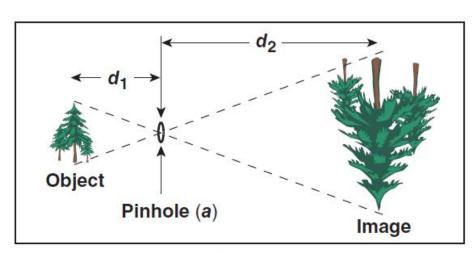# X rays can not be concentrated by lenses

- **X-ray refractive indices are less than unity,** $n \lesssim 1$

- **For those with lower refractive indices, the absorption is also strong**

- **X-ray mirrors can be made through**

  - **Bragg reflection**

  - **External total reflection with a small grazing angle**
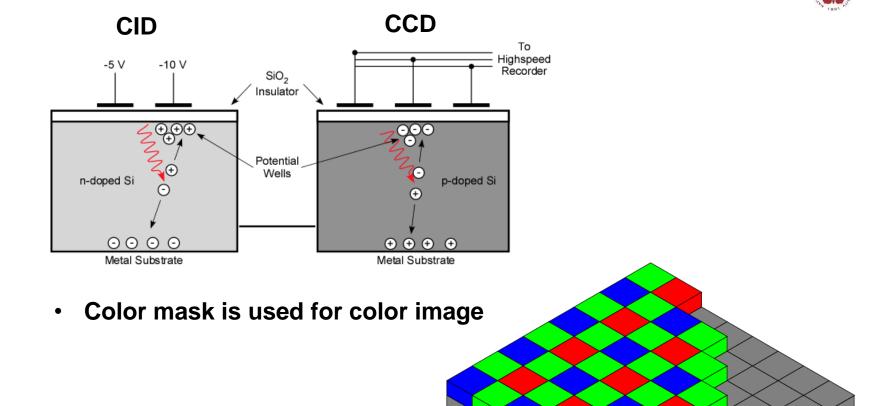
The simplest imaging device is a pinhole camera

Kodak Brownie camera

- Magnification = $\dfrac{d_2}{d_1}$

- Infinite depth of field (variable magnification)

- Pinhole diameter determines
  - resolution $\sim a$
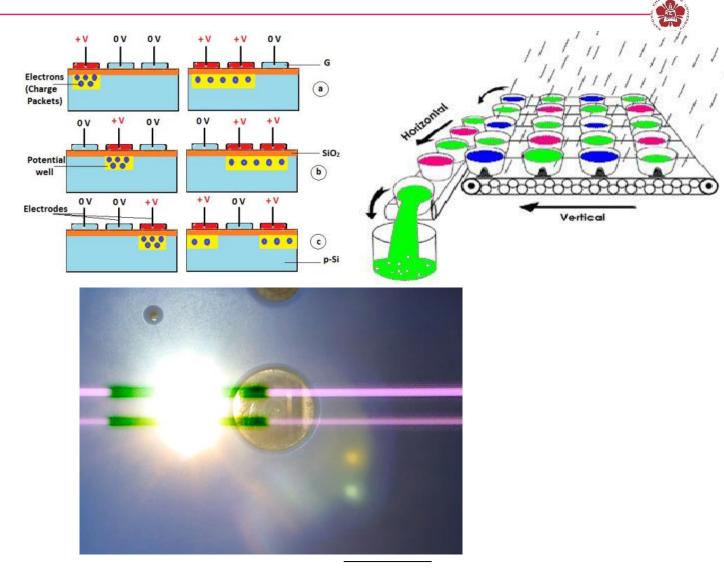 - light collection: $\Delta\Omega = \dfrac{\pi}{4}\dfrac{a^2}{d_1^2}$

Imaging optics (e.g., lenses) can be used for higher resolutions with larger solid angles.

E13982a

2D images can be taken using charge injection device (CID) or charge coupled device (CCD)

CID

CCD

-5 V   -10 V

SiO_2 Insulator

To Highspeed Recorder

Potential Wells

n-doped Si

p-doped Si

Metal Substrate

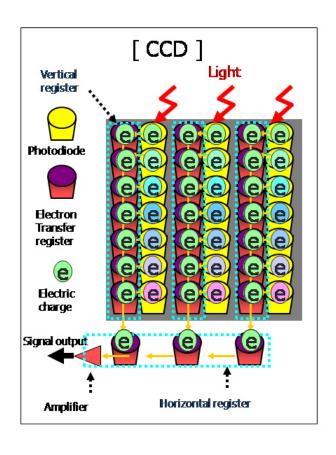Metal Substrate

- **Color mask is used for color image**
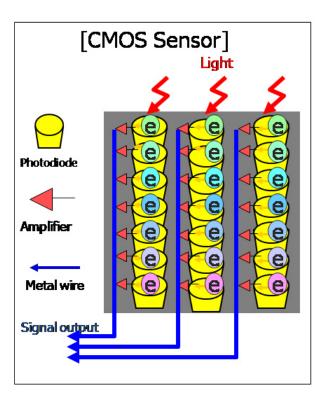
Charges are transferred along the array for readout in CCD

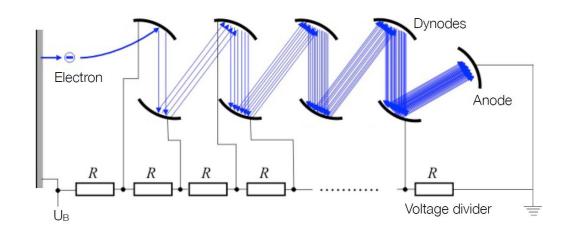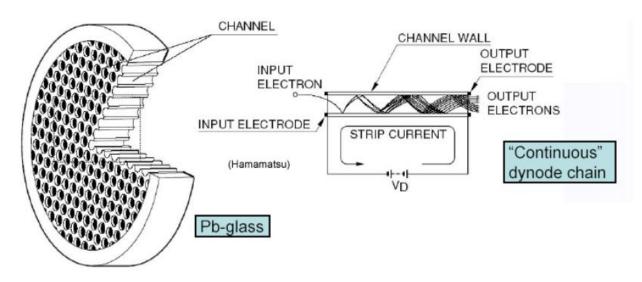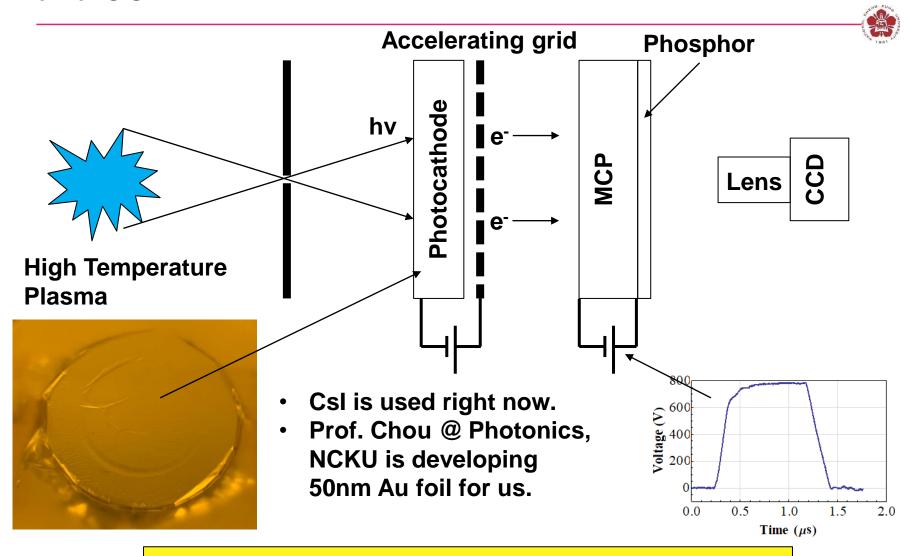**CCD readout:**

Signal is readout individually in CMOS sensor

The number of electrons can be increased through photomultipliers or microchannel plate (MCP)
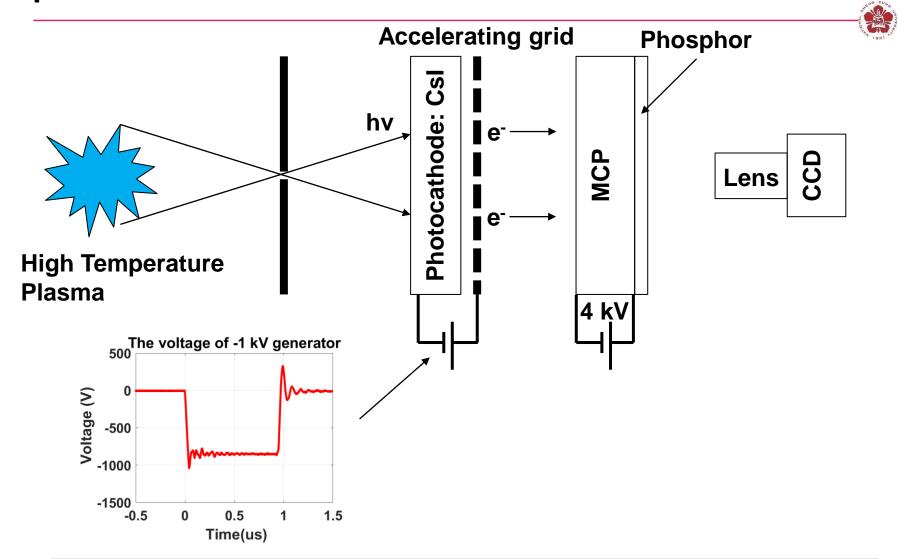

Electron / Dynodes / Anode / R R R R R / Voltage divider / U_B

CHANNEL / CHANNEL WALL / OUTPUT ELECTRODE / INPUT ELECTRON / OUTPUT ELECTRONS / INPUT ELECTRODE / STRIP CURRENT / (Hamamatsu) / V_D / "Continuous" dynode chain / Pb-glass

X-rays are imaged using photocathode, MCP, phosphor, and CCD

Accelerating grid

Phosphor

hv

Photocathode

e⁻

e⁻

MCP

Lens

CCD

High Temperature Plasma

- **CsI is used right now.**
- **Prof. Chou @ Photonics, NCKU is developing 50nm Au foil for us.**

- **Images can be gated using fast high voltage pulses.**
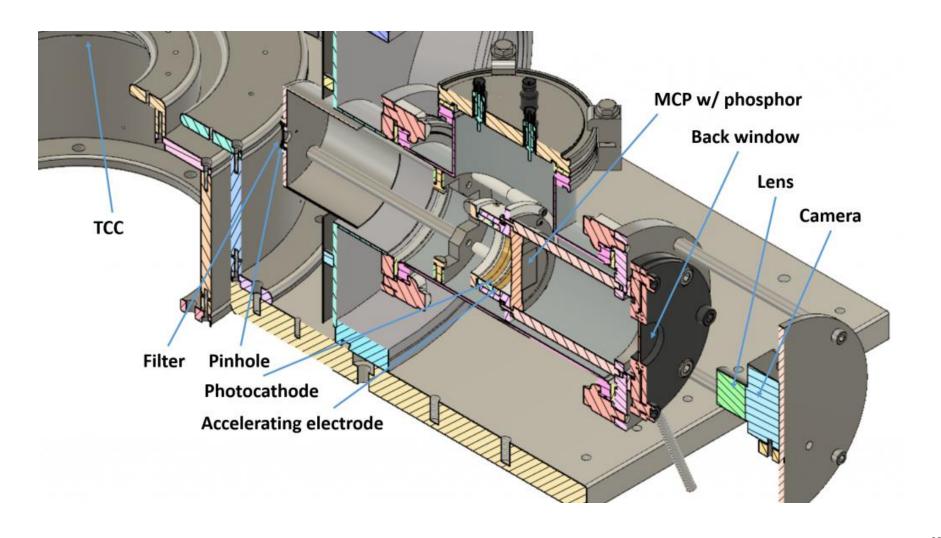
A negative high-voltage pulse is used in our x-ray pinhole camera

Accelerating grid

Phosphor

hv

Photocathode: CsI

e⁻

e⁻

MCP

Lens

CCD

High Temperature Plasma

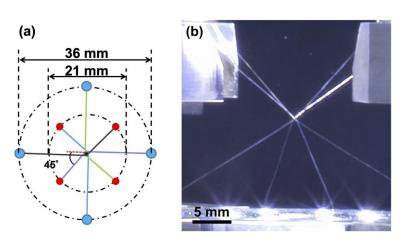4 kV

The voltage of -1 kV generator

- **The x-ray camera with a shutter opening time of ≤ 10 ns will be built.**
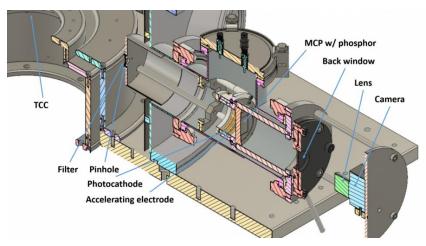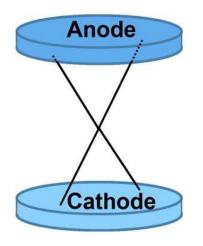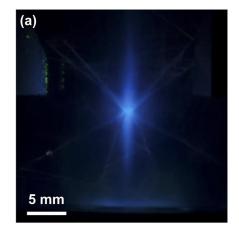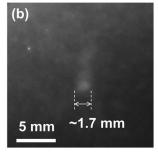
A pinhole camera was designed and was built

TCC

Filter Pinhole

Photocathode

Accelerating electrode

MCP w/ phosphor

Back window

Lens

Camera

We demonstrated using x-ray pinhole camera to capture the radiation from an imploded x pinch

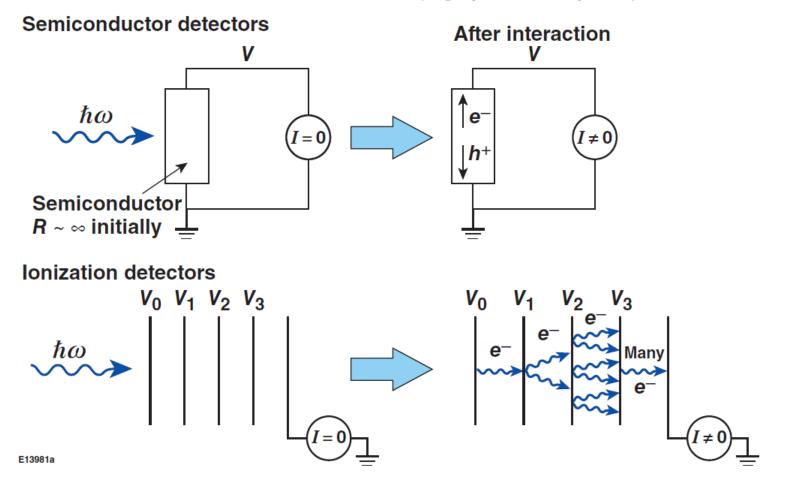P.-Y. Chang *et al.*, Rev. Sci. Instrum **93**, 043505 (2022)

Electronic detectors provide rapid readout
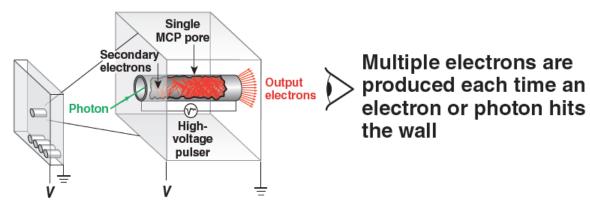
- **Electronic detectors are typically semiconductors or ionization-based stacks (e.g., photomultipliers)**

Semiconductor detectors

V

$\hbar\omega$

$I = 0$

Semiconductor
$R \sim \infty$ initially

After interaction

V

e^-

h^+

$I \neq 0$

Ionization detectors

V_0 V_1 V_2 V_3

$\hbar\omega$

$I = 0$

V_0 V_1 V_2 V_3

e^-
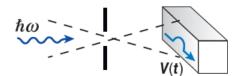
e^-

e^-

Many

e^-

$I \neq 0$

E13981a

A framing camera provides a series of time-gated 2-D images, similar to a movie camera

- The building block of a framing camera is a gated microchannel-plate (MCP) detector

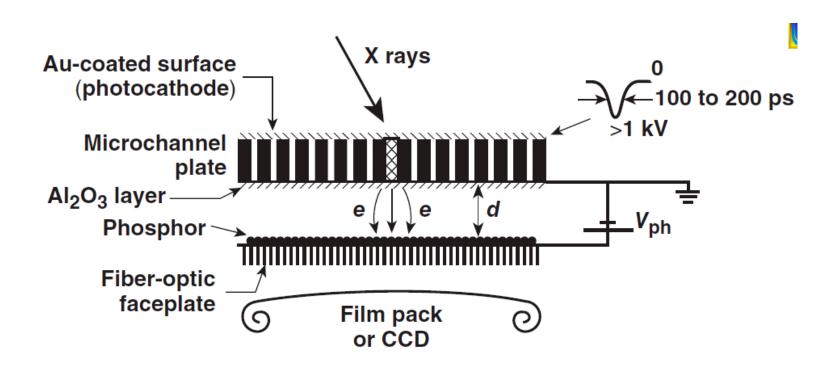- An MCP is a plate covered with small holes, each acts as a photomultiplier

Single MCP pore

Secondary electrons

Photon

Output electrons

High-voltage pulser

Multiple electrons are produced each time an electron or photon hits the wall

V   V

- A voltage pulse is sent down the plate, gating the detector

$\hbar\omega$

$V(t)$

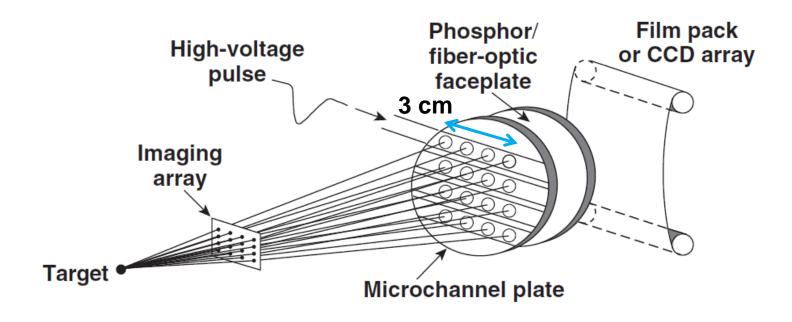The detector is only on when the voltage pulse is present

E13986b

A framing camera detector consists of a microchannel plate (MCP) in front of a phosphor screen

- Electrons are multiplied through MCP by voltage V_c

- Images are recorded on film behind phosphor

- Insulating Al_2O_3 layer allows for V_{ph} to be increased, thereby improving the spatial resolution of phosphor

E7795b

Two-dimensional time-resolved images are recorded using x-ray framing cameras
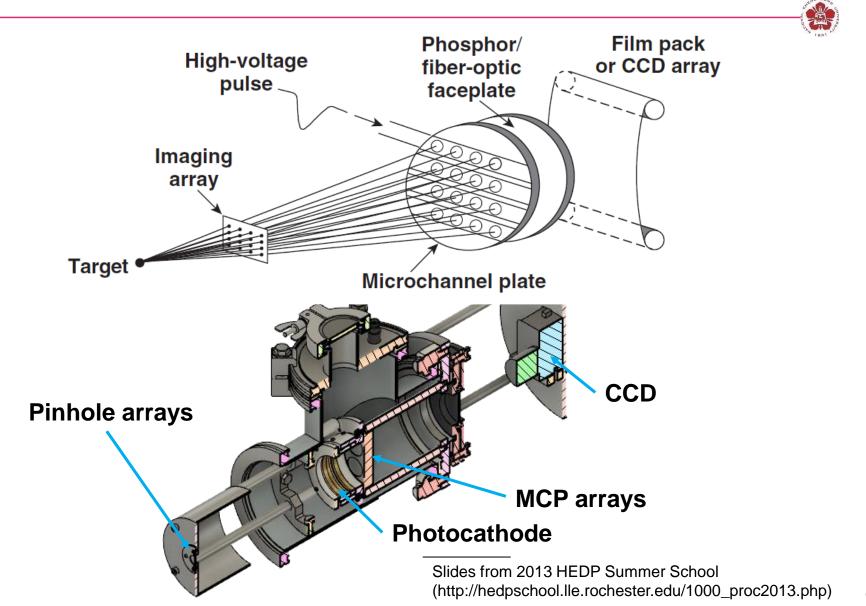

- Temporal resolution = 35 to 40 ps

- Imaging array: Pinholes: 10- to 12-μm resolution, 1 to 4 keV

- Space-resolved x-ray spectra can be obtained by using Bragg crystals and imaging slits

E7105b

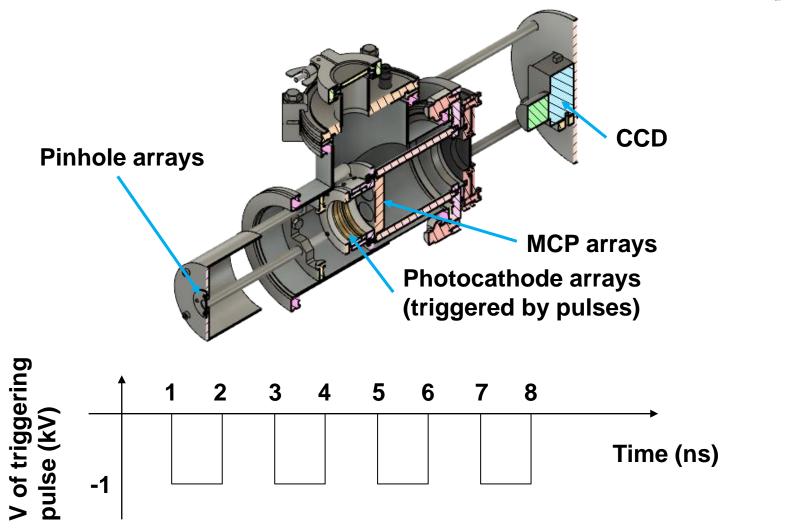$$\text{Ex:} \quad \Delta t = \frac{3 \text{ cm}/3}{3 \times 10^{10} \text{ cm/s}} = 33 \text{ ps}$$

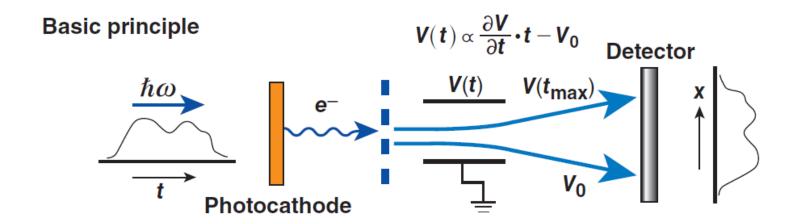# X-ray framing cameras for recording two-dimensional time-resolved images will be built by the end of 2021

Slides from 2013 HEDP Summer School
(http://hedpschool.lle.rochester.edu/1000_proc2013.php)

Each pinhole camera will be triggered separately

Pinhole arrays

CCD

MCP arrays

Photocathode arrays (triggered by pulses)

V of triggering pulse (kV)

1 2 3 4 5 6 7 8

Time (ns)

-1
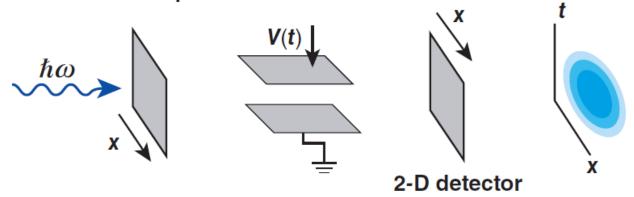
A streak camera provides temporal resolution of 1-D data

Basic principle

$$V(t) \propto \frac{\partial V}{\partial t} \cdot t - V_0$$

Detector

$\hbar\omega$

e^-

$V(t)$ $V(t_{max})$

x

Photocathode

V_0

A streak camera can provide 2-D information

$\hbar\omega$

$V(t)$

x

t

x

x

2-D detector

E13984b
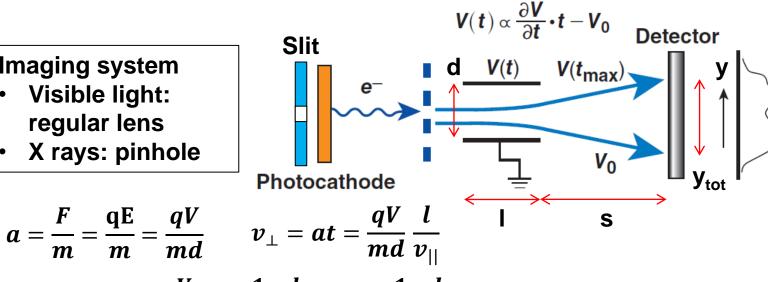
A temporal resolution higher than 15 ps is expected

Imaging system
- **Visible light: regular lens**
- **X rays: pinhole**

$$V(t) \propto \frac{\partial V}{\partial t} \cdot t - V_0$$

Slit

Detector

d $V(t)$ $V(t_{max})$ **y**

e^-

V_0

y_{tot}

Photocathode

l **s**

$$a = \frac{F}{m} = \frac{qE}{m} = \frac{qV}{md} \qquad v_\perp = at = \frac{qV}{md}\frac{l}{v_\parallel}$$

$$y = s\,\mathrm{Tan}\theta = s\frac{V_\perp}{V_\parallel} = \frac{1}{2E_k}\frac{l}{d}sqV = \frac{1}{2E_k}\frac{l}{d}sq(V_0 + V't)$$

- **Let d=10 mm, l=20 mm, s=50 mm, E_k=1 keV, V=-200 ~ 200 V**
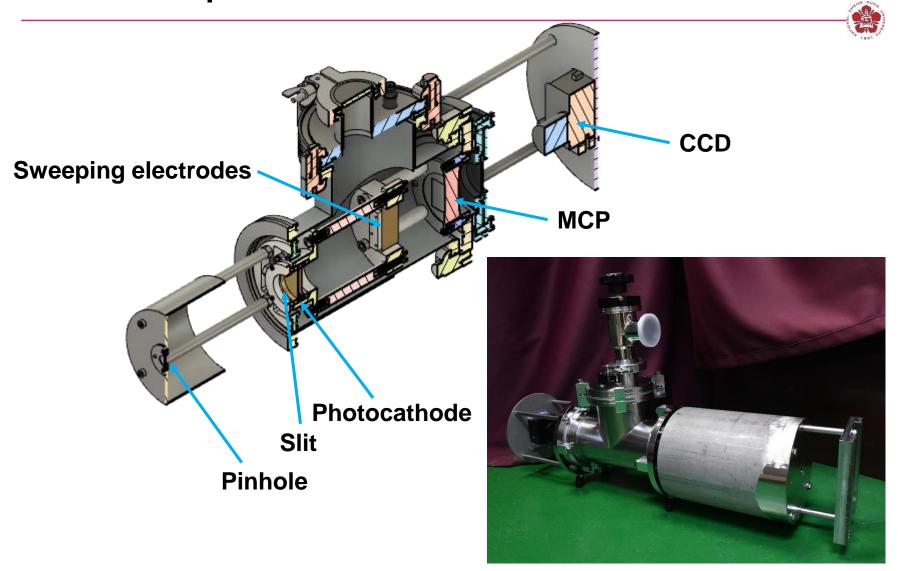
$$V' \equiv \frac{V_{tot}}{t_{tot}} = 0.06\,\mathrm{kV/ns} \qquad y_{tot} = 15\mathrm{mm} \qquad y_{tot} = 15\mathrm{mm}$$

- **Temporal resolution:**

$$\delta t = \delta y\frac{2E_k d}{lsqV'} = 15\,\mathrm{ps} \ \ \text{for} \ \ \delta y = 45\mu\mathrm{m}$$
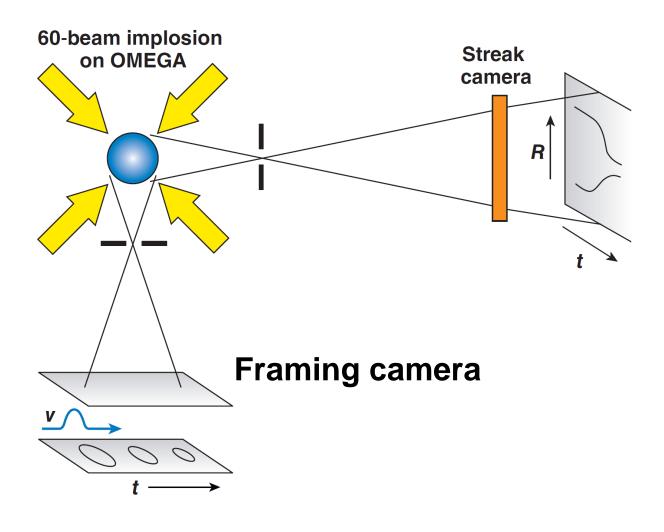
- **δt will be adjusted by changing E_k.**

A streak camera with temporal resolution of 15 ps has been developed

CCD

Sweeping electrodes

MCP

Photocathode

Slit

Pinhole

Shell trajectories can be measured using framing camera or streak camera

60-beam implosion on OMEGA

Streak camera

Framing camera
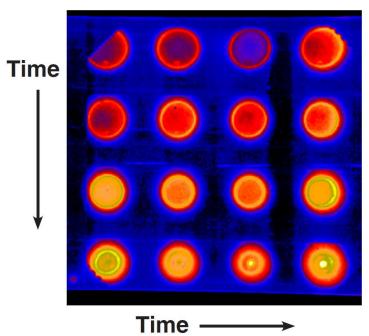
Comparison of images from framing camera versus streak camera

Framing-camera image
6× magnification

Shot 13377

Time

Time ⟶
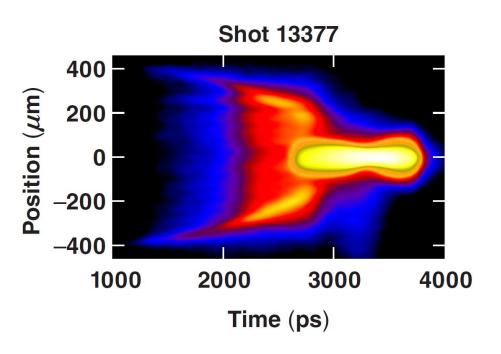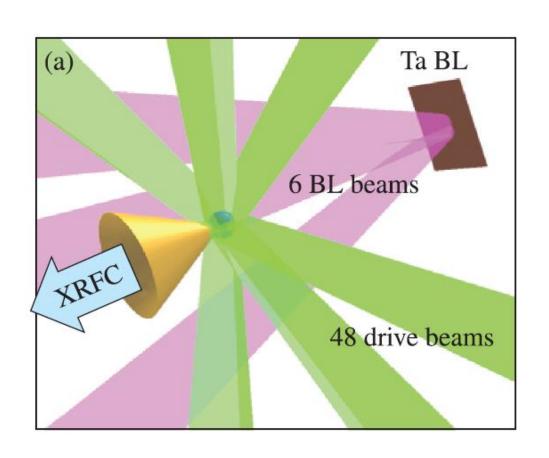
Streak-camera image

Shot 13377

The optical density can be measured using the absorption of a backlighter
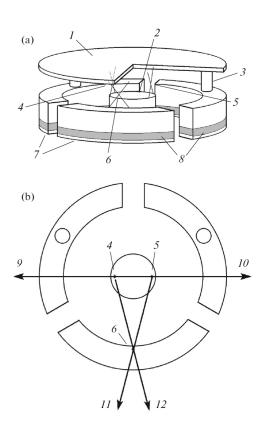
(a) Ta BL

6 BL beams

XRFC

48 drive beams

$$I = \int I(\varepsilon)\exp(-\mu(\varepsilon)\rho\delta)d\varepsilon$$

$$I = I_{\mathrm{BL}}\exp(-\bar{\mu}\rho\delta)$$

$$\ln I = \ln I_{BL} - \mu\rho r$$
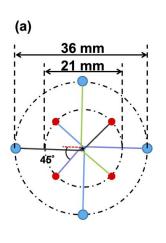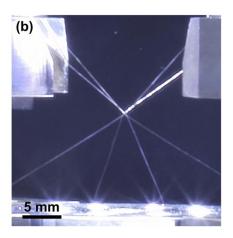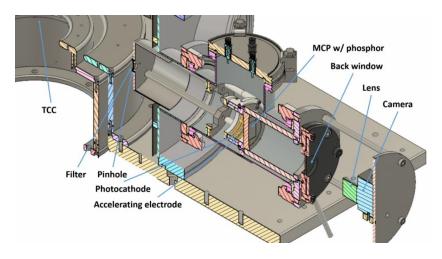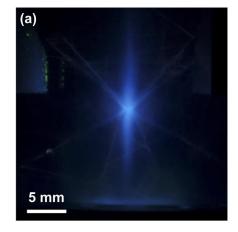
G. Fiksel *et al.*, Phys. Plasmas **19**, 062704 (2012)
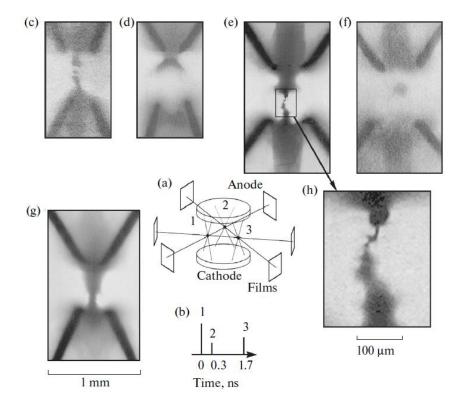
Fig. 44. X-ray radiographs obtained in the system of three parallel 2 × 12.5-μm Mo X-pinches: (a) arrangement of the pinches and films, (b) temporal positions and relative intensities of probing X-ray pulses, (c) image of X-pinch 1 in the radiation of X-pinch 2, (d) image of X-pinch 1 in the radiation of X-pinch 3, (e) image of X-pinch 2 in the radiation of X-pinch 1, (f) image of X-pinch 2 in the radiation of X-pinch 3, (g) image of X-pinch 3 in the radiation of X-pinch 1 emission, and (h) enlarged fragment of the image.
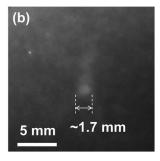
S. A. Pikuz *et al.*, Plasma Phys. Rep. **41**, 291 (2015)

We demonstrated using x-ray pinhole camera to capture the radiation from an imploded x pinch
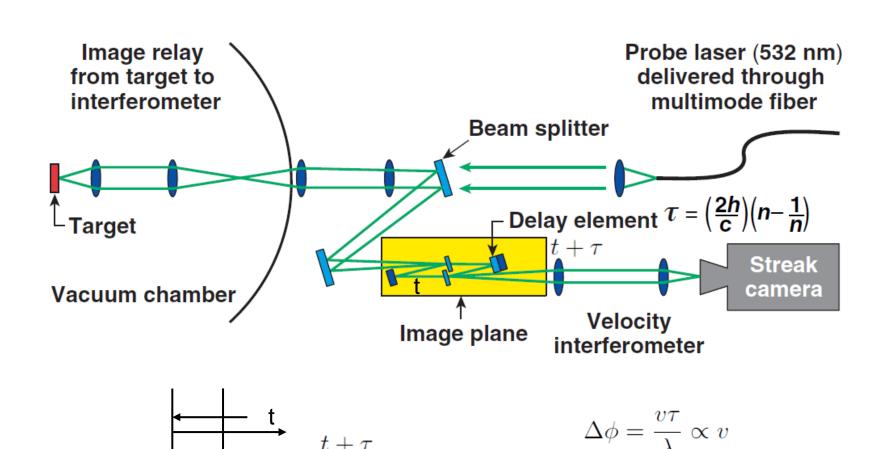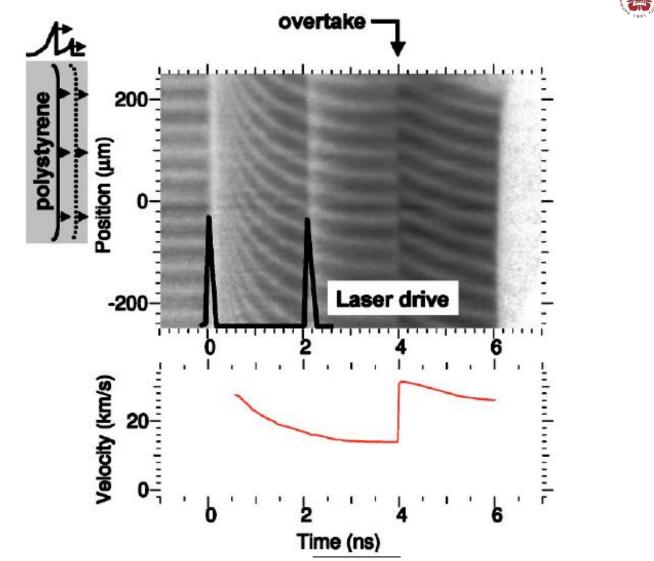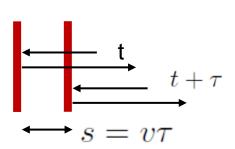

P.-Y. Chang *et al.*, Rev. Sci. Instrum **93**, 043505 (2022)

Shock velocities are measured using time-resolved Velocity Interferometer System for Any Reflector (VISAR)

Image relay from target to interferometer

Target

Vacuum chamber

Beam splitter

Probe laser (532 nm) delivered through multimode fiber

Delay element $\tau = \left(\frac{2h}{c}\right)\left(n - \frac{1}{n}\right)$

$t + \tau$

Image plane

Velocity interferometer

Streak camera

$t + \tau$

$s = v\tau$

$\Delta\phi = \frac{v\tau}{\lambda} \propto v$

http://hedpschool.lle.rochester.edu/1000_proc2013.php   78

Shock velocities are measured using time-resolved Velocity Interferometer System for Any Reflector (VISAR)

polystyrene
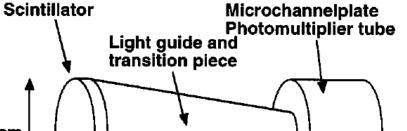
overtake

Position (µm)

Laser drive

Velocity (km/s)

Time (ns)

t

$t + \tau$

$s = v\tau$

P. M. Celliers *et al.*, Rev. Sci. Insytum. **75**, 4916 (2004)

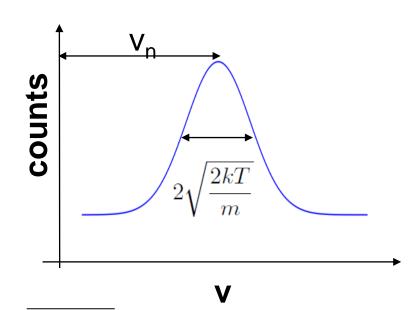# Neutron average temperature is obtained using Neutron Time of Flight (NToF)

$$D + D \longrightarrow He^3 \, (0.82 \text{ MeV}) + n \, (2.45 \text{ MeV})$$

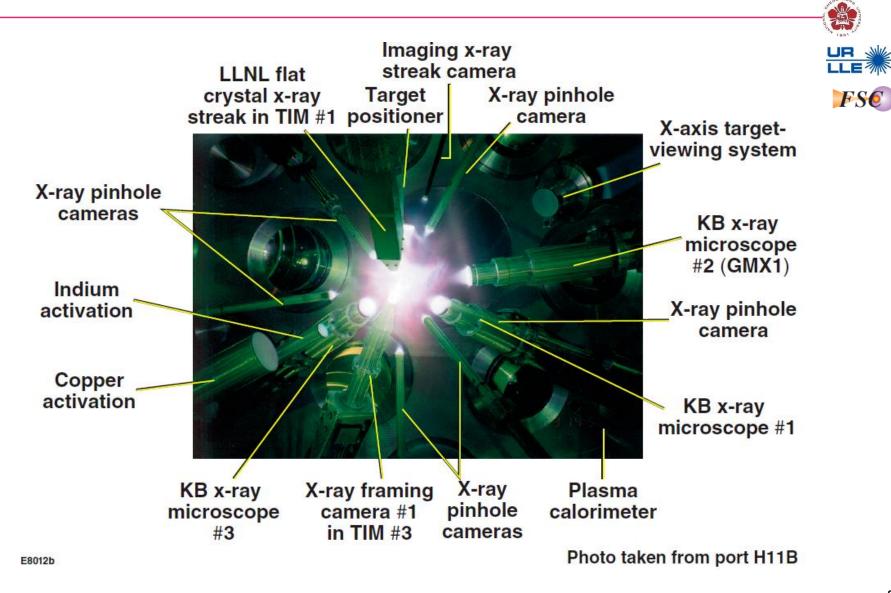$$D + T \longrightarrow He^4 \, (3.5 \text{ MeV}) + n \, (14.1 \text{ MeV})$$

$$s \;=\; vt \qquad v \;=\; \frac{s}{t}$$

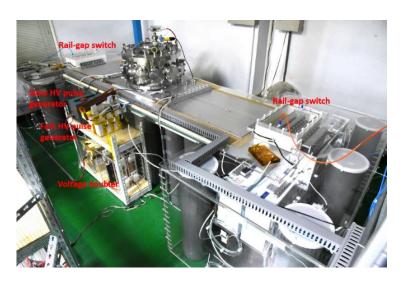$$f(v) = \sqrt{\left(\frac{m}{2\pi kT}\right)} \exp\left(-\frac{mv^2}{2kT}\right)$$

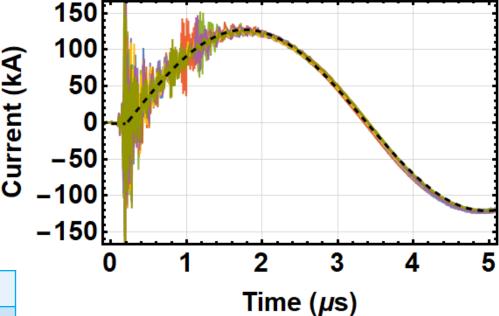T. J. Murphy *et al.*, Rev. Sci. Instrum. **72**, 773 (2001)

The OMEGA Facility is carrying out ICF experiments using a full suite of target diagnostics

Photo taken from port H11B

E8012b

A peak current of ~135 kA with a rise time of ~1.6 us is provided by the pulsed-power system
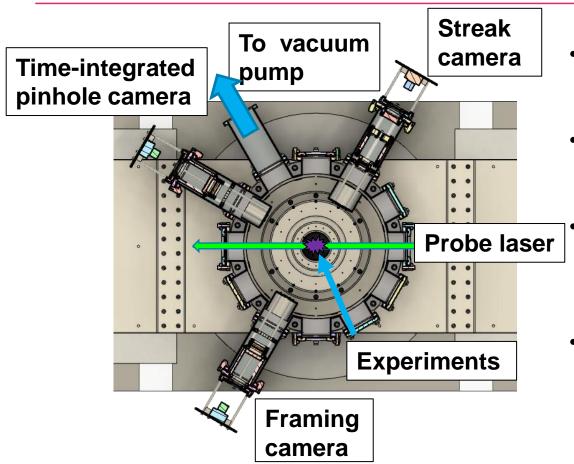
Capacitance (µF)	5
V_{charge} (kV)	20
Energy (kJ)	1
Inductance (nH)	204 $\pm$ 4
Rise time (quarter period, ns)	1592 $\pm$ 3
I_{peak} (kA)	135 $\pm$ 1

A suit of diagnostics in the range of (soft) x-ray are being built

Time-integrated pinhole camera

To vacuum pump

Streak camera

Probe laser

Experiments

Framing camera

- **Pinhole camera:**
  - **Magnification: 1x**
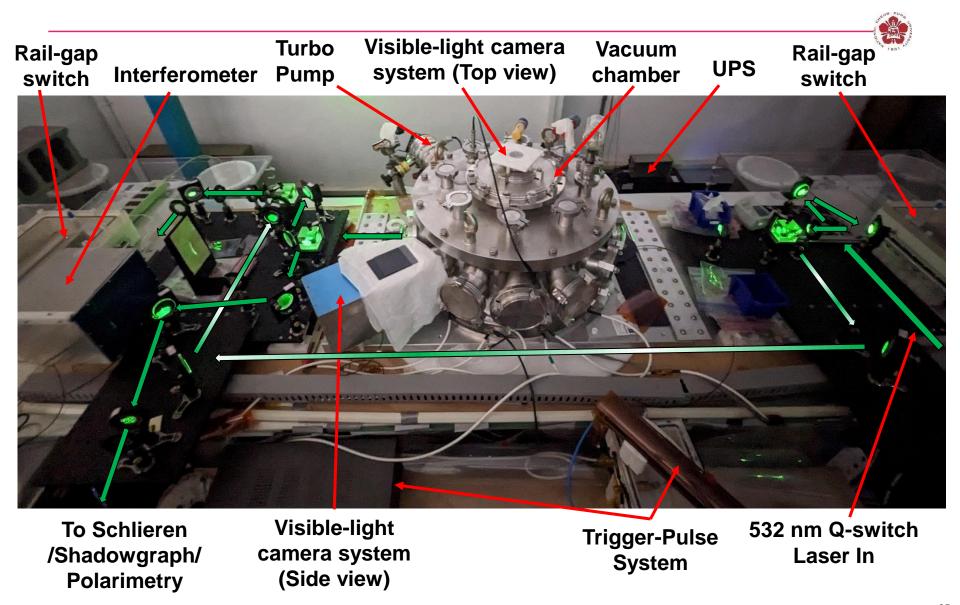 - **Exposure time: 1 us**
- **Streak camera:**
  - **Magnification: 1x**
  - **Temporal resolution: 15 ps**
- **Framing camera:**
  - **Magnification: 0.3x**
  - **Temporal resolution: ~ns using 4 individual MCPs**
- **Laser probing:**
  - **For interferometer, schlieren, shadowgraphy, Thomson scattering.**
  - **Temporal resolution: ~300 ps using stimulated brillouin scattering (SBS) pulse compression in water**
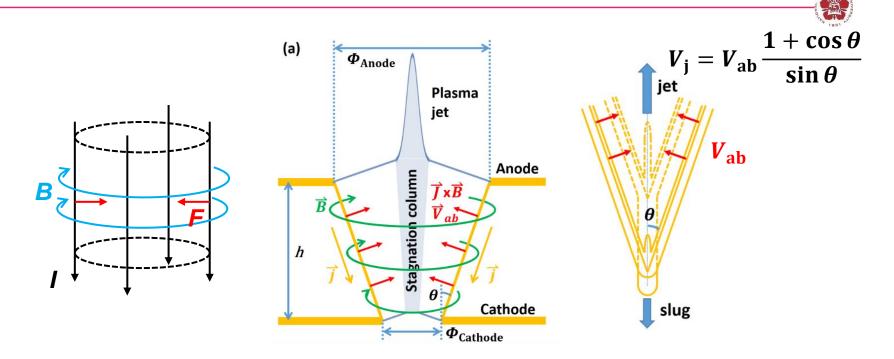
- **CsI are used as the photocathode for all x-ray imaging system.**
- **Au photocathode may be used in the future.**

Time-resolved imaging system with temporal resolution in the order of nanoseconds was implemented

Plasma edge detection

B field measurement

Density measurement

Varies diagnostics were integrated to the system

A plasma jet can be generated by a conical-wire array due to the nonuniform z-pinch effect
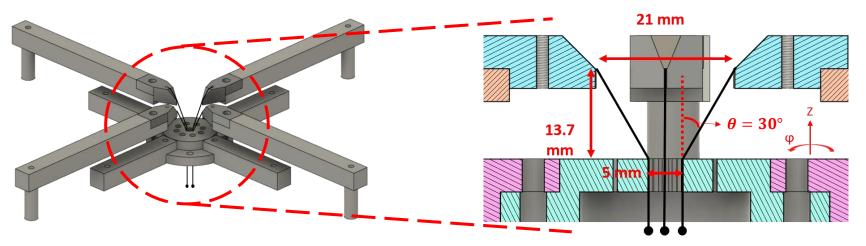

$$V_j = V_{ab} \frac{1 + \cos\theta}{\sin\theta}$$

1. Wire ablation : corona plasma is generated by wire ablations.
2. Precursor : corona plasma is pushed by the $\vec{J} \times \vec{B}$ force and accumulated on the axis forming a precursor.
3. Plasma jet is formed by the nonuniform z-pinch effect due to the radius difference between the top and the bottom of the array.
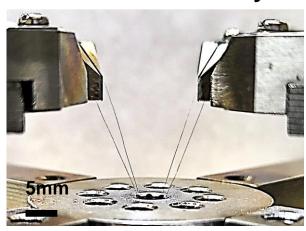
D. J. Ampleforda, et al., Phys. Plasmas 14, 102704 (2007)
G. Birkhoff, et al., J. Applied Physics 19, 563 (1948)

Our conical-wire array consists of 4 tungsten wires with an inclination angle of 30° with respect to the axis

21 mm

13.7 mm
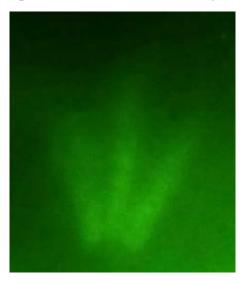
5 mm

$\theta = 30°$

Z

φ

- **Conical-wire array**

5mm

1 cm

- **Material : Tungsten.**
- **Number of wires : 4.**
- **Diameter : 20 μm.**

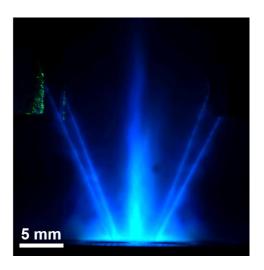# Self-emission of the plasma jet in the UV to soft x-ray regions was captured by the pinhole camera

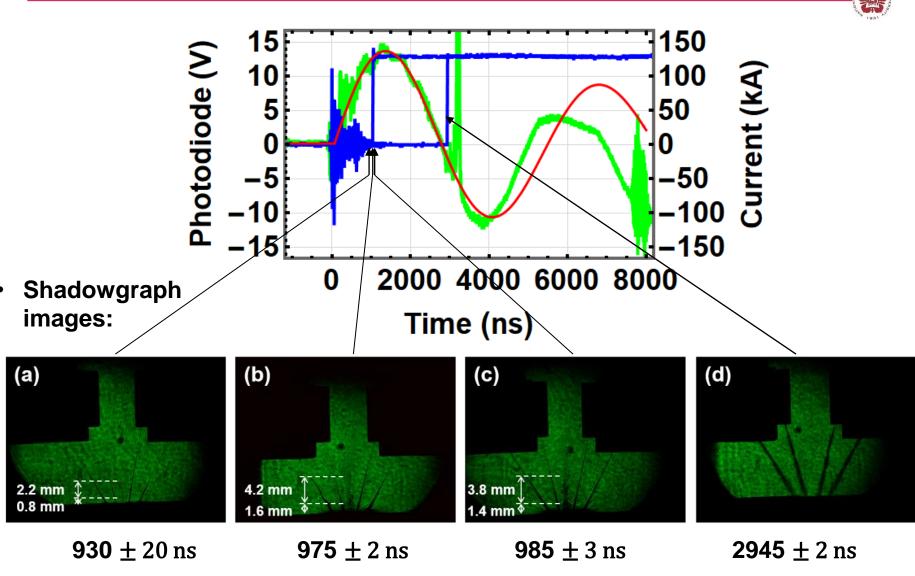- **Image in UV/soft x ray**

(Brightness is increased by 40 %.)

- **Pinhole diameter: 0.5 mm, i.e., spatial resolution: 1 mm.**
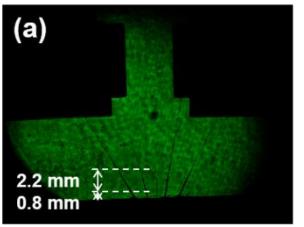
- **Image in visible light**

5 mm

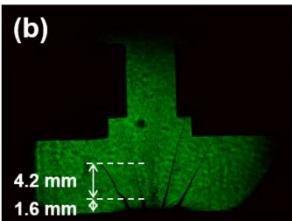**(Enhanced by scaling the intensity range linearly from 0 − 64 to 0 − 255.)**

Plasma jet propagation was observed using laser diagnostics

- **Shadowgraph images:**

(a) 2.2 mm / 0.8 mm — **930 ± 20 ns**

(b) 4.2 mm / 1.6 mm — **975 ± 2 ns**
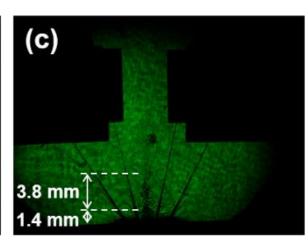
(c) 3.8 mm / 1.4 mm — **985 ± 3 ns**

(d) — **2945 ± 2 ns**

Length of the plasma jet at different time was obtained by the Schlieren images at different times

- **Shadowgraph images:**

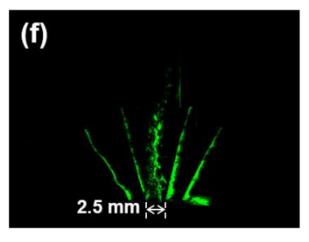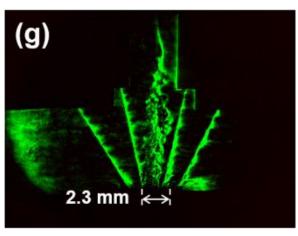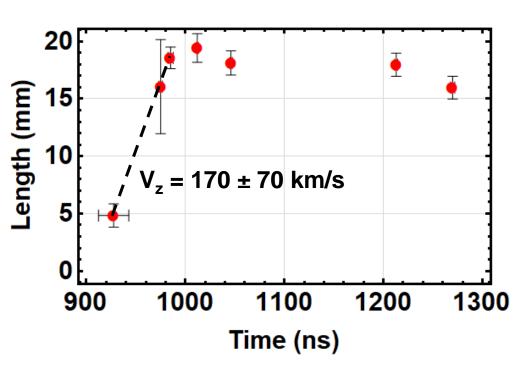(a) 2.2 mm / 0.8 mm (b) 4.2 mm / 1.6 mm (c) 3.8 mm / 1.4 mm

- **Schlieren images:**

(e) 1.8 mm (f) 2.5 mm (g) 2.3 mm
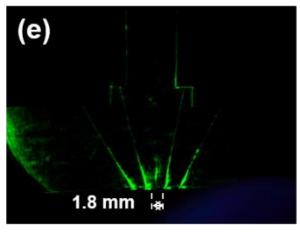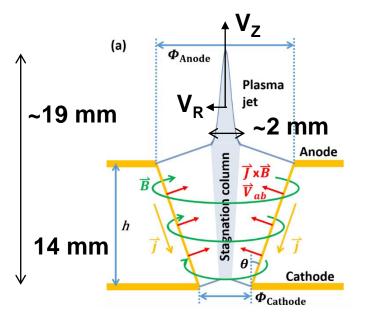
930 $\pm$ 20 ns   **975 $\pm$ 2 ns**   **985 $\pm$ 3 ns**

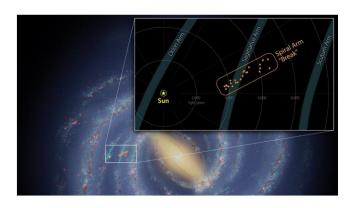# The measured plasma jet speed is 170 ± 70 km/s with the corresponding Mach number greater than 5
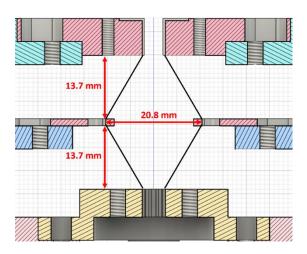
$$M = \frac{V_Z}{V_R} \geq \frac{Z}{r} \approx \frac{(19 - 14)\ \text{mm}}{\dfrac{2\ \text{mm}}{2}} = 5$$

$$V_{ab} = V_j \frac{\sin\theta}{1 + \cos\theta} = 50 \pm 20\ \text{km/s}$$
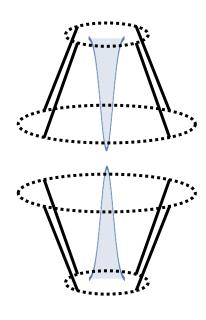
Plasma disk can be formed when two head-on plasma jets collide with each other

- **Astronomers Find a 'Break' in One of the Milky Way's Spiral Arms.**

Plasma disk can be formed when two head-on plasma jets collide with each other
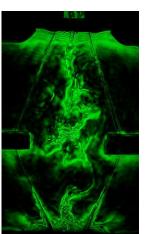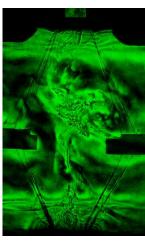
Schlieren

Interferometer
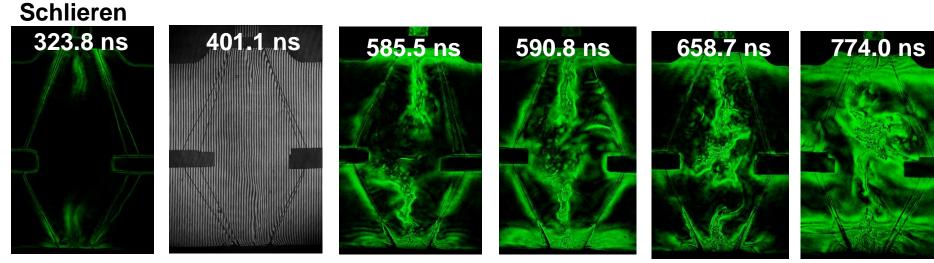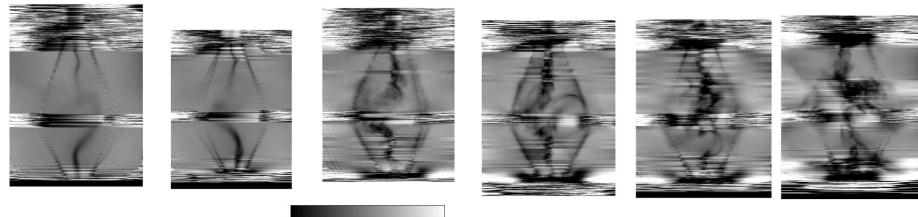
323.8 ns   506.2 ns   585.5 ns   590.8 ns   658.7 ns   774.0 ns

Plasma disk can be formed when two head-on plasma jets collide with each other

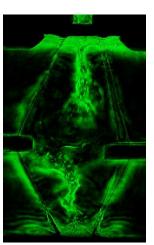**Schlieren**

323.8 ns   401.1 ns   585.5 ns   590.8 ns   658.7 ns   774.0 ns
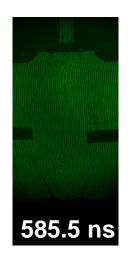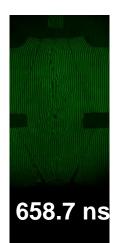
Interferometer $-2\pi \sim 2\pi \Rightarrow 0 \sim 4.2 \times 10^{17}$ cm^{-2} $\Rightarrow 8.4 \times 10^{17}$ cm^{-3} for l= 5mm

-6 -4 -2 0 2 4 6 Φ(rad)

Energetic charged particles losses most of its energy right before it stops

Momentum transfer:

$$\Delta p_\perp = \int F_\perp \, dt = \int F_\perp \frac{dt}{dx} dx = \int F_\perp \frac{dx}{v}$$
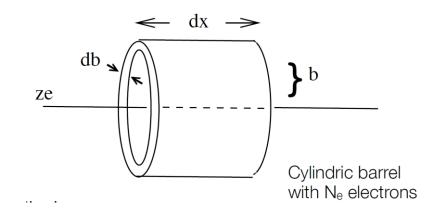
$$= \int_{-\infty}^{\infty} \frac{ze^2}{(x^2 + b^2)} \cdot \frac{b}{\sqrt{x^2 + b^2}} \cdot \frac{1}{v} \, dx = \frac{ze^2 b}{v} \left[\frac{x}{b^2 \sqrt{x^2 + b^2}} \right]_{-\infty}^{\infty} = \frac{2ze^2}{bv}$$

$\Delta p_\parallel$: averages to zero

$$\Delta E(b) = \frac{\Delta p^2}{2 m_e} \qquad N_e = n \cdot (2\pi b) \cdot db \, dx$$

$$-dE(b) = \frac{\Delta p^2}{2 m_e} \cdot 2\pi n b \, db \, dx$$

Cylindric barrel with N_e electrons
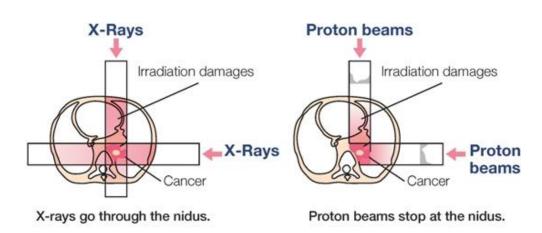
$$-\frac{dE}{dx} = \frac{4\pi \, n \, z^2 e^4}{m_e v^2} \cdot \int_{b_{min}}^{b_{max}} \frac{db}{b} = \frac{4\pi \, n \, z^2 e^4}{m_e v^2} \ln \frac{b_{max}}{b_{min}}$$

Proton therapy takes the advantage of using Bragg peak

Energy Loss of Alphas of 5.49 MeV in Air
(Stopping Power of Air for Alphas of 5.49 MeV)

X-rays go through the nidus.

Proton beams stop at the nidus.

http://www.shi.co.jp/quantum/eng/product/proton/proton.html

There are two suggested website for getting the information of proton stopping power in different materials

http://www.nist.gov/pml/data/star/

http://www.srim.org/

The thickness of a filter can be decided from the range data from NIST website

COPPER

To download data in spreadsheet (array) form, choose a delimiter and use the checkboxes in the table heading. After downloading, save the output by using your browser's Save As feature.

Delimiter:
- ● space
- ○ | (vertical bar)
- ○ tab (some browsers may use spaces instead)
- ○ newline

Download data Reset

$$\frac{dE}{\rho dx} \qquad \rho x$$

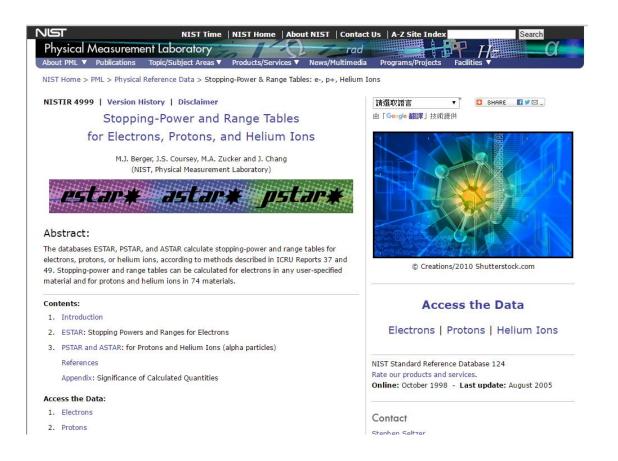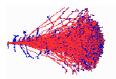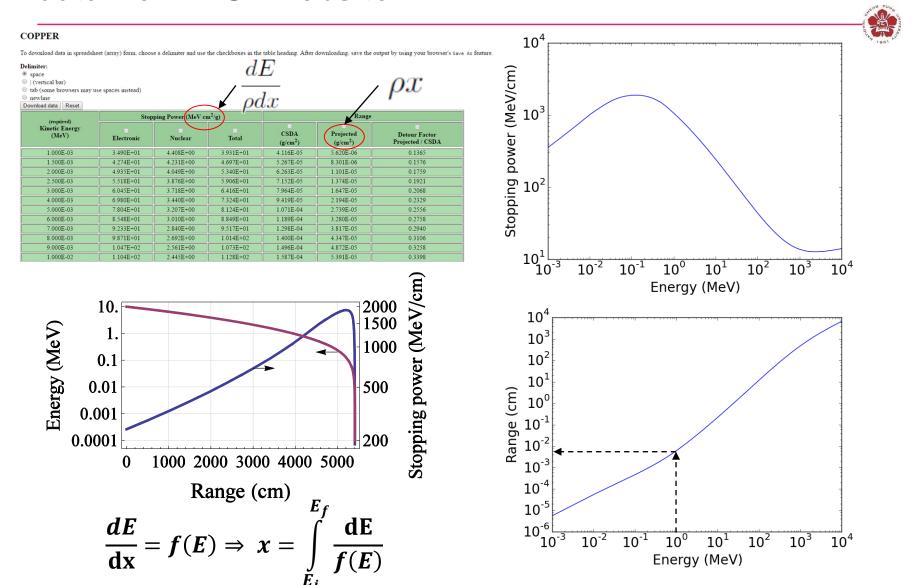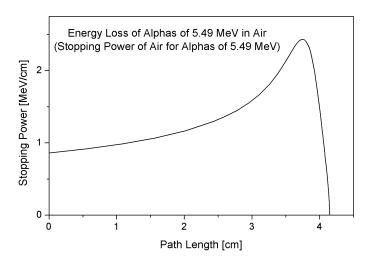| (required) Kinetic Energy (MeV)	Stopping Power (MeV cm²/g)			Range		
	Electronic	Nuclear	Total	CSDA (g/cm²)	Projected (g/cm²)	Detour Factor Projected / CSDA
1.000E-03	3.490E+01	4.408E+00	3.931E+01	4.116E-05	5.620E-06	0.1365
1.500E-03	4.274E+01	4.231E+00	4.697E+01	5.267E-05	8.301E-06	0.1576
2.000E-03	4.935E+01	4.049E+00	5.340E+01	6.263E-05	1.101E-05	0.1759
2.500E-03	5.518E+01	3.876E+00	5.906E+01	7.152E-05	1.374E-05	0.1921
3.000E-03	6.045E+01	3.718E+00	6.416E+01	7.964E-05	1.647E-05	0.2068
4.000E-03	6.980E+01	3.440E+00	7.324E+01	9.419E-05	2.194E-05	0.2329
5.000E-03	7.804E+01	3.207E+00	8.124E+01	1.071E-04	2.739E-05	0.2556
6.000E-03	8.548E+01	3.010E+00	8.849E+01	1.189E-04	3.280E-05	0.2758
7.000E-03	9.233E+01	2.840E+00	9.517E+01	1.298E-04	3.817E-05	0.2940
8.000E-03	9.871E+01	2.692E+00	1.014E+02	1.400E-04	4.347E-05	0.3106
9.000E-03	1.047E+02	2.561E+00	1.073E+02	1.496E-04	4.872E-05	0.3258
1.000E-02	1.104E+02	2.445E+00	1.128E+02	1.587E-04	5.391E-05	0.3398

$$\frac{dE}{dx} = f(E) \Rightarrow x = \int_{E_i}^{E_f} \frac{dE}{f(E)}$$

Proton therapy takes the advantage of using Bragg peak

Energy Loss of Alphas of 5.49 MeV in Air
(Stopping Power of Air for Alphas of 5.49 MeV)

X-rays go through the nidus.

Proton beams stop at the nidus.

Saha equation gives the relative proportions of atoms of a certain species that are in two different states of ionization in thermal equilibrium

$$\frac{n_{r+1}n_e}{n_r} = \frac{G_{r+1}g_e}{G_r}\frac{(2\pi m_e KT)^{3/2}}{h^3}\exp\left(-\frac{\chi_r}{KT}\right)$$

- n_{r+1}, n_r: Density of atoms in ionization state r+1, r (m^{-3})

- n_e: Density of electrons (m^{-3})

- G_{r+1}, G_r: Partition function of ionization state r+1, r

- g_e=2: Statistical weight of the electron

- m_e: Mass of the electron

- χ_r: Ionization potential of ground level of state r to reach to the ground level of state r+1

- T: Temperature

- h: Planck's constant

- K: Boltzmann constant

Supplement to Ch. 6 of Astrophysics Processes by Hale Bradt
(http://homepages.spa.umn.edu/~kd/Ast4001-2015/NOTES/n052-saha-bradt.pdf)

Some backgrounds of quantum mechanics

- **Planck blackbody function:**

$$u(v, T) = \frac{8\pi h v^3}{c^3} \frac{1}{e^{hv/KT} - 1} \left(W/m^3 \text{ Hz}\right)$$

- **Boltzmann formula:**

  - **g_i, g_j: statistical weight**

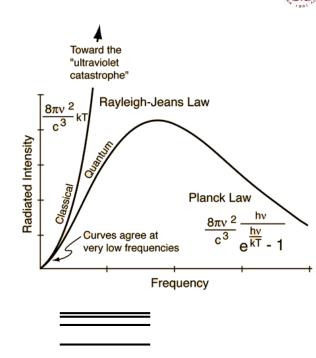$$\frac{n_i}{n_j} = \frac{g_i e^{-\epsilon_i/KT}}{g_j e^{-\epsilon_j/KT}} = \frac{g_i}{g_j} e^{-hv_{ij}/KT} \qquad \frac{g_i}{g_j} = \frac{2J_i + 1}{2J_j + 1}$$
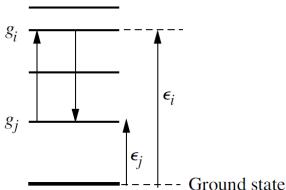
  (J: angular momenta quantum number)

  - **Number in the ith state to the total atom:**

$$\frac{n_i}{n} = \frac{n_i}{\Sigma n_j} \equiv \frac{g_i e^{-\epsilon_i/KT}}{G} \qquad G \equiv \Sigma g_j e^{-\epsilon_j/KT}$$

  G: partition function of statistical weight for the atom, taking into account all its excited states.

Toward the "ultraviolet catastrophe"

Rayleigh-Jeans Law

$\frac{8\pi v^2}{c^3} kT$

Radiated Intensity

Classical

Quantum

Curves agree at very low frequencies

Planck Law

$\frac{8\pi v^2}{c^3} \frac{hv}{e^{\frac{hv}{kT}} - 1}$

Frequency

g_i

g_j

ϵ_i

ϵ_j

Ground state

Einstein coefficient

- **Probability of electron energy transition:**
    - **Excitation (↑):** $P_{\mathrm{ji}} = B_{\mathrm{ji}} u(\nu, T)$
    - **De-excitation (↓):** $P_{\mathrm{ij}} = A_{\mathrm{ij}} + B_{\mathrm{ij}} u(\nu, T)$
- **In thermal equilibrium:**

$$n_i(A_{\mathrm{ij}} + B_{\mathrm{ij}} u) = n_j B_{\mathrm{ji}} u$$

$$\frac{g_i}{g_j} e^{-x}(A_{\mathrm{ij}} + B_{\mathrm{ij}} u) = B_{\mathrm{ji}} u$$

$$x \equiv \frac{h\nu}{KT}$$

$$u = a(e^x - 1)^{-1}$$

$$a \equiv \frac{8\pi h\nu^3}{c^3}$$
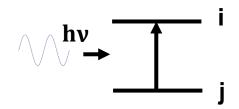
$$a\left(e^x B_{\mathrm{ji}} - \frac{g_i}{g_j} B_{\mathrm{ij}}\right) = (e^x - 1)\frac{g_i}{g_j} A_{\mathrm{ij}}$$

- **The Einstein coefficients are independent of T or ν.**

$$x \to 0, e^x \to 1$$

$$x \to \infty, e^x \to \infty$$
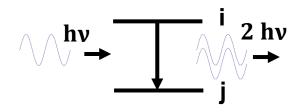
$$\frac{B_{\mathrm{ij}}}{B_{\mathrm{ji}}} = \frac{g_j}{g_i}$$

$$aB_{\mathrm{ji}} = \frac{g_i}{g_j} A_{\mathrm{ij}} \qquad \frac{A_{\mathrm{ij}}}{B_{\mathrm{ij}}} = \frac{8\pi h\nu^3}{c^3}$$
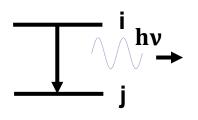
- **Photoexcitation:**

- **Induced radiation:**

- **Spontaneous radiation:**

Saha equation is derived using the transition between different ionization states
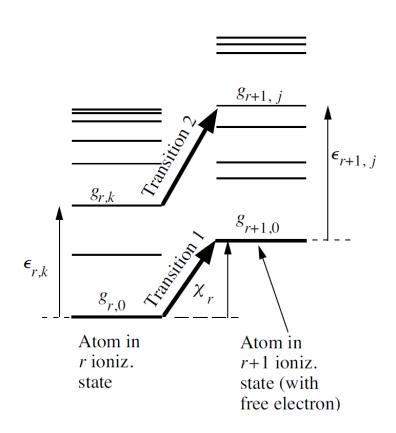
- **Required photon energy for transition 1 from the ground state of r ionization state to the ground state of r+1 ionization state:**

$$h\nu = \chi_r + \frac{p^2}{2m}$$

Energy of the free electron

- **Required photon energy for transition 2 from the energy level k of r ionization state to the energy level j of r+1 ionization state:**

$$h\nu = \chi_r + \epsilon_{r+1,j} - \epsilon_{r,k} + \frac{p^2}{2m}$$

Saha equation is derived using the transition between different ionization states

- **Photoionization:**

$$R_{\text{pi}} = n_{r,k} u(\nu) B_{r,k \to r+1,j}$$

- **Induced radiation:**

$$R_{\text{ir}} = n_{r+1,j} n_{e,p}(p) u(\nu) B_{r+1,j \to r,k}$$

- **Spontaneous emission:**
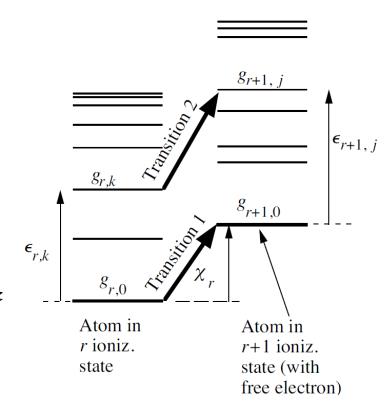
$$R_{\text{sr}} = n_{r+1,j} n_{e,p}(p) A_{r+1,j \to r,k}$$

- **In thermal equilibrium:**

$$n_{r+1,j} n_{e,p} A_{r+1,j \to r,k} + n_{r+1,j} n_{e,p} u B_{r+1,j \to r,k}$$
$$= n_{r,k} u B_{r,k \to r+1,j}$$

- **Einstein coefficients:**

$$\frac{B_{r,k \to r+1,j}}{B_{r+1,j \to r,k}} = \frac{g_{r+1,j}}{g_{r,k}} \frac{g_e 4\pi p^2}{h^3} \qquad \frac{A_{r+1,j \to r,k}}{B_{r+1,j \to r,k}} = \frac{8\pi h \nu^3}{c^3}$$

Atom in r ioniz. state

Atom in $r+1$ ioniz. state (with free electron)

Saha equation - continued

$$n_{r+1,j}n_{e,p}A_{r+1,j\to r,k} + n_{r+1,j}n_{e,p}uB_{r+1,j\to r,k} = n_{r,k}uB_{r,k\to r+1,j}$$

$$n_{r+1,j}n_{e,p}\frac{A_{r+1,j\to r,k}}{B_{r+1,j\to r,k}} + n_{r+1,j}n_{e,p}u = n_{r,k}u\frac{B_{r,k\to r+1,j}}{B_{r+1,j\to r,k}}$$

$$\frac{n_{r+1,j}n_{e,p}}{n_{r,k}} = \left(\frac{A_{r+1,j\to r,k}}{uB_{r+1,j\to r,k}} + 1\right)^{-1}\frac{B_{r,k\to r+1,j}}{B_{r+1,j\to r,k}} \qquad \frac{B_{r,k\to r+1,j}}{B_{r+1,j\to r,k}} = \frac{g_{r+1,j}}{g_{r,k}}\frac{g_e 4\pi p^2}{h^3}$$

$$n_{e,p}(p) = \frac{n_e 4\pi p^2}{(2\pi mKT)^{3/2}}\exp\left(-\frac{p^2}{2mKT}\right) \qquad \frac{A_{r+1,j\to r,k}}{B_{r+1,j\to r,k}} = \frac{8\pi h\nu^3}{c^3}$$

$$\frac{n_{r+1,j}n_e}{n_{r,k}} = \frac{(2\pi mKT)^{3/2}}{4\pi p^2}\exp\left(\frac{p^2}{2mKT}\right)\left[\frac{c^3}{8\pi h\nu^3}\left(e^{h\nu/KT}-1\right)\frac{8\pi h\nu^3}{c^3}+1\right]^{-1}\frac{g_{r+1,j}}{g_{r,k}}\frac{g_e 4\pi p^2}{h^3}$$

$$\frac{n_{r+1,j}n_e}{n_{r,k}} = \frac{(2\pi mKT)^{3/2}}{h^3}\frac{g_{r+1,j}g_e}{g_{r,k}}\exp\left[\frac{1}{KT}\left(\frac{p^2}{2m}-h\nu\right)\right]$$

Saha equation - continued

$$\frac{n_{r+1,j}n_e}{n_{r,k}} = \frac{(2\pi mKT)^{3/2}}{h^3} \frac{g_{r+1,j}g_e}{g_{r,k}} \exp\left[\frac{1}{KT}\left(\frac{p^2}{2m} - h\nu\right)\right]$$

$$\frac{n_{r+1,j}n_e}{n_{r,k}} = \frac{(2\pi mKT)^{3/2}}{h^3} \frac{g_{r+1,j}g_e}{g_{r,k}} \exp\left[\frac{1}{KT}\left(\frac{p^2}{2m} - \chi_r - \epsilon_{r+1,j} + \epsilon_{r,k} - \frac{p^2}{2m}\right)\right]$$

$$\frac{n_{r+1,j}n_e}{n_{r,k}} = \frac{(2\pi mKT)^{3/2}}{h^3} \frac{g_{r+1,j}\exp\left(\frac{\epsilon_{r+1,j}}{KT}\right)g_e}{g_{r,k}\exp\left(\frac{\epsilon_{r,k}}{KT}\right)} \exp\left(-\frac{\chi_r}{KT}\right)$$

$$\frac{n_{r,k}}{n_r} = \frac{g_{r,k}e^{-\epsilon_{r,k}/KT}}{G_r} \qquad\qquad G_r = \Sigma g_{r,k}e^{-\epsilon_{r,k}/KT}$$

$$\frac{n_{r+1,j}}{n_{r+1}} = \frac{g_{r+1,j}e^{-\epsilon_{r+1,j}/KT}}{G_{r+1}} \qquad\qquad G_{r+1} = \Sigma g_{r+1,j}e^{-\epsilon_{r+1,j}/KT}$$

$$\frac{n_{r+1}n_e}{n_r} = \frac{G_{r+1}g_e}{G_r} \frac{(2\pi m_eKT)^{3/2}}{h^3} \exp\left(-\frac{\chi_r}{KT}\right)$$

Saha equation – example: hydrogen plasma of the sun

- **Photosphere of the sun – hydrogen atoms in an optically thick gas in thermal equilibrium at temperature T=6400 K.**

    – **Neutral hydrogen (r state / ground state)**

    $$G_r = \Sigma g_{r,k} = g_{r,0} + g_{r,1}\exp\left(-\frac{\epsilon_{r,1}}{KT}\right) + \cdots = 2 + 8\exp\left(-\frac{10.2\text{eV}}{0.56\text{eV}}\right) + \cdots$$

    $$= 2 + 9.8 \times 10^{-8} + \cdots \approx 2$$

    – **Ionized state (r+1 state)**

    $$G_{r+1} = \Sigma g_{r+1,j} = g_{r+1,0} + g_{r+1,1}\exp\left(-\frac{\epsilon_{r+1,1}}{KT}\right) + \cdots \approx 1$$

    – **Other information:** $\quad g_e = 2 \qquad \chi_r = 13.6\text{eV}; KT = 0.56\text{eV} \qquad n_{r+1} = n_e$

    $$\frac{n_{r+1}^2}{n_r} = 2.41 \times 10^{21}\frac{1 \times 2}{2}(6400)^{3/2}\exp\left(-\frac{13.6}{0.56}\right) = 3.5 \times 10^{16}m^{-3}$$

It is mostly neutral in the photosphere of the sun

- **Assuming 50 % ionization:**

$$n_{r+1} = n_r = 3.5 \times 10^{16} m^{-3} \qquad n = n_{r+1} + n_r = 7 \times 10^{16} m^{-3}$$

- **At lower densities n at the same temperature, there should be fewer collisions leading to recombination and thus the plasma to be more than 50 % ionization.**

- **In the photosphere of the sun:**
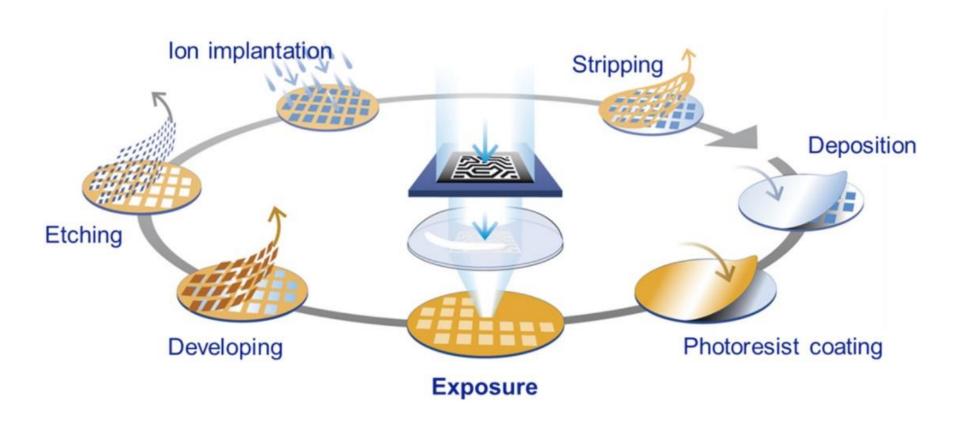
$$\rho \sim 3 \times 10^{-4} \, \text{kg}/m^3 \to n = 2 \times 10^{23} m^{-3} \gg 7 \times 10^{16} m^{-3}$$

   $\Rightarrow$ **Less than 50 % ionization**

- **Use the total number density to estimate the ionization percentage:**

$$n_{r+1} + n_r = 2 \times 10^{23}$$

$$\frac{n_{r+1}}{n_r} = 4 \times 10^{-4} @ 6400K$$

A semiconductor device is fabricated by many repetitive production process

Ion implantation

Stripping

Deposition

Etching

Developing

Exposure

Photoresist coating
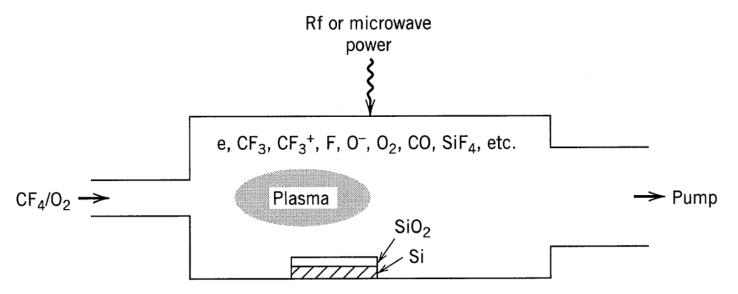
Reference for material processing

- **Principles of plasma discharges and materials processing, 2nd edition, by Michael A. Lieberman and Allan J. Lichtenberg**

- **http://www.eecs.berkeley.edu/~lieber/**

- **Materials science of thin films, 2nd edition, by Milton Ohring**

- **Plasma etching, by Dennis M. Manos and Daniel L. Flamm**

- **Industrial plasma engineering, volume 1, by J. Reece Roth**
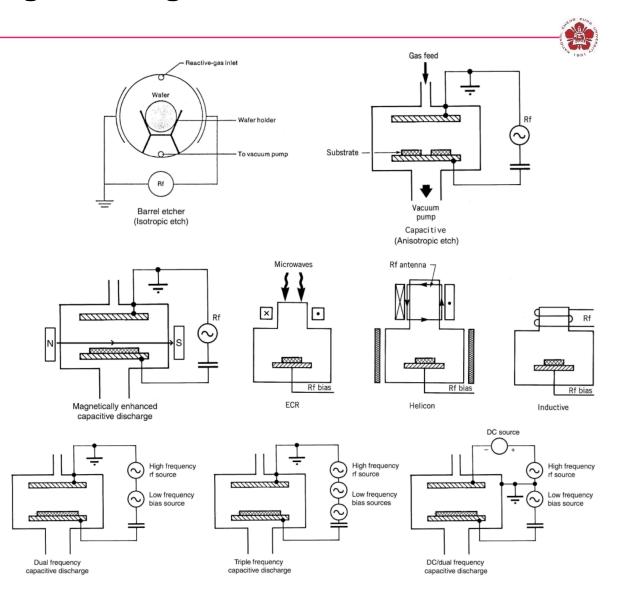
Evolution of etching discharges

1st generation
(1 source, multi-wafer, low density)

2nd generation
(2 sources, single-wafer, high density)

3rd generation
(multi-sources, single-wafer, moderate density)
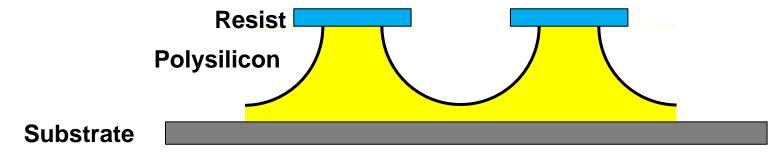
There are two types of etching: isotropic vs anistropic

- **Isotropic etching**

Resist

Polysilicon

Substrate

- **Anisotropic etching**

Resist
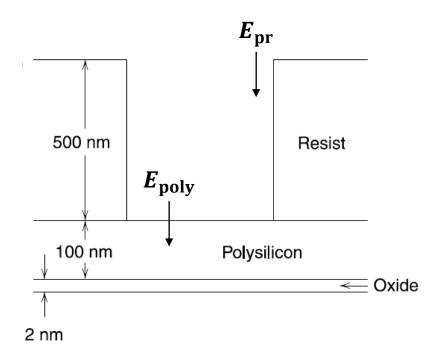
Polysilicon

Substrate

Plasma etch requirements – etch rate
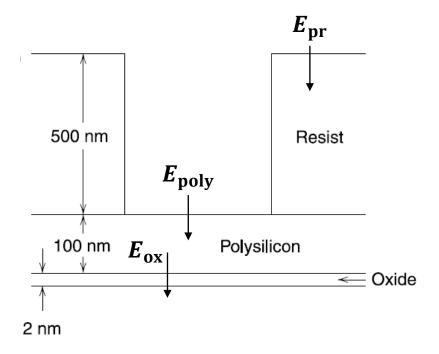
- **Etch time needs to be within a few minutes:**

$$E_{pr} \geq 250 \, nm/min$$

$$E_{poly} \geq 50 \, nm/min$$

Principles of plasma discharges and materials processing, 2nd edition, by Michael A. Lieberman and Allan J. Lichtenberg

Plasma etch requirements - selectivity

- **Selectivity between polysilicon and resist:**
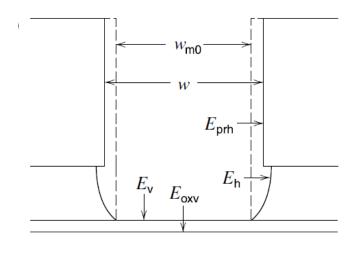
$$s = \frac{E_{\text{poly}} \triangle t}{E_{\text{pr}} \triangle t} >> \frac{100\text{nm}}{500\text{nm}} = 0.2$$
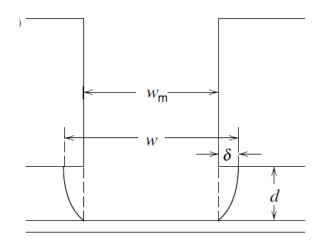
- **Assuming 20% non-uniformity on the wafer:**

$$s = \frac{E_{\text{poly}} \triangle t}{E_{ox} \triangle t} >> \frac{20\% \times 100\text{nm}}{2\text{nm}} = 10$$

Principles of plasma discharges and materials processing, 2nd edition, by Michael A. Lieberman and Allan J. Lichtenberg

Plasma etch requirements – Anisotropy

- **Anisotropy**

$$a_h = \frac{E_v}{E_h} = \frac{d}{\delta}$$

$$w = w_m + 2\delta$$
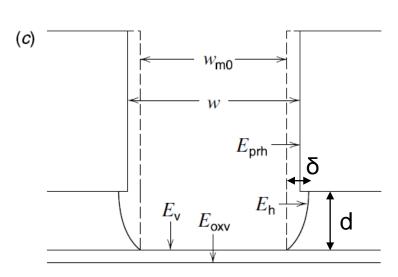
$$a_h \geq \frac{2d}{w - w_m}$$

- **The smallest feature size where $w_m = 0$:**

$$w \approx \frac{2d}{a_h}$$

Principles of plasma discharges and materials processing, 2nd edition, by Michael A. Lieberman and Allan J. Lichtenberg

# Plasma etch requirements – Anisotropy including etching on photoresist
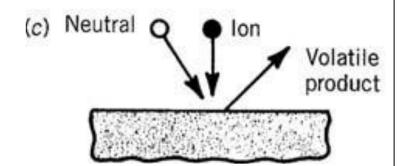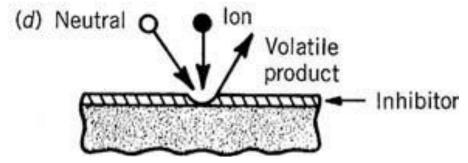

$$a_h^{-1} \equiv \frac{E_h}{E_v}$$

$$\left(\frac{\delta}{d} > 0.1\right)$$

$$\left(\frac{\delta}{d} < 0.1\right)$$

$$\frac{E_{prh}}{E_v} \equiv s_{pr}^{-1}$$
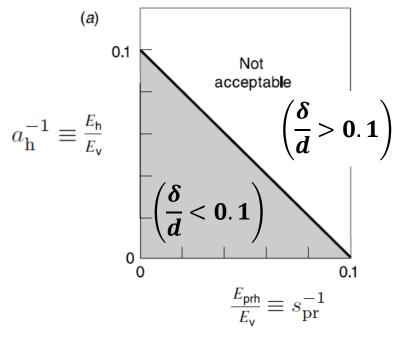
$$\delta \approx (E_h + E_{prh})\, t$$

$$t = \frac{d}{E_v}$$

$$\delta \approx d\frac{E_h + E_{prh}}{E_v}$$

$$\frac{E_h + E_{prh}}{E_v} \approx \frac{\delta}{d}$$
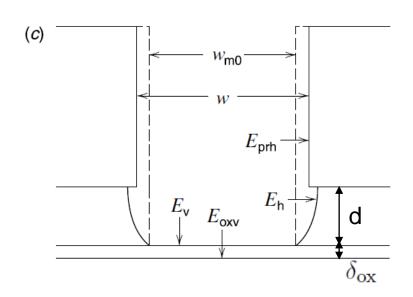
$$\frac{E_h}{E_V} + \frac{E_{prh}}{E_V} = a_h^{-1} + s_{pr}^{-1} \approx \frac{\delta}{d} \equiv 0.1$$

- The contribution of the horizontal etching is from both E_h and E_{prh}.

Plasma etch requirements – Uniformity on selectivity and anisotropy
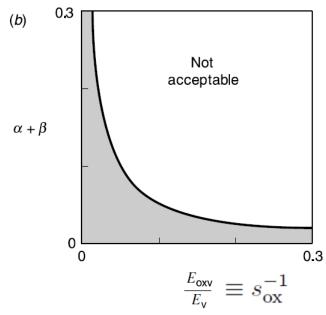
$$d \to d(1 \pm \alpha) \qquad E_v \to E_v(1 \pm \beta)$$

where α, β are variations.

$$t_{\max} = \frac{d(1 + \alpha)}{E_v(1 - \beta)} \approx \frac{d}{E_v}(1 + \alpha + \beta)$$

$$t_{\min} = \frac{d(1 - \alpha)}{E_v(1 + \beta)} \approx \frac{d}{E_v}(1 - \alpha - \beta)$$

$$\delta_{ox} = (t_{\max} - t_{\min})E_{oxv}$$

$$= \frac{d}{E_v}2(\alpha + \beta)E_{oxv}$$
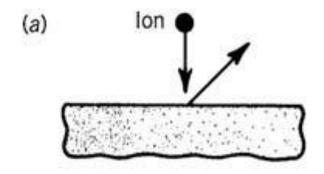
$$2(\alpha + \beta)\frac{E_{oxv}}{E_v} = \frac{\delta_{ox}}{d}$$

Principles of plasma discharges and materials processing, 2nd edition, by Michael A. Lieberman and Allan J. Lichtenberg

117
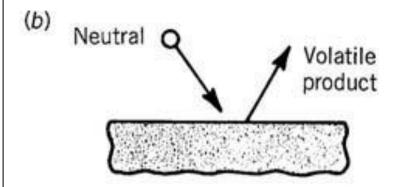
There are four major plasma etching mechanisms

- **Sputtering**

- **Pure chemical etching**

- **Ion energy-driven etching**

- **Ion-enhanced inhibitor etching**
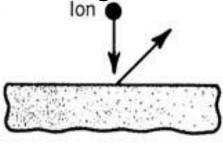
Principles of plasma discharges and materials processing, 2nd edition, by Michael A. Lieberman and Allan J. Lichtenberg

Sputtering is an unselective but anisotropic process
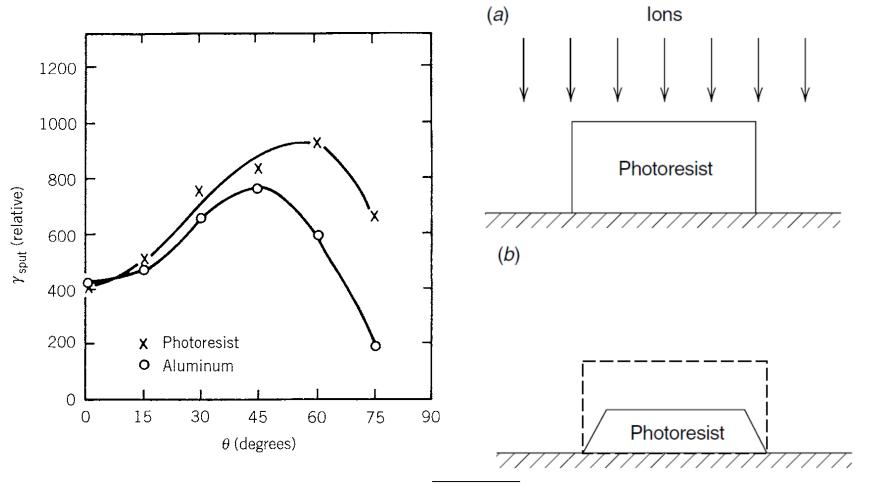
- **Unselective process.**

- **Anisotropic process, strongly sensitive to the angle of incidence of the ion.**

- **Sputtering rates of different materials are roughly the same.**

- **Sputtering rates are generally low because the yield is typically of order one atom per incident ion.**

- **Sputtering is the only one of the four etch processes that can remove nonvolatile products from a surface.**

- **The process is generally under low pressure since the mean free path of the sputtered atoms must be large enough to prevent redeposition on the substrate or target.**

Ion

Principles of plasma discharges and materials processing, 2nd edition, by Michael A. Lieberman and Allan J. Lichtenberg

Topographical patterns might not be faithfully transferred during sputter etching

Principles of plasma discharges and materials processing, 2nd edition, by Michael A. Lieberman and Allan J. Lichtenberg
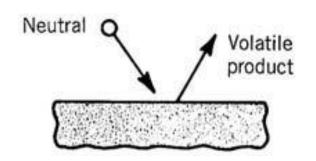
Atoms or molecules chemically react with the surface to form gas-phase products

- **Highly chemically selective, e.g.,**

$$Si(s) + 4F \longrightarrow SiF_4(g)$$
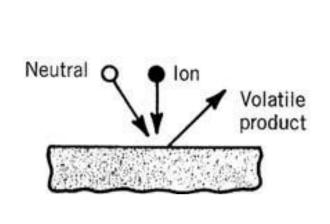
$$photoresist + O(g) \longrightarrow CO_2(g) + H_2O(g)$$
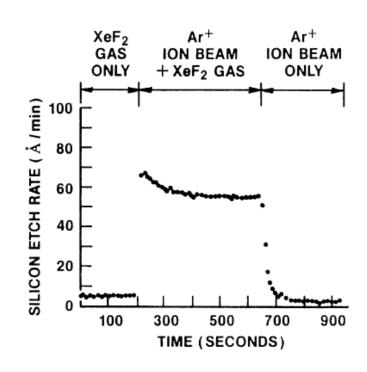
- **Almost invariably isotropic.**

- **Etch products must be volatile.**

- **The etch rate can be quite large.**

- **Etch rate are generally not limited by the rate of arrival of etchant atoms, but by one of a complex set of reactions at the surface leading to formation of etch products.**

The discharge supplies both etchants and energetic ions to the surface

Neutral ○   ● Ion

Volatile product

XeF$_2$ GAS ONLY | Ar$^+$ ION BEAM + XeF$_2$ GAS | Ar$^+$ ION BEAM ONLY

SILICON ETCH RATE (Å / min)

100
80
60
40
20
0

100   300   500   700   900

TIME (SECONDS)

- **Low chemical etch rate of silicon substrate in XeF2 etchant gas.**

- **Tenfold increase in etch rate with XeF$_2$ + 500 V argon ions, simulating ion-enhanced plasma etching.**

- **Very low "etch rate" due to the physical sputtering of silicon by ion bombardment alone.**

Plasma etching, by Daniel L. Flamm and G. Kenneth Herb

Ion-enhanced energy-driven etching has the characteristic of both sputtering and pure chemical etching
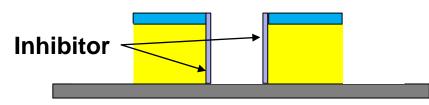
- **Chemical in nature but with a reaction rate determined by the energetic ion bombardment.**

- **Product must be volatile.**

- **Highly anisotropic.**

Ion-enhanced inhibitor etching

An inhibitor species is used

- **Inhibitor precursor molecules that absorb or deposit on the substrate form a protective layer or polymer film.**

- **Etchant is chosen to produce a high chemical etch rate of the substrate in the absence of either ion bombardment or the inhibitor.**

- **Ion bombardment flux prevents the inhibitor layer from forming or clears it as it forms.**

- **Where the ion flux does not fall, the inhibitor protects the surface from the etchant.**

- **May not be as selective as pure chemical etching.**

- **A volatile etch product must be formed.**

- **Contamination of the substrate and final removal of the protective inhibitor film are other issues.**

Inhibitor

Comparison of different processes

	Sputtering etching	Pure chemical etching	Ion energy-driven etching	Ion-enhanced Inhibitor etching
Selectivity	X	O	O	O
Anisotropic	O	X	O	O
Volatile product	X	O	O	O

TABLE 15.1. Etch Chemistries Based on Product Volatility

Material	Etchant Atoms
Si, Ge	F, Cl, Br
SiO_2	F, F + C
Si_3N_4, silicides	F
Al	Cl, Br
Cu	Cl ($T > 210°C$)
C, organics	O
W, Ta, Ti, Mo, Nb	F, Cl
Au	Cl
Cr	Cl, Cl + O
GaAs	Cl, Br
InP	Cl, C + H

Deposition and implementation
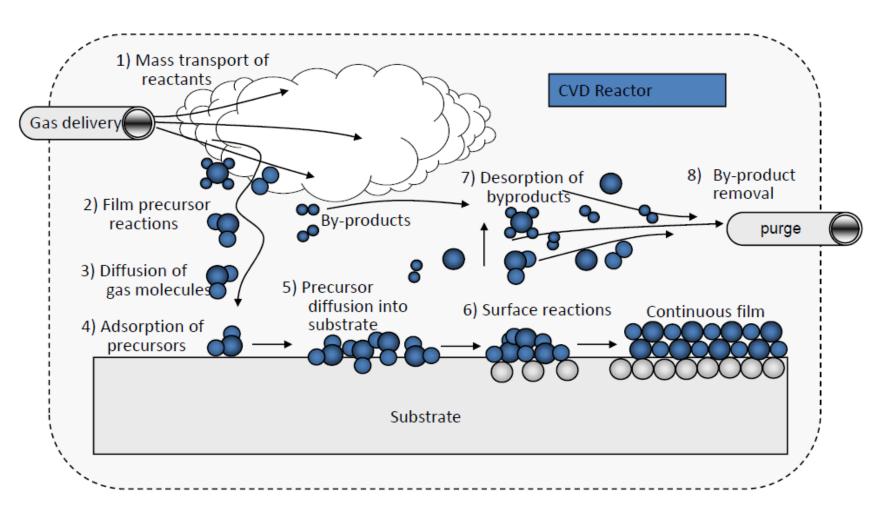
- **Plasma-assisted deposition, implantation, and surface modification are important material processes for producing films on surfaces and modifying their properties**

- **Example processes:**

  - **Plasma-enhanced chemical vapor deposition (PECVD)**

  - **Sputter deposition / physical vapor deposition (PVD)**

  - **Plasma-immersion ion implantation (PIII)**

Chemical Vapor Deposition (CVD)

1) Mass transport of reactants

CVD Reactor

Gas delivery

2) Film precursor reactions

By-products

7) Desorption of byproducts

8) By-product removal

purge

3) Diffusion of gas molecules

5) Precursor diffusion into substrate

6) Surface reactions

Continuous film

4) Adsorption of precursors

Substrate
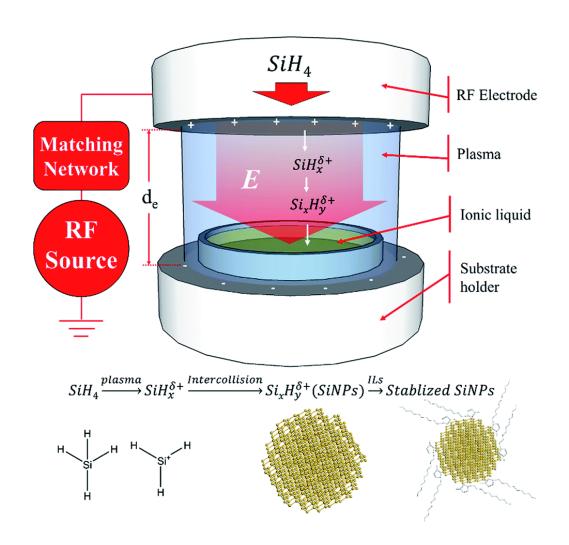
Plasma-enhanced chemical vapor deposition (PECVD)

Films can be deposited in low temperatures using plasma deposition

- **Device structures are sensitive to temperature, high-temperature deposition processes cannot be used in many cases.**

- **High-temperature films can be deposited at low temperatures.**

- **Unique films not found in nature can be deposited, e.g., diamond.**

Working temperature is determined by the desired film properties
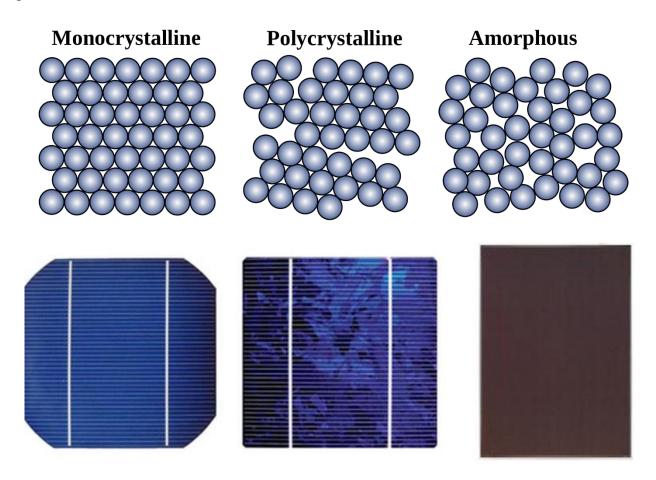
- **CVD – consists of a thermally activated set of gas-phase and surface reactions that produce a solid product at a surface.**

- **PECVD – gas-phase and the surface reactions are controlled or modified by the plasma properties.**

- **Te~2-5 eV in PECVD is much greater than the substrate temperature, the temperature in PECVD is much less that CVD.**

- **Deposition rates are usually not very sensitive to the substrate temperature T.**

- **Film properties such as composition, stress, and morphology, are functions of T.**

- **Low-temperature PECVD films are amorphous, not crystalline, which can more easily be achieved with chemical vapor deposition (CVD).**

Example of using PECVD – amorphous silicon
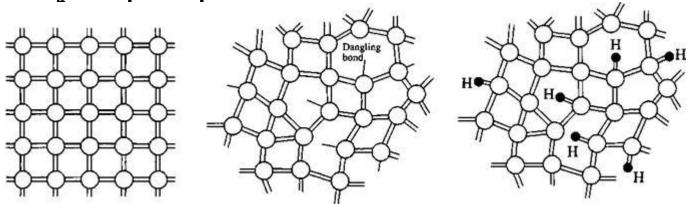
- **Amorphous silicon thin films are used in solar cells**

Monocrystalline   Polycrystalline   Amorphous

Example of using PECVD – amorphous silicon

- **H is required so that SiH$_4$ is used**

  - **For the material to be semiconducting.**

  - **Terminate the dangling bonds.**

  - **The dangling bonds are created by ion bombardment (SiH$_3^+$) which also removes hydrogen from the surface.**

  - **SiH$_3$ and SiH$_2$ radicals are important precursors for film growth while SiH$_4$ also participates in surface reactions.**
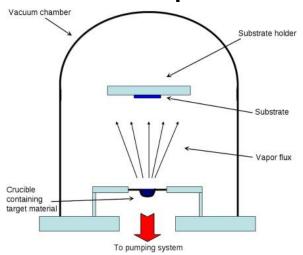
Physical vapor deposition can be achieved by heating the deposited material
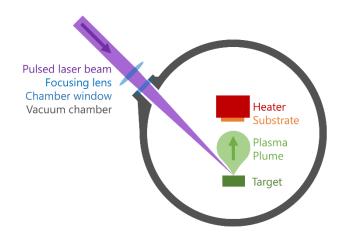
- **Thermal evaporator**
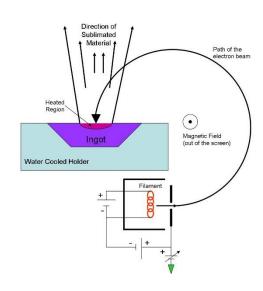
- **Electron-beam evaporator**

- **Pulsed-laser deposition**

https://en.wikipedia.org/wiki/Pulsed_laser_deposition
Engineered biomimicry by A. Lakhtakia and R. J. Martin-Palma
https://en.wikipedia.org/wiki/Electron-beam_physical_vapor_deposition
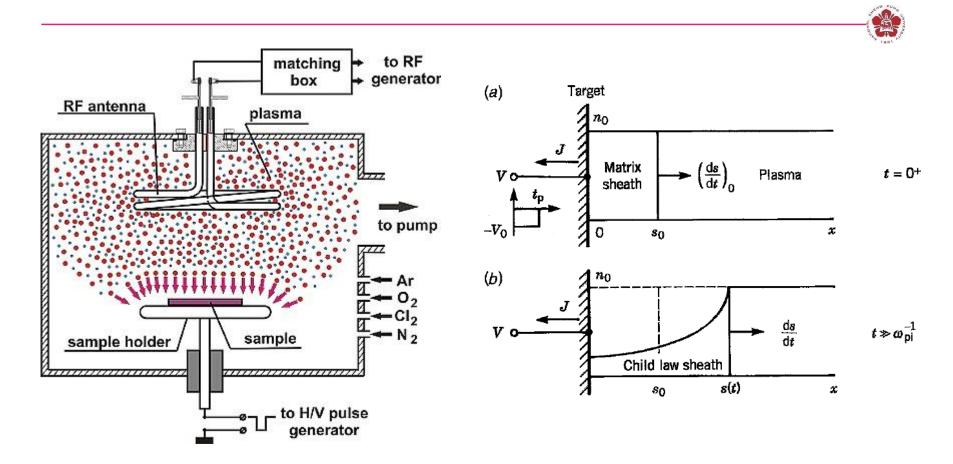
Sputtering deposition
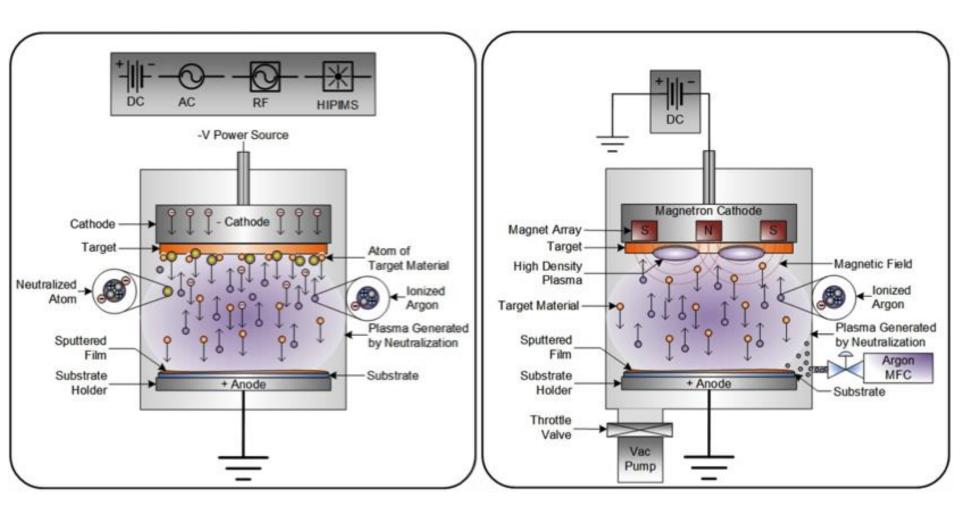
Plasma-immersion ion implantation (PIII)

- **Silicon doping – ions such as B, P, As are implanted**

- **Surface hardening of metals – N, C are implanted**

Magnetron sputtering provides higher deposition rates than conventional sputtering
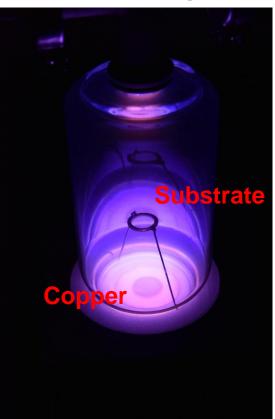
Demonstration experiments – magnetron sputtering
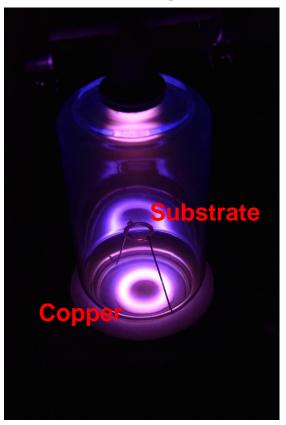
- **System**
- **Without magnet**
- **With magnet**
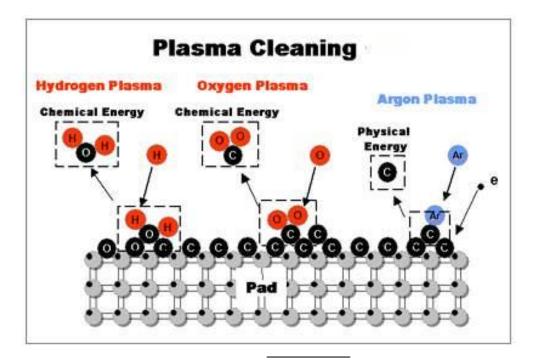
Plasma can be used for cleaning surface

- **Cleaning mechanisms:**
  - **Chemical reactions by free radicals**
  - **Physical sputtering by high energy ions**

馗鼎奈米科技股份有限公司
https://www.ecplaza.net/products/plasma-cleaning_111807

Free radicals are generated and used in chemical reactions

$$e^- + H_2 \rightarrow 2H\bullet \qquad e^- + O_2 \rightarrow 2O\bullet \qquad O\bullet + O_2 \rightarrow O_3$$

- **Highly reactive free radicals generated in plasma may react with the hydrocarbon contaminants of surface oxide.**

- **Both H• and O• can react with grease or oil on surface to form volatile hydrocarbons.**

$$\text{H}\bullet_{(g)} + C_nH_{2n+2(s)} \rightarrow \text{CH}_{4(s)}$$

$$\text{O}\bullet_{(g)} + C_nH_{2n+2(s)} \rightarrow \text{CO}_{(s)} + \text{CH}_xO_{y(g)} + H_2O_{(g)}$$

- O• is more reactive than H•. But O• may also react with surface metal to form oxide, deteriorating the material properties. Nevertheless, H• can make metal oxide back to metal.

$$\text{O}\bullet + \text{Me} \rightarrow \text{MeO}$$

$$\text{H}\bullet + \text{MeO} \rightarrow \text{Me} + H_2O$$

The effect of chemical reactions is increased as the pressure increases

- **Advantages:**

    - **Stable gas products are formed.**

    - **No redeposition problem.**

    - **High etching selectivity.**

- **Disadvantages:**

    - **Higher concentration of H_2 or O_2 is required to ensure an appropriate etching rate.**

    - **H_2 safety or O_2 strong oxidation ability needs to be monitored.**

High energy ions are used in physical sputtering cleaning

- **Ions generated in plasma can be accelerated toward the substrate to physically bombard away the atoms of contaminants.**

- **The physical sputtering rate increases as the following quantities increase:**

    - **Plasma density;**

    - **Accelerating voltage;**

    - **Mass of bombardment atoms.**

- **The physical sputtering is also enhanced by lowering the pressure.**

- **High cathode bias is used.**

- **Ar^+ has strong sputtering effect.**

The physical sputtering rate increases with higher cathode bias and Ar concentration and lower pressure

- **Advantages:**

    - **Highly efficient cleaning effect can be achieved.**

    - **Gas consumption rate can be very low.**
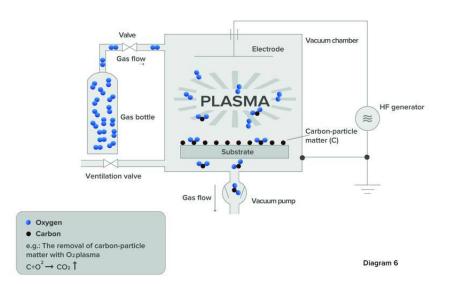
- **Disadvantages:**

    - **Etching problems – non-selective etching by physical sputtering.**

    - **Redeposition problems: the products sputtered out may be highly unstable and tend to deposit again downstream.**
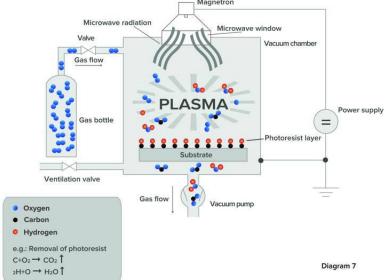
Plasma cleaning examples

Low-pressure plasma system: Generation with a low-frequency or high-frequency generator

Low-pressure plasma system: Cleaning with a microwave generator

Diagram 6

Diagram 7
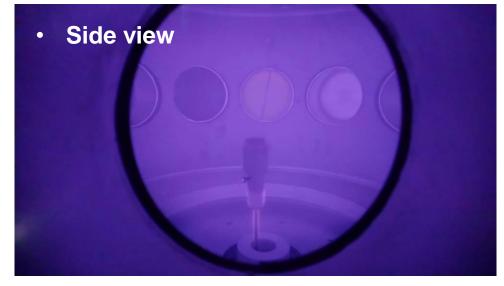
Plasma cleaning needs to work in the regime of abnormal glow discharge

Filled with Ar

High-voltage feedthrough

High-voltage power supply

- Top view

- Side view
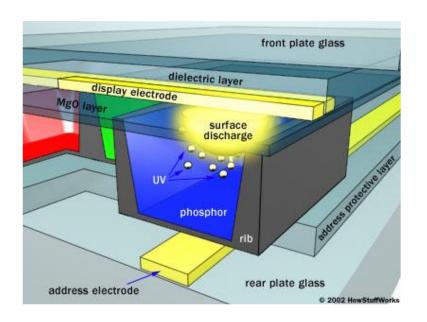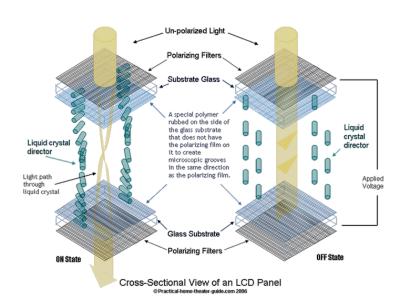
Light source and display systems

Plasma display panel (PDP)

Liquid crystal display (LCD)

Outlines
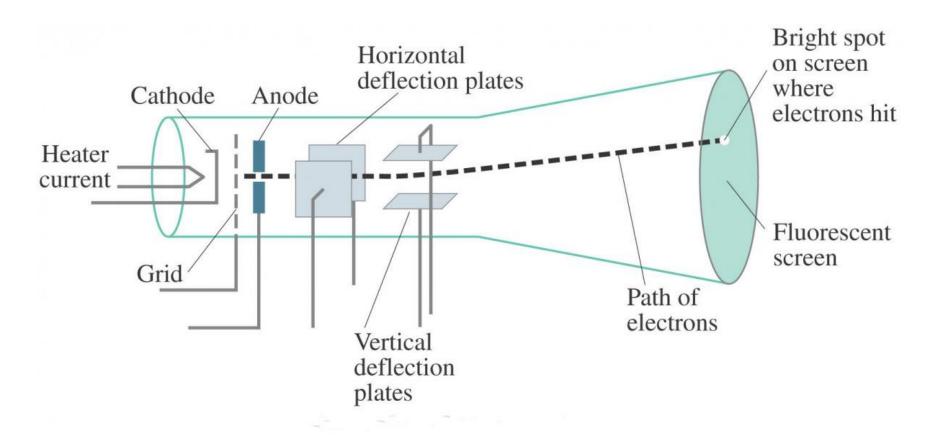
- **Cathode Ray Tube**

- **Color space (CIE 1931 color spaces)**

- **History of plasma display panel (PDP)**

- **Design of PDP**

- **Liquid crystal display (LCD)**

- **LCD vs PDP**
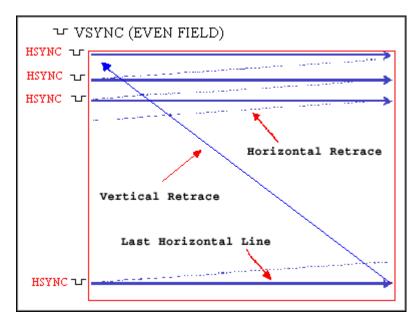
Cathode Ray Tube uses electron beams to light the fluorescent screen

Cathode   Anode   Horizontal deflection plates

Heater current

Grid

Vertical deflection plates

Bright spot on screen where electrons hit

Fluorescent screen

Path of electrons
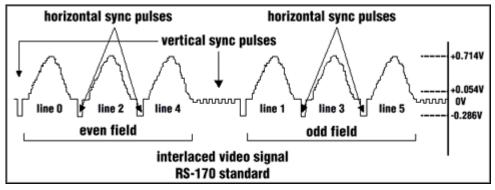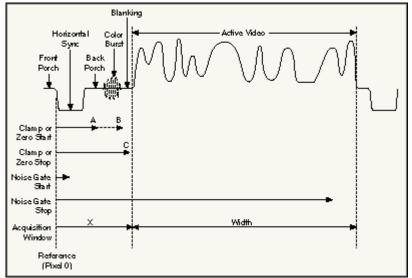
The image is shown by scanning through the whole screen with the single electron beam
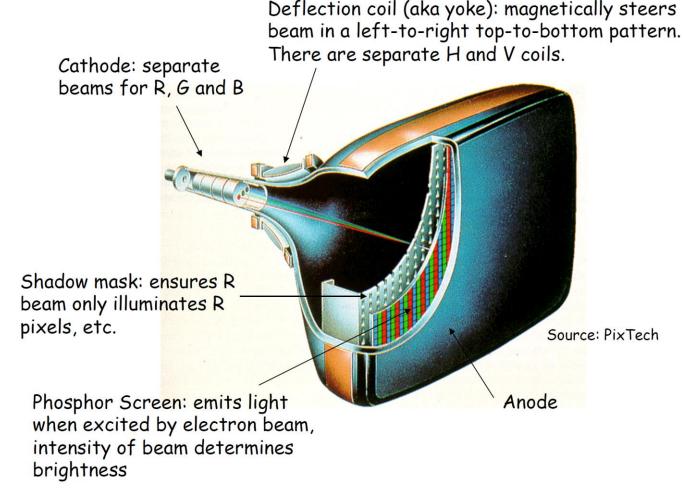
Color image is formed by using three electron beams scanning through three different color channels

Cathode: separate beams for R, G and B

Deflection coil (aka yoke): magnetically steers beam in a left-to-right top-to-bottom pattern. There are separate H and V coils.

Shadow mask: ensures R beam only illuminates R pixels, etc.

Phosphor Screen: emits light when excited by electron beam, intensity of beam determines brightness

Anode

Source: PixTech
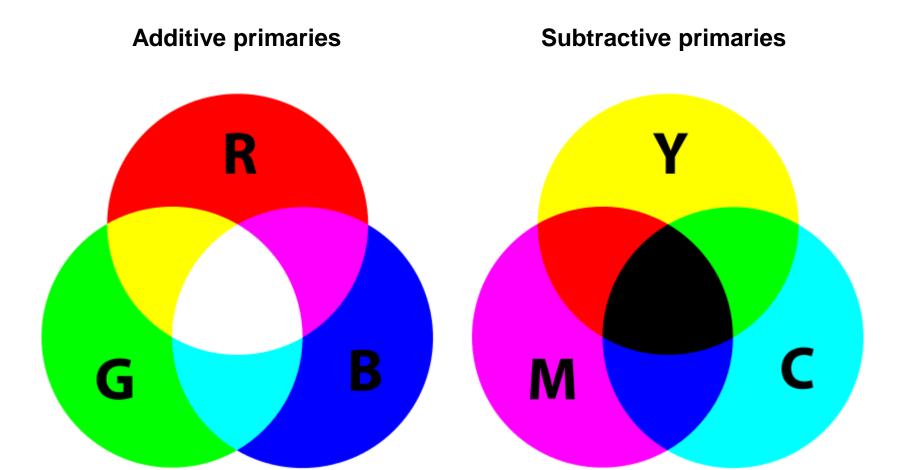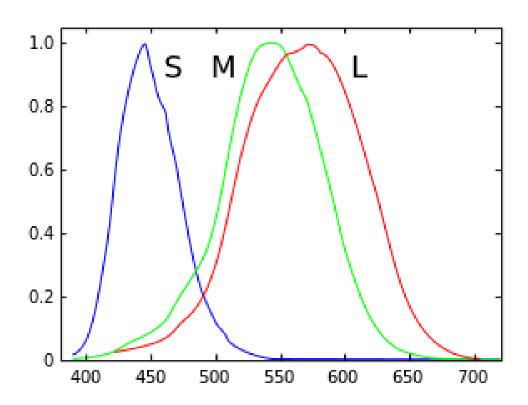
Color can be created using three primary colors

Additive primaries

Subtractive primaries
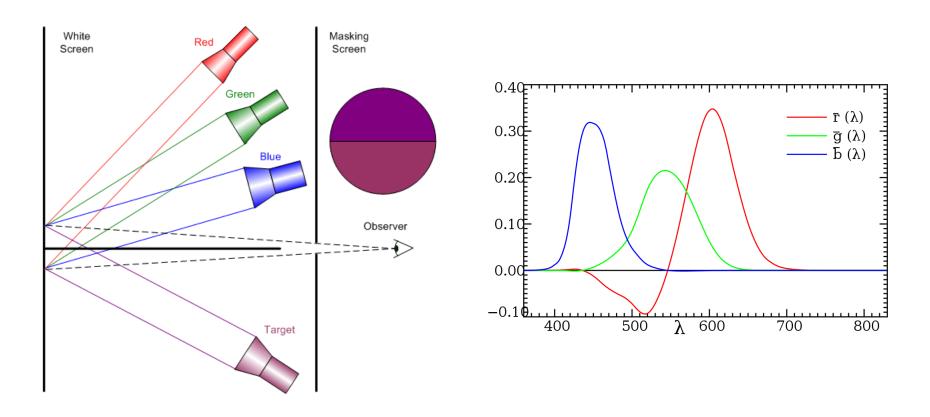
Human retina has three kinds of "cones" that have different spectral response
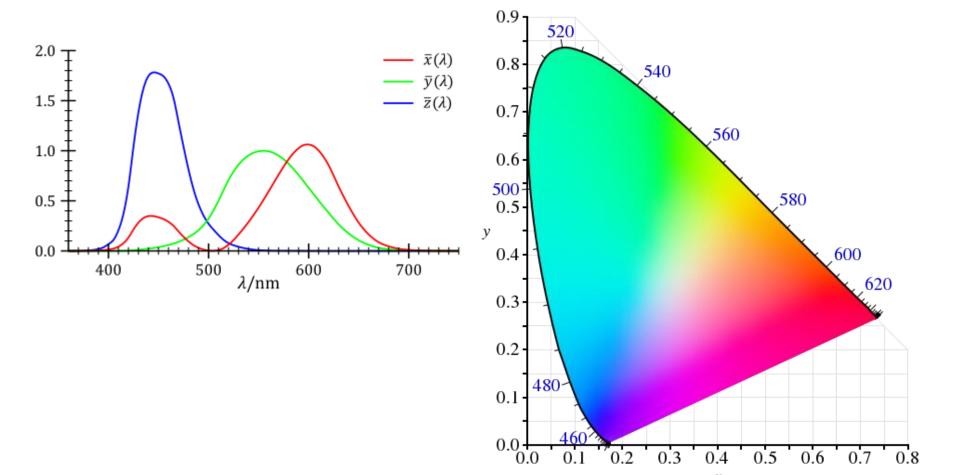
Spectral response of retina "cones" are tested using light sources with single wavelength

The CIE 1931 color space chromaticity diagram is the standard color space
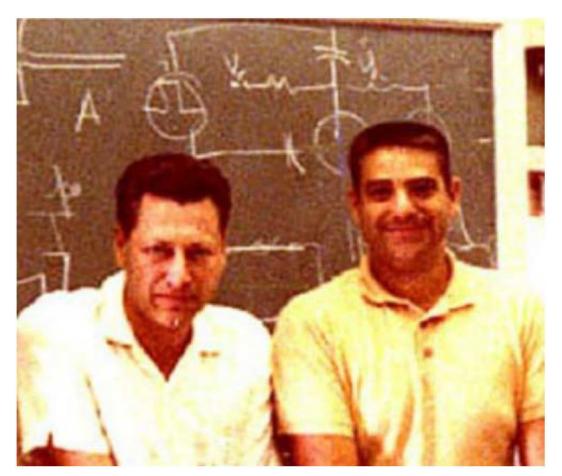
Plasma display panel was invented at the University of Illinois in 1967

Prof. H. Gene Slottow   **Prof. Donald L. Bitzer**

PDP was invented due to a need for Programmed Logic for Automatic Teaching Operations (PLATO) in 1960s

1981 Plato V
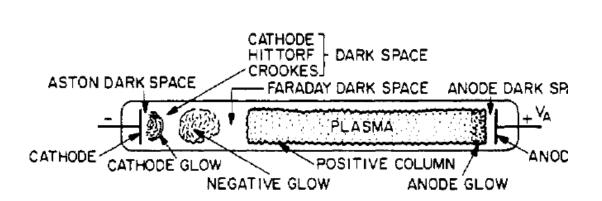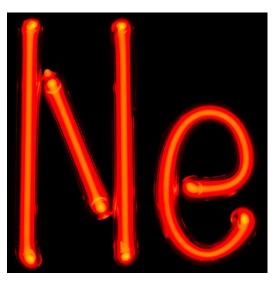
https://topwallpapers.pw/computer/keyboards-computers-history-teletype-typewriters-desktop-hd-wallpaper-1035981/
https://en.wikipedia.org/wiki/Punched_tape
https://en.wikipedia.org/wiki/PLATO_(computer_system)

The positive column in a glow discharge is used to excite phosphors in color PDP
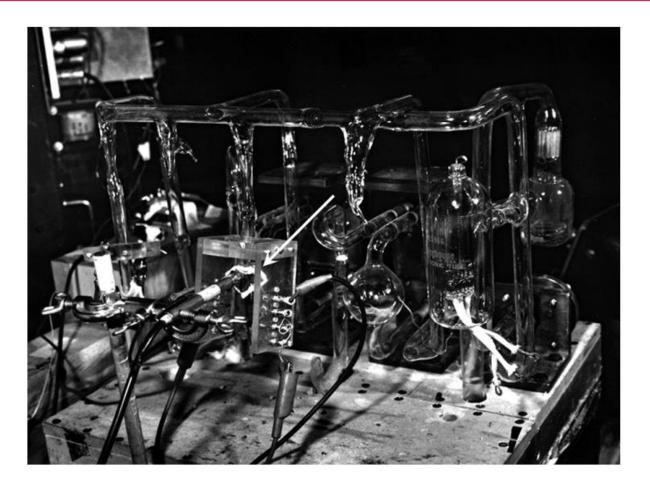
- **Majority of monochrome PDPs use the negative glow as the light source**
- **The positive column is used to excite phosphors in fluorescent lamps and in color PDPs**

Early plasma panel (PD) attached to the glass vacuum system used for the first plasma displays at UI
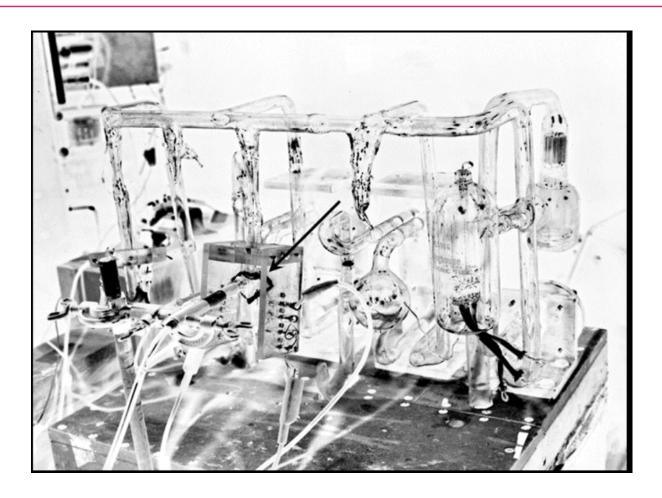
- **It had the same alternating sustain voltage, neon, gas, and dielectric glass insulated electrodes that are used for plasma TVs today.**

Early plasma panel (PD) attached to the glass vacuum system used for the first plasma displays at UI
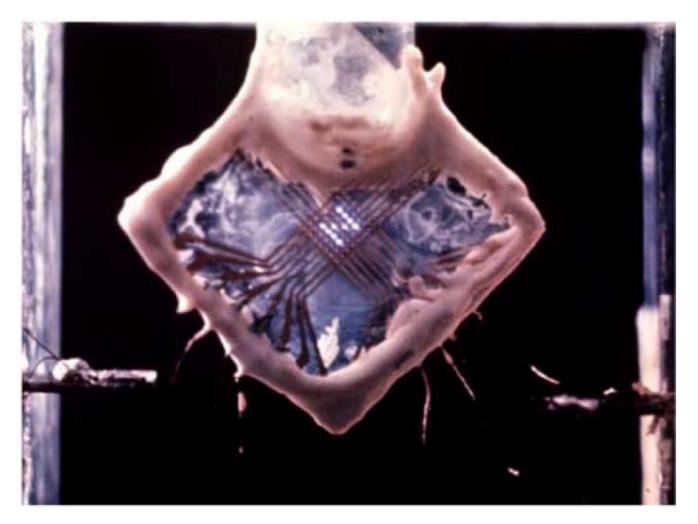
- It had the same alternating sustain voltage, neon, gas, and dielectric glass insulated electrodes that are used for plasma TVs today.

Early 4x4 pixel panel has achieved matrix addressability for the first time
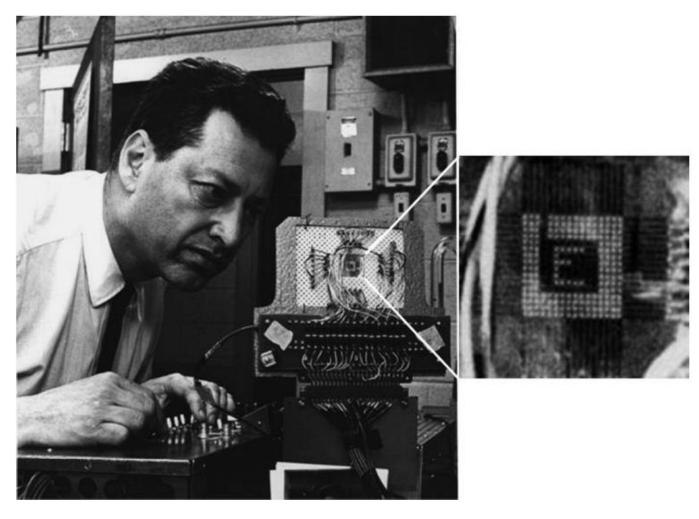
L. F. Weber, IEEE Trans. Plas. Scien., *34*, 268, 2006

159

Early 4x4 pixel panel has achieved matrix addressability for the first time

L. F. Weber, IEEE Trans. Plas. Scien., *34*, 268, 2006
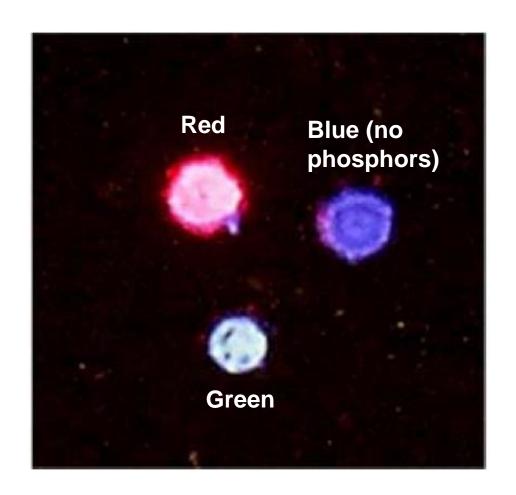
A 16x16 pixel PD, developed in 1967, needed to be addressed manually
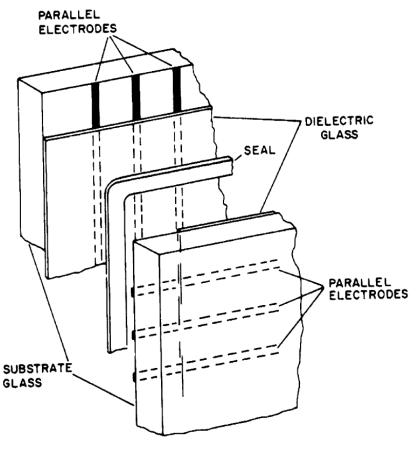
First color PD was three cell prototype with red and green color phosphors excited by a xenon gas discharge

Open-cell structure developed in 1968
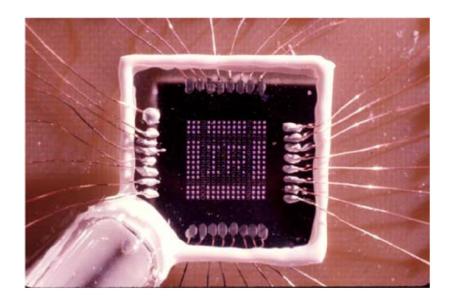
- **It could be baked under vacuum at 350 ºC to drive out contaminants.**

L. F. Weber, IEEE Trans. Plas. Scien., *34*, 268, 2006

163
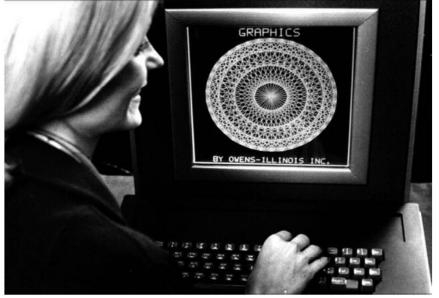
More progress
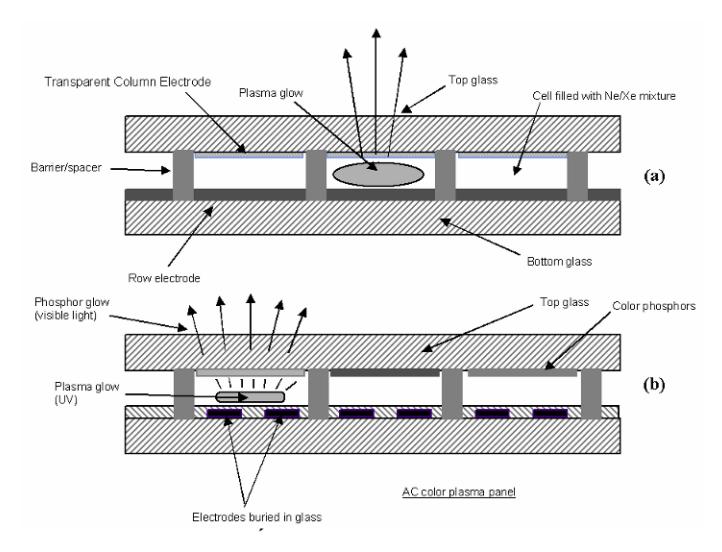
1968, University of Illinois
16x16 pixels

1971, Owens-Illinois
512x512 pixels
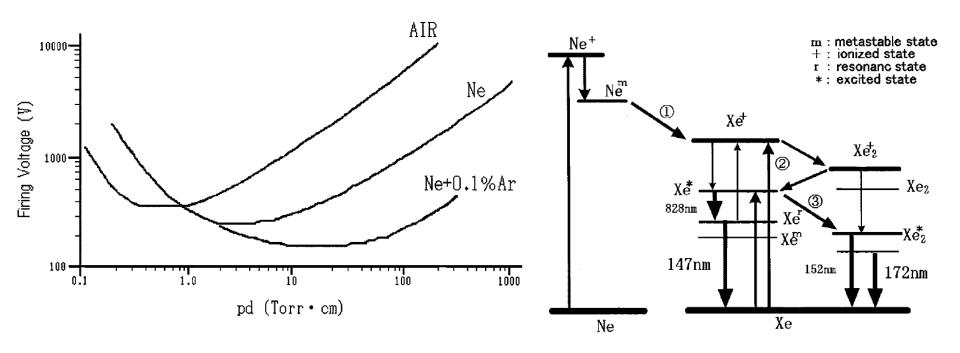
Color PDPs had short display lifetime due to the degradation of color phosphors caused by ion sputtering

Transparent Column Electrode

Plasma glow

Top glass

Cell filled with Ne/Xe mixture

Barrier/spacer

(a)

Row electrode

Bottom glass

Phosphor glow (visible light)

Top glass

Color phosphors

Plasma glow (UV)

(b)

Electrodes buried in glass

AC color plasma panel
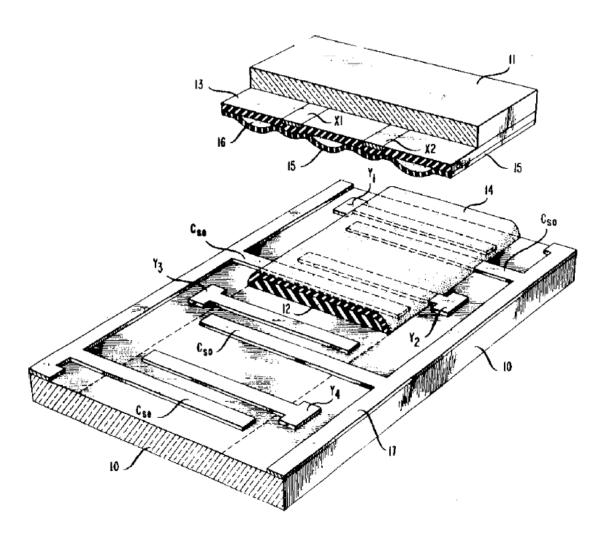
A lower breakdown voltages can be obtained with very small amounts of added gas
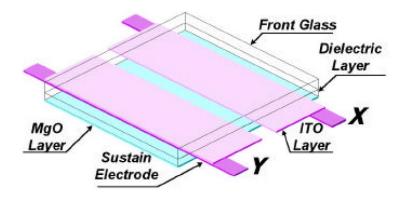
AT&T three-electrode patent
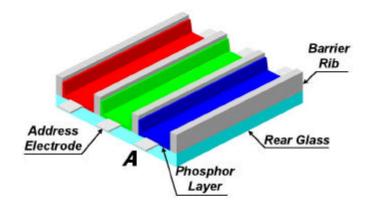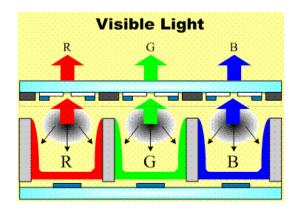
Reflective phosphor geometry is used in most of today's plasma TVs
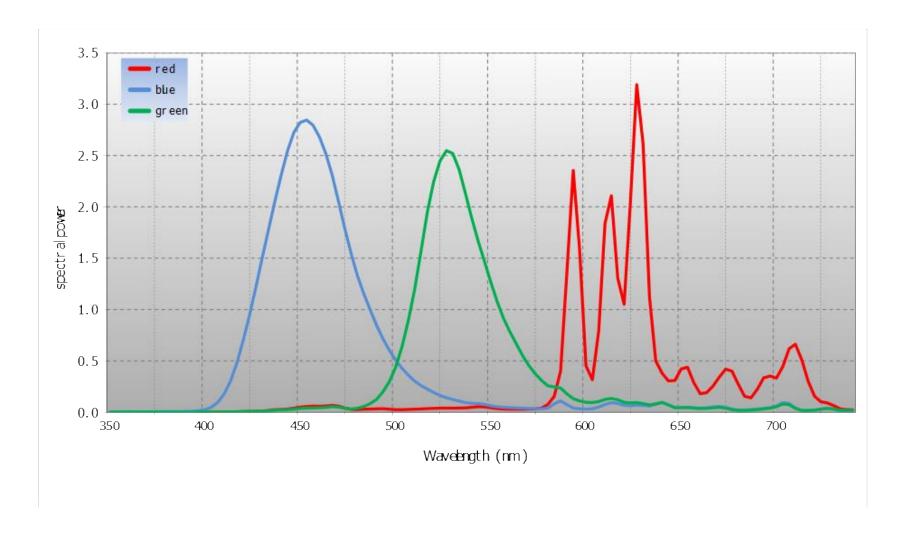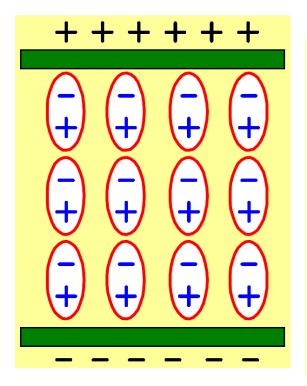
Spectrum of the different phosphors
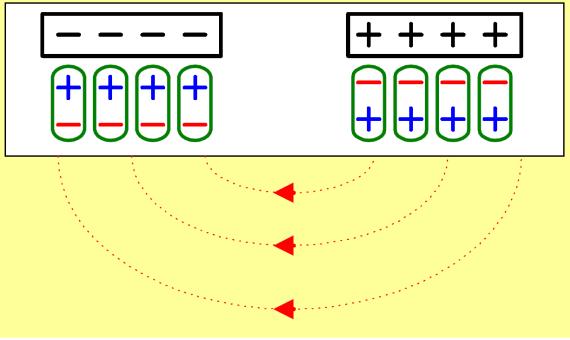
The foundation of AC discharge
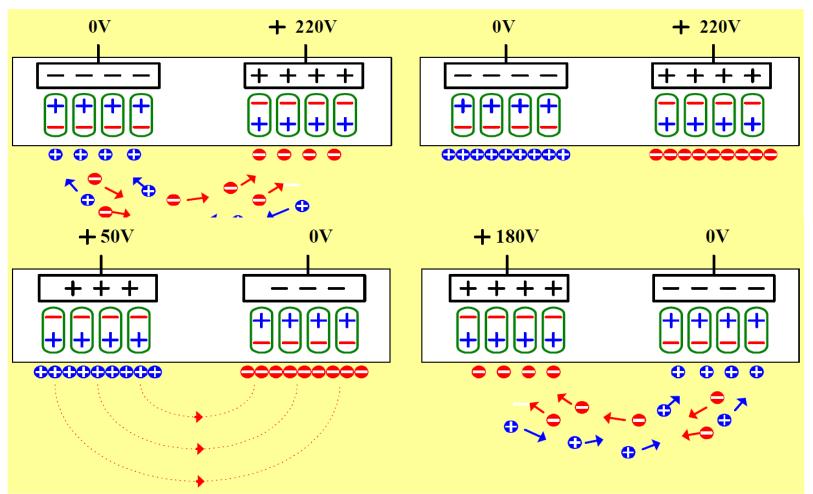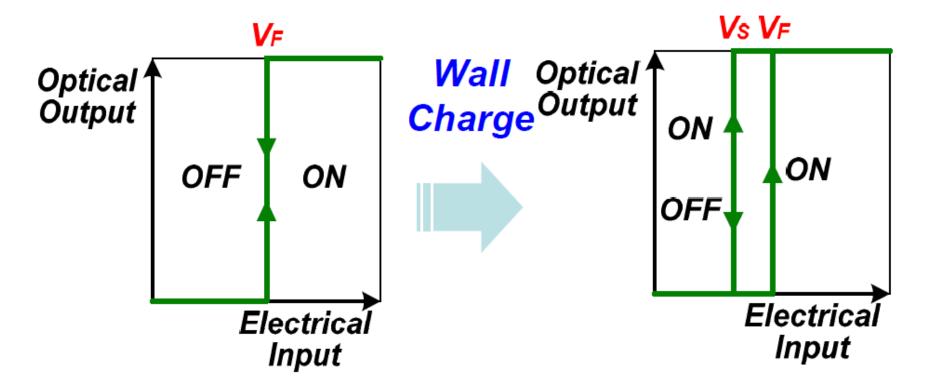
The plasma can be sustained using ac discharged

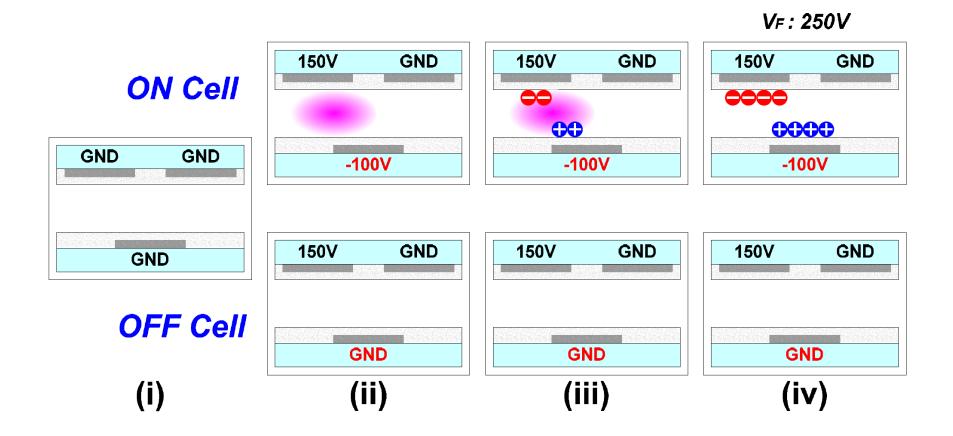- **Wall discharge reduced the required discharge voltage**

Wall discharge reduced the required discharge voltage
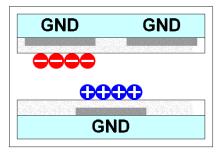
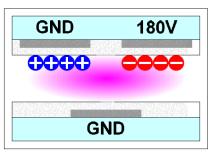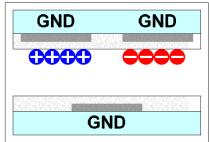# ON/OFF State Selection

$V_F : 250V$

ON Cell

OFF Cell

(i)   (ii)   (iii)   (iv)

Sustain discharge

ON Cell

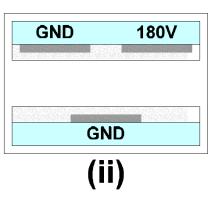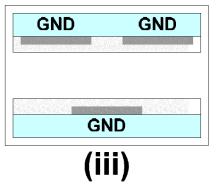| (i)	(ii)	(iii)	(iv)
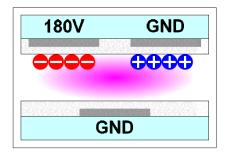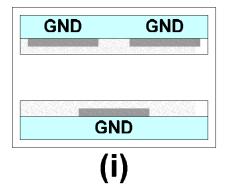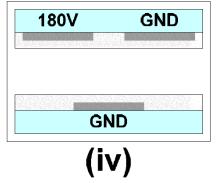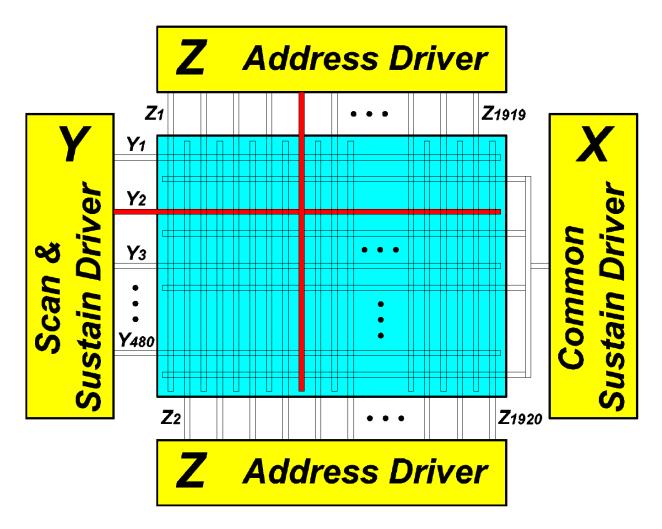
Address and sustain electrodes are connected to different drivers

Slides from Prof. Heung-Sik Tae, School of Electronic and Electrical Engineering, Kyungpook National University

175
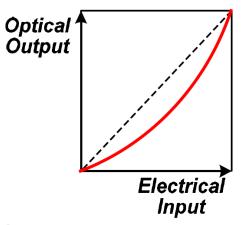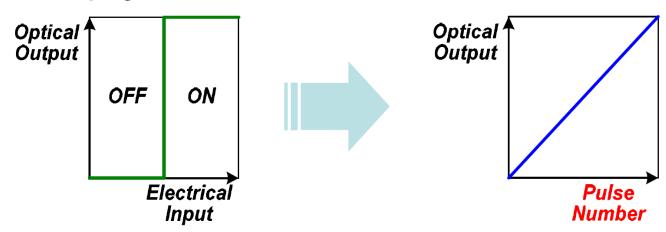
PDP pixel can only be either ON or OFF

- Cathode Ray Tube :

- Plasma Display Panel :

Slides from Prof. Heung-Sik Tae, School of Electronic and Electrical Engineering, Kyungpook National University

176

PDP luminance is controlled by using number of light pulses

- CRT : Control the Luminance using Electron Beam Intensity

Luminance Ratio 2 : 1

- PDP : Control the Luminance using Number of Light Pulses

Luminance Ratio 2 : 1

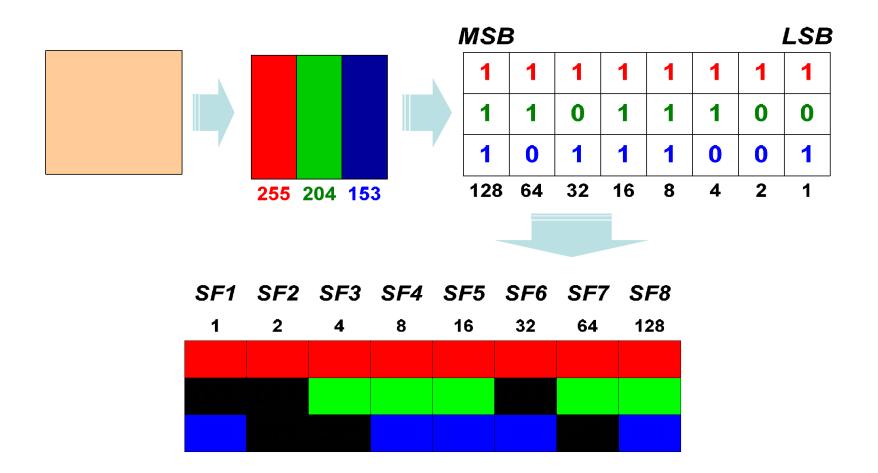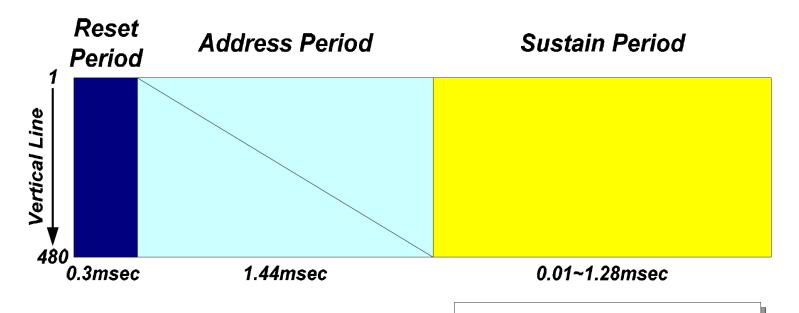# A single field is divided into 8 subfield

MSB							LSB
1	1	1	1	1	1	1	1
1	1	0	1	1	1	0	0
1	0	1	1	1	0	0	1
128	64	32	16	8	4	2	1

255 204 153

SF1	SF2	SF3	SF4	SF5	SF6	SF7	SF8
1	2	4	8	16	32	64	128

Slides from Prof. Heung-Sik Tae, School of Electronic and Electrical Engineering, Kyungpook National University

178

Composition of each subfield

Reset Period   **Address Period**   **Sustain Period**

Vertical Line

1

480

0.3msec   1.44msec   0.01~1.28msec
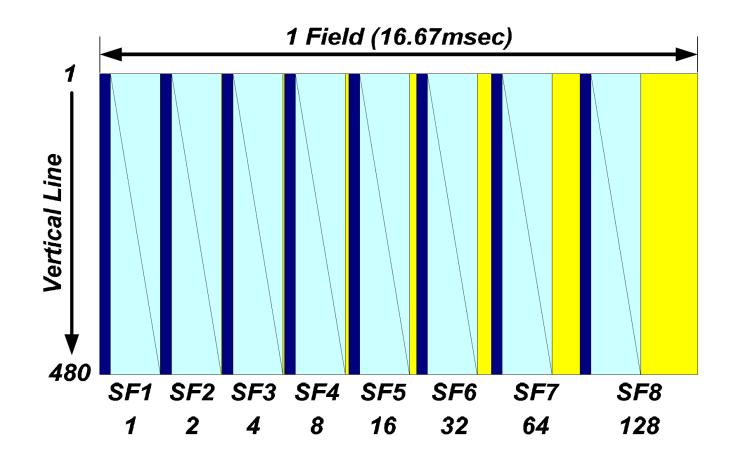
Spec : VGA (640*480)
        8 Subfield
        0.03msec Address Pulse
        100KHz Sustain Freq.

8 subfield in one TV-Field (ADS)

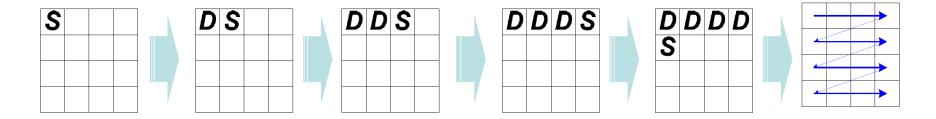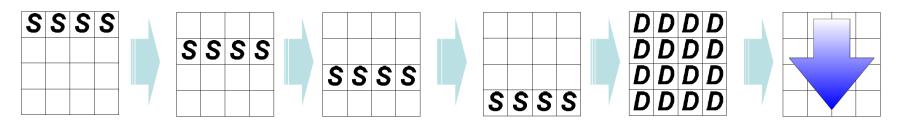# PDP uses line-by-line scanning

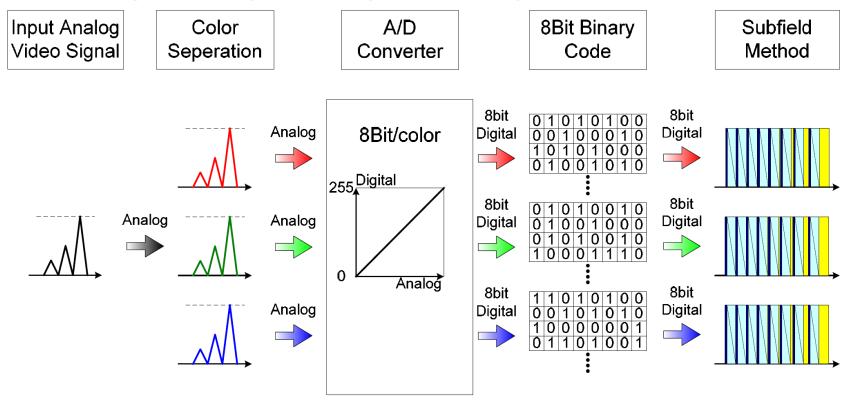- Cathode Ray Tube : Cell-by-Cell Scanning

- PDP : Line-by-Line Scanning

Slides from Prof. Heung-Sik Tae, School of Electronic and Electrical Engineering, Kyungpook National University

181

Video signal processing

- Analog Video Signal ⇨ Digital Pulse Signal

| Input Analog Video Signal | Color Seperation | A/D Converter | 8Bit Binary Code | Subfield Method |

Addressing period

Original Image   SF1   SF2   SF3

SF4   SF5   SF6   SF7   SF8

Displaying period

Original Image   SF1   SF2   SF3
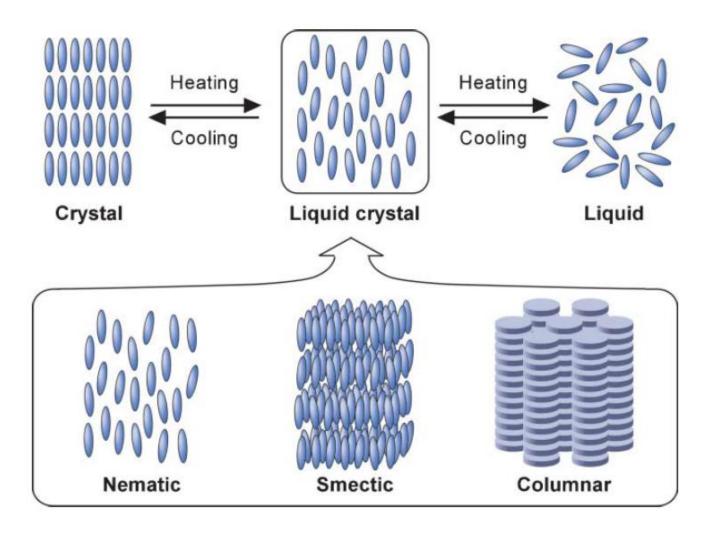
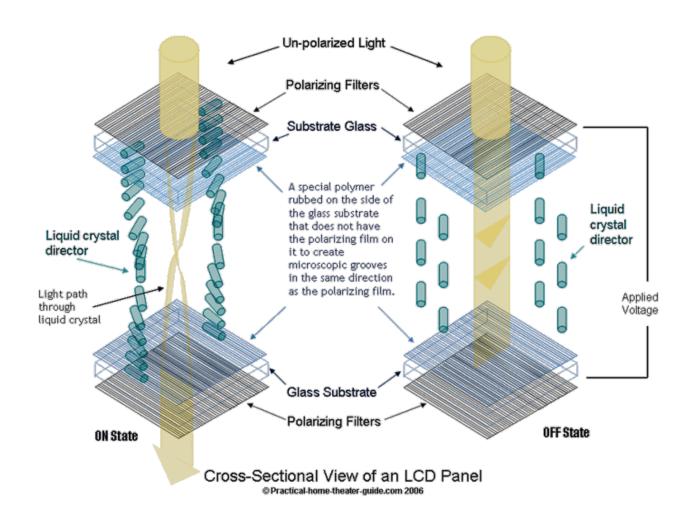SF4   SF5   SF6   SF7   SF8

Liquid crystal are a special state of matter between liquid and crystal
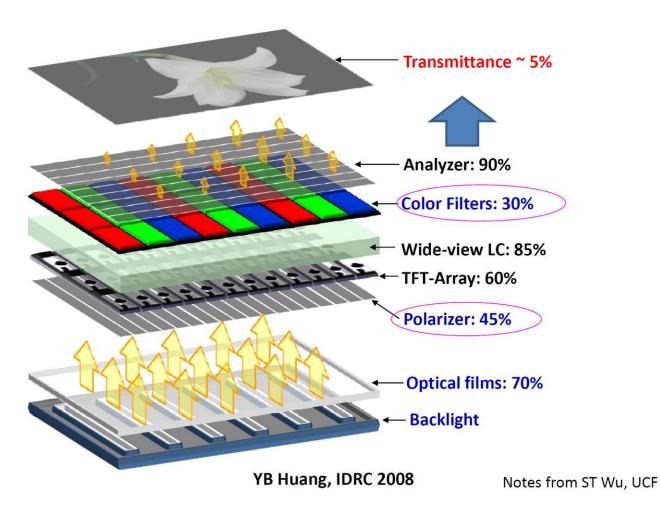
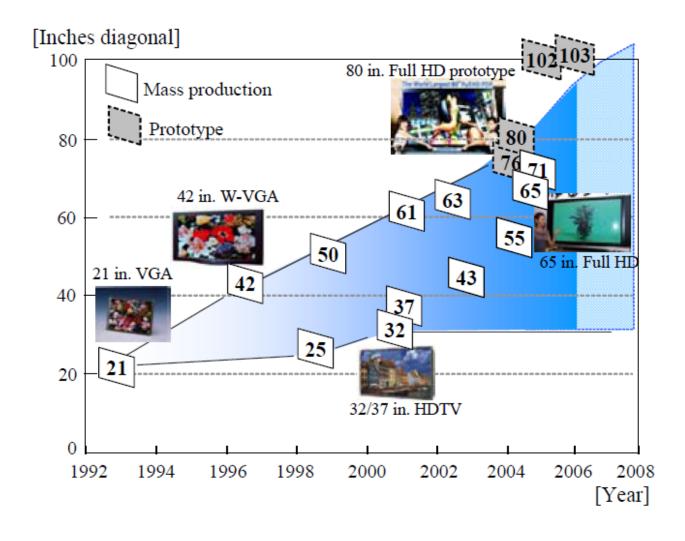# Linear polarization of a light can be rotated by miss aligned liquid crystal

Cross-Sectional View of an LCD Panel
© Practical-home-theater-guide.com 2006

Structure of Liquid crystal display (LCD)

Transmittance ~ 5%

Analyzer: 90%

Color Filters: 30%

Wide-view LC: 85%

TFT-Array: 60%

Polarizer: 45%

Optical films: 70%

Backlight

YB Huang, IDRC 2008

Notes from ST Wu, UCF

http://www6.cityu.edu.hk/cityu25/events/engineering/pdf/proftang.pdf
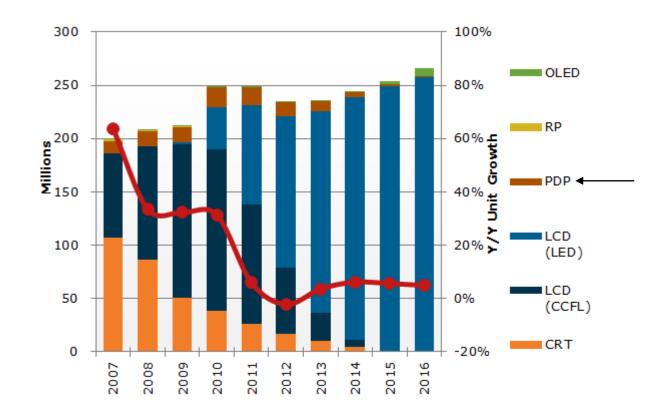
Optimistic projection of PDP market

Reality
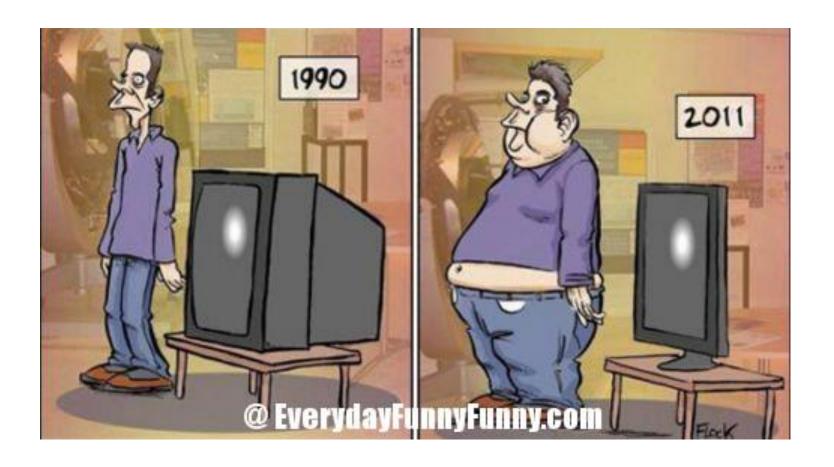
TV Shipment Growth by Technology

Too many reasons that PDP died!

- **Bright showroom conditions put plasmas at a distinct disadvantage versus LED-lit LCDs**

- **Aesthetics may have played a role in hastening plasma's demise**

- **UHD/4K caught on quickly**

- **Screen-size limitations also played a part in plasmas plight**

- **You can't bend a plasma**

- **Plasmas were harder to deal with than LCDs**

- **While OLED is still in the early stages of development, there's no question it offers greater potential than plasma**

- **Energy efficiency may have played a part in putting plasma out to pasture**

- **Plasma was the original flat-panel technology, People just thought of it as old technology.**

- **Projectors improved in quality and prices dropped**

http://www.avsforum.com/forum/40-oled-technology-flat-panels-general/2080650-10-reasons-plasma-died.html
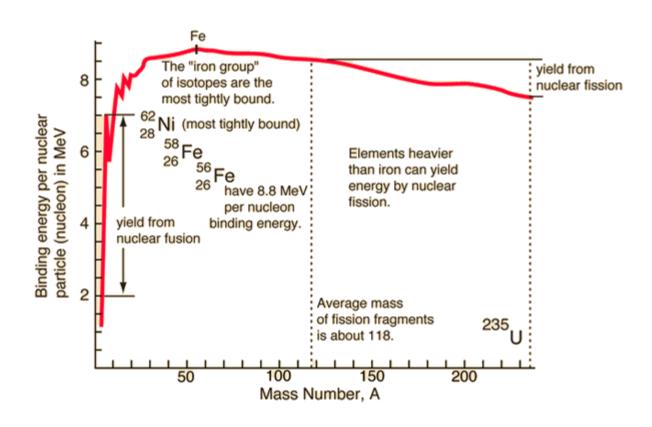
Let's stand up and do exercise!!
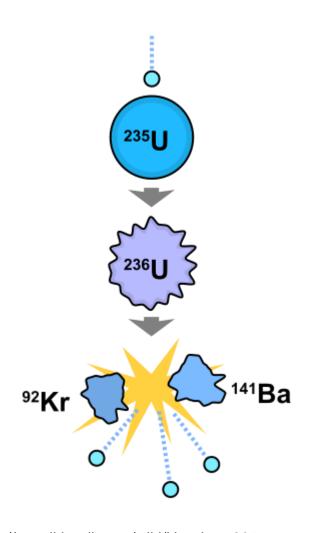
The hydrogen bomb

The "iron group" of isotopes are the most tightly bound

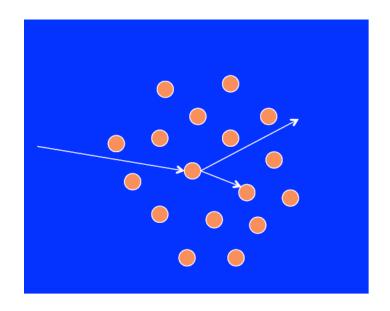# Chain reaction can happen in U^{235} fission reaction

- **~ 200 million electron volts (MeV)/fission, ~million times more than chemical reactions**
- **Energy for bombs, or for civilian power can generate huge amounts of energy (and toxicity) in a small space with a modest amount of material**
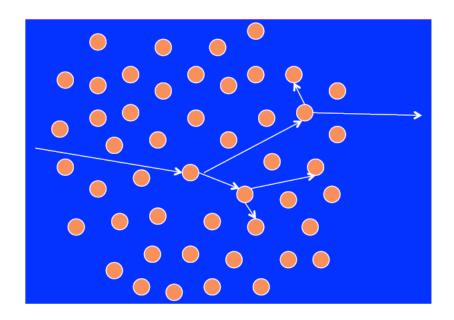- **Source of safety, security issues for nuclear power**

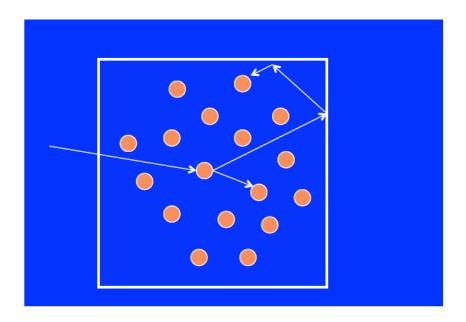# The neutrons are leaking out and stopping the chain reaction in a sub-critical mass
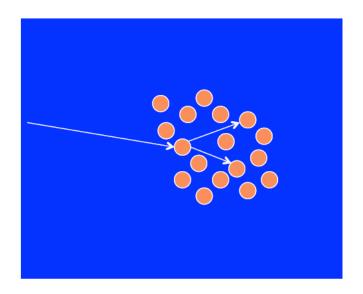
Solution 1: add more material

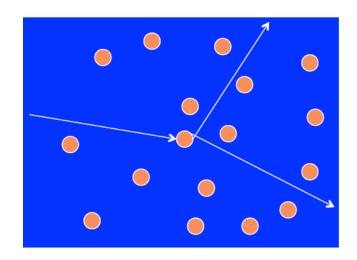# Solution2: reflect the neutron back in

Solution 3: increase the density

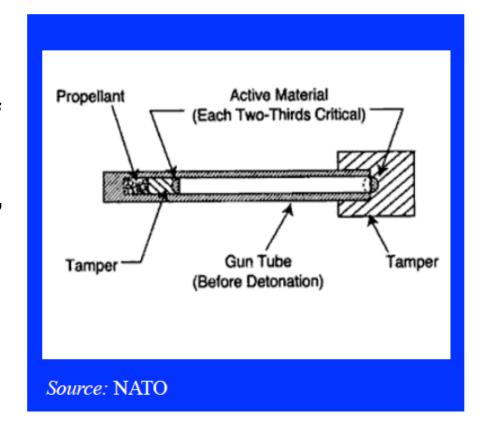# How to get the material together before it blows apart?

- **There are always neutrons around**
- **Once chain reaction starts, material will heat up, expand, stop reaction**
- **How to get enough material together fast enough?**

Gun-type bomb

- **Simple, reliable – can be built without testing**
- **Highly inefficient – require lots of nuclear material (50-60 kg of 90% enriched HEU)**
- **Can only get high yield with HEU, not plutonium**
- **Hiroshima bomb: cannon that fired HEU projectile into HEU target**

Source: NATO

Hiroshima Bomb – "Little Boy"

Gun Type – Easiest to design and build (Hiroshima bomb was never tested)

About 13 kiloton explosive yield

Talk given by Dr. Charles D. Ferguson, President, Federation of American Scientists, Department of Physics, Colloquium, American University, 2012

Atomic bomb is very destructive

Hiroshima: August 6, 1945   Nagasaki: August 9, 1945

Talk given by Dr. Charles D. Ferguson, President, Federation of American Scientists, Department of Physics, Colloquium, American University, 2012

The fusion process

Deuterium (H-2)
Tritium (H-3)
3.5 MeV Alpha Particle (He-4)
14.1 MeV Neutron

Deuterium-Tritium Fusion Reaction
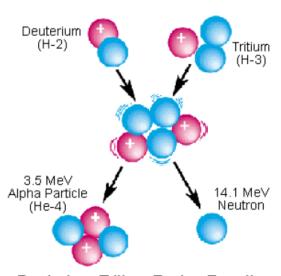
$^2H + ^3H \Rightarrow ^4He + n + Q \equiv 17.6\ \text{MeV}$

Energy release $Q = 17.6\ \text{MeV}$

In comparison

$^2H + ^2H \Rightarrow ^1H + ^3H + Q \equiv 4.0\ \text{MeV}$
$^2H + ^2H \Rightarrow ^3He + n + Q \equiv 3.2\ \text{MeV}$
$^3H + ^3H \Rightarrow ^4He + 2n + Q \equiv 11.3\ \text{MeV}$
$^{235}U + n \Rightarrow X_A + X_B + 3n + Q \approx 200\ \text{MeV}$

Fusionable Material, deuterium ^2H (D) and tritium ^3H (t):

Deuterium: natural occurrence (heavy water) (0.015%).

Tritium: natural occurrence in atmosphere through cosmic ray bombardment; radioactive with $T_{1/2} = 12.3$ y.

"Advantages" of hydrogen bomb

Fusion of ^{2}H+^{3}H:

$$\frac{Q}{A} = \frac{17.6\ MeV}{(3+2)\ amu} = 3.5\ \frac{MeV}{amu}$$

Fission of ^{235}U:

$$\frac{Q}{A} = \frac{200\ MeV}{236\ amu} = 0.85\ \frac{MeV}{amu}$$

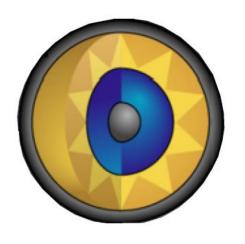Fusion is 4 times more powerful than fission and generates 24 times more neutrons!

Neutron production:

$$^2H+^3H: \quad \frac{n}{A} = \frac{1}{5} = 0.2$$

$$^{235}U + n: \quad \frac{n}{A} = \frac{2}{236} = 0.0085$$

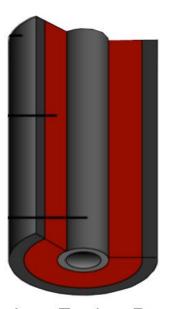# Hydrogen bomb uses a fission bomb to initiate the fusion reaction

Fuel

Primary Fission Device

Core: ^{239}Pu, ^{235}U, plus ^{2}H+^{3}H booster

Shell: ^{238}U tamper

High explosive lenses
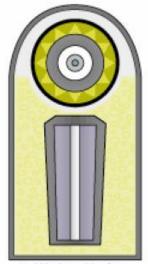
Secondary Fusion Device
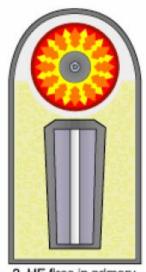
Radiation channel

^{239}Pu sparkplug

^{6}Li, ^{2}H, ^{3}H fusion cell

^{238}U tamper

Event sequence

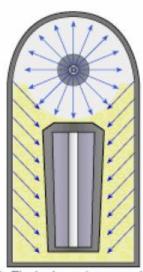1. Warhead before firing; primary (fission bomb) at top, secondary (fusion fuel) at bottom, all suspended in polystyrene foam.

2. HE fires in primary, compressing plutonium core into supercriticality and beginning a fission reaction.

3. Fissioning primary emits X-rays which reflect along the inside of the casing, irradiating the polystyrene foam.

4. Polystyrene foam becomes plasma, compressing secondary, and plutonium sparkplug begins to fission.

5. Compressed and heated, lithium-6 deuteride fuel begins fusion reaction, neutron flux causes tamper to fission. A fireball is starting to form...

Additional pressure from recoil of exploding shell (ablation)!

You don't want to build a hydrogen bomb!

Illustration From October 2002
Issue of "Popular Mechanics" (pg. 69)